

Biotransformation, trace analysis and effects of perfluoroalkyl and polyfluoroalkyl substances

vorgelegt von
Dipl.-Ing. (FH)
Tobias Frömel
aus Idstein

Von der Fakultät III – Prozesswissenschaften –
der Technischen Universität Berlin
zur Erlangung des akademischen Grades
Doktor der Ingenieurwissenschaften
Dr.-Ing.

genehmigte Dissertation

Promotionsausschuss

Vorsitzender: Prof. Dr. rer. nat. Wolfgang Rotard

Berichter: Prof. Dr.-Ing. Martin Jekel

Berichter: Prof. Dr.-Ing. Thorsten Reemtsma

Berichter: Prof. Dr. rer. nat. Thomas P. Knepper

Tag der wissenschaftlichen Aussprache: 06.07.2012

Berlin 2012

D 83

Abstract

Perfluoroalkyl and polyfluoroalkyl substances are environmental contaminants with adverse properties owing to the presence of the particularly strong C-F bond.

In this thesis, the biotransformation potential of fluorotelomer ethoxylates (FTEOs) was assessed under aerobic conditions. After investigation of the technical FTEO mixture by electrospray-mass spectrometry (ESI-MS) techniques, it could be shown that two pathways are possible, one involving oxidation to ω -oxidized carboxylates (FTEOCs), which can be stable under certain conditions, and another pathway releasing perfluorocarboxylates, in function of the perfluoroalkyl chain length of the FTEO. After successful synthesis of two short-chain FTEOCs, these compounds were quantified in a wastewater treatment plant (WWTP) effluent by solid phase extraction and high performance liquid chromatography coupled to ESI-MS/MS. Alongside the FTEOCs, a set of perfluorocarboxylates and perfluoroalkane sulfonates was determined in seventeen WWTP effluent samples and four surface water samples.

The biotransformation behavior of three building blocks of potential novel environmentally friendly fluorosurfactants was investigated. It could be shown that 6-(trifluoromethoxy)-hexan-1-ol released 100% inorganic fluoride, whereas 3-(trifluoromethoxy)-propan-1-ol yielded only 15% fluoride. The remainder was shown to be organically bound as the non-degradable 3-(trifluoromethoxy)-propanoic acid. The building block 1-(2,2,3,3,4,4,4-heptafluorobutoxy)-propan-2-ol expectedly released perfluorobutanoic as the persistent transformation product.

The toxicity of the dead-end transformation product PFBA towards the green algae *Pseudokirchneriella subcapitata* and towards the Cladoceran *Chydorus sphaericus* was assessed with standardized tests. The results suggested no acute toxicity of these compounds at environmental levels. Other

fluorinated compounds were included in the screening suggesting a general increase of toxicity with longer perfluoroalkyl chain length. However, the functional group itself showed a major effect on toxicity.

The mass spectrometric fragmentation characteristics of the compounds studied in this thesis were carefully scrutinized. Comparison of different fluorotelomer-based compounds revealed a general fragmentation pattern for these compounds after negative electrospray ionization and collision-induced dissociation, which can be utilized to screen for novel fluorotelomer-based contaminants hereafter.

Abstract

Polyfluorierte und perfluorierte Verbindungen stellen eine Gruppe von Umweltkontaminanten dar, die aufgrund der starken C-F-Bindung besonders negative ökologische Eigenschaften besitzen.

In dieser Arbeit wurde das Biotransformations-Potenzial von Fluortelomerethoxylaten (FTEO) unter aeroben Bedingungen untersucht. Nach Ermittlung der molekularen Zusammensetzung eines technischen FTEO-Gemischs mittels Elektrospray-Massenspektrometrie (ESI-MS) konnte aufgezeigt werden, dass zwei Transformationswege möglich sind, wobei einer dieser Wege über ω -oxidierte Carboxylate (FTEOCs), welche unter bestimmten Bedingungen nicht weiter abbaubar sind, verläuft. Ein anderer Abbauweg mündet in Perfluorcarboxylaten. Nach erfolgreicher Synthese zweier kurzkettiger FTEOCs konnten diese Verbindungen mithilfe einer Methode basierend auf Festphasenextraktion und HPLC-ESI-MS/MS in einer Kläranlagenablaufprobe nachgewiesen und quantifiziert werden. Neben den FTEOCs konnten eine Reihe von Perfluorcarboxylaten und Perfluoralkansulfonaten in siebzehn Kläranlagenabläufen und vier Oberflächengewässern bestimmt werden.

Die Untersuchung der Bioabbaubarkeit dreier potentieller Bausteine für neue, umweltfreundliche Fluortenside ergab, dass 6-(Trifluormethoxy)-hexan-1-ol 100% anorganisches Fluorid freisetzte. Die homologe Verbindung 3-(Trifluormethoxy)-propan-1-ol hingegen setzte lediglich 15% Fluorid frei, wobei das verbleibende Fluor in der nicht weiter abbaubaren 3-(Trifluormethoxy)-propansäure organisch gebunden blieb. Der dritte Baustein - 1-(2,2,3,3,4,4,4-Heptafluorbutoxy)-propan-2-ol – führte erwartungsgemäß zur persistenten Verbindung Perfluorbutansäure.

Die Toxizität der Perfluorbutansäure gegenüber der Algenspezies *Pseudokirchneriella subcapitata* und dem Kleinkrebs *Chydorus sphaericus* wurde anschließend ermittelt. Die toxikologischen Kenndaten ergaben keine akute Gefährdung dieser Organismen bei umweltrelevanten Konzentrationen. Weitere fluorierte Verbindungen wurden untersucht, wobei gezeigt werden konnte, dass die Toxizität mit zunehmender Kettenlänge im Allgemeinen zunimmt, die funktionelle Gruppe jedoch einen signifikanten Einfluss auf die Toxizität hat.

Die massenspektrometrische Fragmentierung aller untersuchten Verbindungen wurde untersucht. Dabei ergab sich ein allgemeiner Fragmentierungsweg für Fluortelomer-basierte Verbindungen unter negativen Elektrospray-Bedingungen und stoßinduzierter Fragmentierung. Diese Erkenntnisse können in Zukunft zur Detektion neuer unbekannter Fluortelomer-basierter Verbindungen verwendet werden.

Acknowledgement

First and foremost, I would like to thank Prof. Dr. Martin Jekel for his supervision and the opportunity to carry out my PhD thesis with him.

I am particularly grateful to Prof. Dr. Thomas P. Knepper for the opportunity to carry out the experimental work in his laboratory, but also for his valuable scientific guidance and supervision, as well as for his openness, but also for his criticism.

I would like to express my thanks to the whole team of the Institute for Analytical Research, including Jutta Müller, Marco Bernhard, Heike Weil, Sascha Klein, Ian Ken Dimzon, Vanessa Gellrich and our former colleague Dr. Manuela Peschka, for the scientific support, the convenient ambiance and simply a great time.

The German Water Chemical Society is highly acknowledged for allowing me the PhD grant for three years of my experimental work.

I thank Willie Peijnenburg for allowing me to carry out the ecotoxicity tests in his laboratory and the European Union for financial support under the ECO-itn project during my stay in The Netherlands. Marja Wouterse, Erik Steenbergen and Evert-Jan van den Brandhof are highly acknowledged for their support with these tests.

I thank I would like to thank Prof. Dr. Monika Buchholz for the assistance with synthesis of transformation products.

The group of Prof. Dr. Mario Thevis is greatly acknowledged for the orbitrap MS measurements.

I thank Karl-Heinz Bauer for the fluoride measurements after UV decomposition.

I would like to thank Dr. Axel Buchholz for the NMR measurements.

Finally, I would like to say thank you to my parents Elke and Thomas Frömel as well as to my girlfriend Valentina Kelsch, who have always been there for me. I am sure I would not have been able to achieve what I have achieved without your presence and help.

1	Introduction	9
1.1	The role of transformation products for sustainable chemistry.....	9
1.2	Fluorinated compounds.....	12
1.3	Chemical and physico-chemical properties of fluorinated compounds.....	13
1.4	Sources and application of perfluorinated and polyfluorinated compounds.....	14
1.5	Environmental occurrence, effects and regulation of PFASs	15
1.6	Biotransformation of fluorinated compounds	17
1.7	Objectives	23
2	Theory.....	25
2.1	Liquid chromatography.....	25
2.2	Mass Spectrometry	26
2.2.1	Application of mass spectrometry and definitions	26
2.2.2	Ion sources	27
2.2.3	Mass analyzers	29
2.3	CID fragmentation of aliphatic fluorinated compounds.....	35
3	Results and discussion	37
3.1	Characterization of a commercial fluorotelomer ethoxylate mixture	37
3.1.1	ESI-MS	37
3.1.2	HPLC-ESI-MS.....	39
3.1.3	Molecular weight distribution	40
3.1.4	Semiquantitative determination of FTEO.....	43
3.1.5	Conclusion	44
3.2	CID fragmentation of FTEO and its TPs	45
3.2.1	Fragmentation of cationic species	45
3.2.2	Fragmentation of anionic species.....	47
3.2.3	Conclusion	55
3.3	Biotransformation of a commercial fluorotelomer ethoxylate mixture	56
3.3.1	FTOH residues in the commercial mixture.....	56
3.3.2	Generation of perfluorocarboxylic acids by biotransformation.....	56

3.3.3	Primary degradation vs. adsorption	57
3.3.4	Temporal evolution of FTEOC.....	59
3.4	Biotransformation of fractionated long-chained fluorotelomer ethoxylates	60
3.4.1	Two-dimensional fractionation of technical fluorotelomer ethoxylate mixture	60
3.4.2	Primary degradation and adsorption.....	61
3.4.3	Formation of transformation products.....	63
3.4.4	Conclusion	67
3.5	Monitoring of PFASs in environmental samples	67
3.5.1	Synthesis of standards	67
3.5.2	Monitoring of FTEO ₁ Cs and classic PFASs in environmental samples	68
3.5.3	Conclusion	72
3.6	Biotransformation of novel fluorosurfactant building blocks	73
3.6.1	3-(Trifluoromethoxy)-1-propanol	73
3.6.2	6-(Trifluoromethoxy)-1-hexanol	78
3.6.3	1-(2,2,3,3,4,4,4-Heptafluorobutoxy)-propan-2-ol.....	83
3.6.4	Conclusion	88
3.7	Ecotoxicological assessment of selected PFASs.....	89
3.7.1	Selection of compounds and background.....	89
3.7.2	Acute toxicity on <i>Pseudokirchneriella subcapitata</i>	90
3.7.3	Acute toxicity to <i>Chydorus sphaericus</i>	95
3.7.4	Conclusions	95
4	Perspectives	97
5	Summary.....	98
6	Annex.....	100
6.1	Materials and methods	100
6.1.1	Solvents, reagents, reference materials and instrumentation	100
6.1.2	HPLC-ESI/MS analysis	101
6.1.3	Biotransformation setup and sample preparation	111
6.1.4	Trace analysis of PFASs in wastewater treatment plant effluents.....	114

6.1.5	Two-dimensional fractionation of FTEO	115
6.1.6	Synthesis of TPs	116
6.1.7	Ecotoxicological experiments	118
6.2	List of abbreviations	119
6.3	List of figures.....	122
6.4	List of tables	124
6.5	List of compounds and their acronyms	125
6.6	List of references.....	130

Parts of this thesis have been published in the following articles and books:

Frömel T., Knepper T. P. Mass spectrometry as an indispensable tool for studies of biodegradation of surfactants. *TrAC Trends in Analytical Chemistry* (2008) 27(11): 1091-1106

Frömel T., Knepper T. P. Fluorotelomer ethoxylates: Sources of highly fluorinated environmental contaminants part I: Biotransformation. *Chemosphere* (2010) 80(11): 1387-1392

Frömel T., Knepper T. P. Biodegradation of Fluorinated Alkyl Substances. *Reviews of Environmental Contamination and Toxicology* (2010) 208: 161-179

Frömel T., Knepper T. P. Mass spectrometric Approaches to reveal PFC biotransformation products. In Knepper, T. P., Lange, F. T. Polyfluorinated chemicals and transformation products (2011), part of Barceló D., Konstantoy, A. G. *The Handbook of Environmental Chemistry*, Springer, Heidelberg, Germany

Ding G. H., Frömel T., van den Brandhof, E. J., Baerselman, R., Peijnenburg, W. J. G. M. Acute toxicity of poly- and perfluorinated compounds to two Cladocerans, *Daphnia magna* and *Chydorus sphaericus*. *Environmental Toxicology and Chemistry* (2012) 31(3): 605-610

1 Introduction

1.1 The role of transformation products for sustainable chemistry

Numerous organic anthropogenic chemicals have been identified and quantified in environmental specimen throughout the past decades [1-9]. Distribution of legacy environmental pollutants results from direct use of these compounds and as such, they are target analytes to analytical chemists. Well-known examples for these compounds are pesticides, pharmaceuticals, surfactants and polychlorinated compounds such as polychlorinated biphenyls and polychlorinated dibenzodioxins. Screening of such target analytes is often carried out effortlessly by routine analysis, because scientists are aware of the chemical structure and physico-chemical properties. As a result, analytical methods can be developed by virtue of these features and even analytically challenging analytes may be measured by customized optimization of protocols.

However, organic anthropogenic compounds in the environment are not confined to those which are directly and intentionally produced by humans. The number of compounds is largely increased when taking into account transformation products (TPs) of organic compounds. These substances may be a result of biotic or abiotic processes, which are summarized in Figure 1.

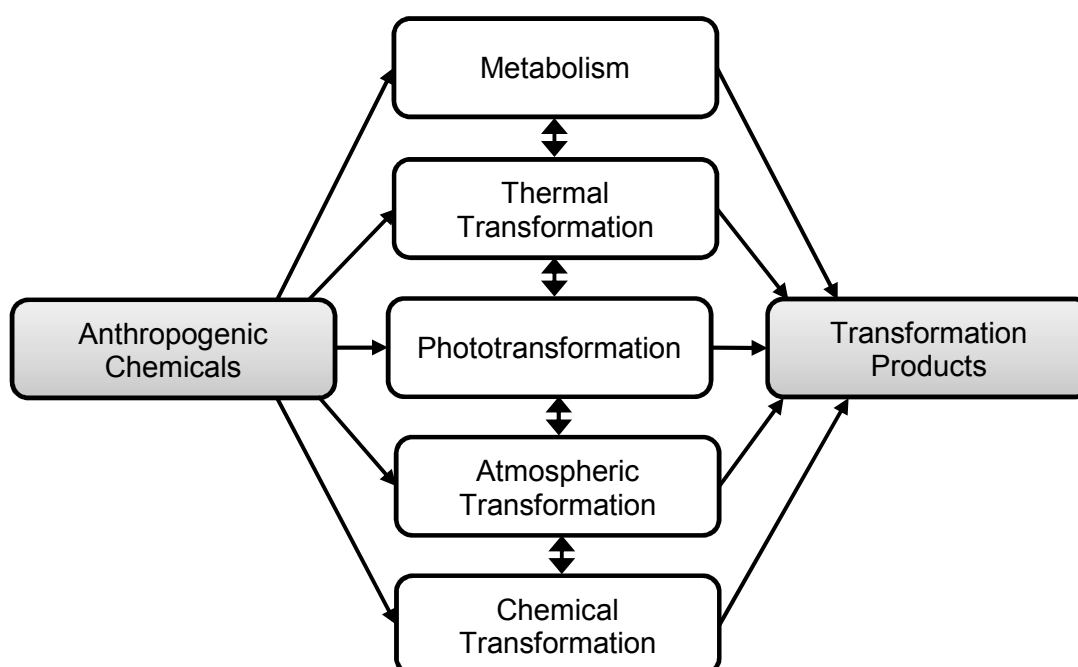


Figure 1: Overview of biotic and abiotic processes involved in the formation of transformation products

Biotic processes involve metabolic enzymatic reactions by higher organisms, such as humans, animals or plants as well as microbial transformations by bacteria, fungi, algae or protozoa. Most of these organisms may transform organic compounds as a source of energy, carbon or other elements the respective compound consists of. Higher organisms may also transform these compounds to facilitate excretion of otherwise toxic compounds.

Microbial transformation is an essential process which is made use of in modern wastewater treatment plants (WWTPs), where organic anthropogenic compounds can be transformed or even entirely degraded [4,8,10-12]. However, even after entering the environment, organic compounds can be transformed microbially due to the ubiquity of microorganisms. Thus, these reactions may occur in all kinds of aqueous environmental compartments and in soil.

Processes without the involvement of enzymatically driven chemical reactions are summarized under the term abiotic processes. These reactions are mediated by photons, chemicals or thermal energy and may occur in different environmental compartments as well as in man-made facilities or factories.

Phototransformation is an important process, which includes the direct or indirect reaction of a compound with sunlight in aqueous solution. Direct phototransformation refers to reactions occurring between the compound and photons, whereas indirect phototransformation describes processes involving mediators such as natural organic matter, which effectively absorbs the photons and induces further reactions with the target compound [13]. Closely related to phototransformation is atmospheric transformation of substances in the gas phase. Under these conditions, hydroxyl radicals are formed and may effectively react with organic molecules [14].

Chemical reactions may be induced notably under harsh conditions, e.g. in drinking water facilities, where ozonation and chlorination are still the methods of choice for disinfection [15]. Both of these chemicals do not only attack microorganisms, but are very reactive towards organic and inorganic compounds. Hence, several toxic TPs have been identified to result from their use, such as the highly carcinogenic N,N-dimethylnitrosamine [16,17]. A particularly important transformation by chemical reaction is hydrolysis, which represents cleavage of esters, amides or similarly labile compounds by the influence of water. Its importance is corroborated by the fact that pollutants in the environment are most often present in aqueous solution.

Thermal transformation has not gained scientists' attraction until the discovery that chlorinated organic compounds may be transformed to the extremely toxic polychlorinated dibenzodioxins or dibenzofuranes under high temperatures [18].

The fact that all of these processes may theoretically proceed consecutively drastically increases the number of possible TPs. An impressive example is the abovementioned formation of N,N-dimethylnitrosamine during chlorination in drinking water facilities. One of the sources

was pinpointed to be dimethylsulfamide, which in turn is a microbial TP of the pesticide tolylfluanide [17].

Adverse effects arising from microbial transformation processes have been first revealed in 1984, when biotransformation of nonylphenol ethoxylates (NPEO) was shown to yield the toxic TP 4-nonylphenol [19]. Although self-commitment of manufacturers lead to reduced use of NPEO shortly after this ascertainment, the fact that the application of NPEO was only restricted in 2003 by the European Union [20] underlines the complexity and tediousness when chemicals are about to be legislated. This in turn emphasizes the need to study environmental fate and effects of compounds before releasing them onto the market.

In addition to the pronounced environmental benefits, this *modus operandi* would facilitate tracing of these TPs in the environment after their release, because analytical chemists could develop specifically designed analytical methods. Unless scientific studies simulating these processes are carried out, detection and identification in environmental samples is usually extremely complex [21] and time-consuming due to the very low concentrations and – even more severely – because non-target analysis has to be performed. Although analytical instrumentation and data evaluation tools have become more and more powerful, target analysis will certainly always be the method of choice, especially at low concentrations.

A shift from pollution reduction by treatment processes after use towards pollution prevention is necessary and inevitable [22], which is also implemented by the European Union Regulation ‘Registration, Evaluation, Authorisation, and Restriction of Chemicals’ (REACH). In the REACH legislation, it is addressed that “a characterisation of possible degradation, transformation, or reaction processes and an estimation of environmental distribution and fate shall be performed” [23], which is required for chemicals exceeding production amounts of more than 100 t/y [24].

The necessity for this mode of action is substantiated by the fact that TPs can be more toxic than their parent compounds, as illustrated in Figure 2, although this figure demonstrates that most of the TPs are indeed less toxic than their parent compound. The sustainability of novel compounds brought onto the market should thus be contemplated integrally, including knowledge on identity, properties and toxicity of TPs. This can only be affected by means of sophisticated analytical methods, such as mass spectrometry (MS) or nuclear magnetic resonance (NMR) spectroscopy. Thus, non-specific biodegradation tests such as those suggested by the Organisation for Economic Co-Operation and Development (OECD) [25] relying on sum parameters cannot evaluate environmental friendliness. For instance, even if a compound is shown to be 90% biodegradable within a short time (based on dissolved organic carbon (DOC) or carbon dioxide evolution tests), the remaining 10% may be present in form of a lower molecular weight toxic TP.

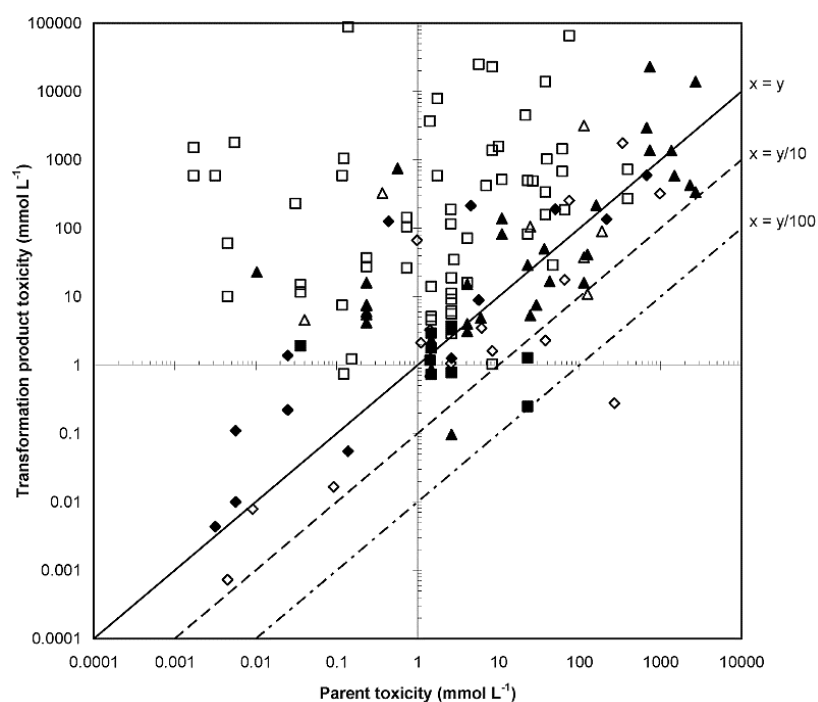


Figure 2: Toxicity of a set of pesticides versus the toxicity of its TP. Toxicity towards fish, daphnids and algae are shown. Reprinted from Ref. [26]. Please notice that the different icons do not reflect the species tested.

Prediction of environmental properties, especially of toxicity and degradability, will certainly play an important role with the implementation of REACH, but it will probably not replace laboratory experiments. The complexity of these properties is extremely complex, because both toxicity and degradability are often linked to their ability to bind to proteins – enzymes or receptors – which depend at least on the species under investigation. With this knowledge, it is recommended to use both *in silico* methods and laboratory methods synergistically.

1.2 Fluorinated compounds

Perfluoroalkyl and polyfluoroalkyl substances (PFASs) are anthropogenic compounds, which are mainly used in technical applications, but also in consumer products. Apart from well-known genuine fluorocarbons, such as polytetrafluoroethylene (PTFE) and perfluoroalkanes, and hydrofluorocarbons, such as polyvinylidene difluoride (PVDF), numerous functionalized highly fluorinated compounds of lower molecular weight have been used in various applications. These will be referred to herein as PFASs. By definition, all fictive hydrogen atoms on an aliphatic carbon backbone are substituted by fluorine in perfluorinated substances, whereas polyfluorinated substances contain one or more C-H bonds.

Among the various substance classes, perfluorinated carboxylic acids (PFCA) and perfluorinated sulfonic acids (PFSA) are the most prominent perfluorinated substances today,

especially perfluorooctanoic acid (PFOA) and perfluorooctane sulfonic acid (PFOS). These compounds have been identified to occur ubiquitously and to exhibit several adverse effects towards humans and the environment, as described in chapter 1.5. And yet, the effects and significance of PFASs to the environment can only be assessed, when all PFASs are taken into account. However, the entirety of PFASs is very difficult to assess, which is substantiated by a list provided by the OECD, where more than 900 compounds are listed, which may degrade to PFCA or PFSA [27]. The spectrum of compound classes ranges from carboxylic acids, sulfonic acids to phosphonic and phosphinic acids, amines, sulfonamides, polyethoxylates, and many more [28].

Only very few indications on naturally occurring defluorinating enzymes have been discovered, which is due to the scarcity of fluorinated molecules in nature and the high bond enthalpy. Indeed, only 4-fluorothreonine, several fluorinated fatty acids as well as fluorocitrate, fluoroacetone and one fluorinated nucleoside derivative (nucleocidin) have been discovered so far [29,30].

1.3 Chemical and physico-chemical properties of fluorinated compounds

Most of the unique and often deleterious effects of PFASs are connected to the properties of fluorine, which can be considered an element of extremes within the periodic table of elements. The most important characteristics with consequences for environmental effects analytical problems of PFASs are summarized in the following.

Fluorine has an atomic number of 9 and a relative atomic weight of 18.9984 u. In contrast to most other elements, fluorine is monoisotopic. Thus, fluoroorganic compounds do not exhibit characteristic isotopic patterns in MS, which is one of the disadvantageous properties of fluorine for the analytical chemist, especially the mass spectrometrists. In contrast, other organohalogens, like organochlorines and organobromines offer very pronounced isotopic patterns, which can be made use of by means of MS.

Fluorine has a very small van der Waals radius of 147 pm [31] and, although very difficult to measure, a covalent radius of approximately 60 pm [32-34]. Associated with this, it has the highest electronegativity in the entire periodic system of 3.98 on Pauling's scale [35], which inevitably causes every bond A-F to have considerably ionic character, unless A is oxygen, nitrogen or fluorine itself [32]. Thus, the C-F bond is better described as $C^{\delta+}-F^{\delta-}$. As a result of these rather ionic interactions, the C-F bond is considered the strongest single bond in organic chemistry with a bond enthalpy of 481 kJ mol⁻¹ in CH₃F, which is substantially higher than that of other bonds [36]. This pronounced bond strength is reflected by the notorious environmental and chemical stability of PFASs.

In mammalian organisms, cytochrome P₄₅₀ monooxygenases can defluorinate certain molecules, but the number of articles on microbial defluorination is very scarce, at least this is true for aliphatic compounds. Aromatic fluoroorganics seem to be more susceptible to defluorination, as the number of scientific papers on defluorination of aromatic compounds exceeds that of aliphatic compounds by far [37].

Another consequence of its low van der Waals radius is a very low electronic polarizability, which causes London forces and surface energies of fluorinated molecules to be very low [38] and may represent a reason for the unique partitioning characteristics of highly fluorinated molecules. They are both hydrophobic and lipophobic/oleophobic [39,40] and, depending on the functional groups attached to the fluorinated carbon chain, have low aqueous solubility. For instance, the aqueous solubility of 8:2-fluorotelomer alcohol (8:2-FTOH) is approximately two orders of magnitude lower than its non-fluorinated counterpart 1-decanol [41]. Furthermore, 8:2-FTOH is rather liquid, whereas 1-decanol is solid, which also implies very low intermolecular forces between 8:2-FTOH molecules. Despite the low intramolecular forces, PFASs tend to show distinct partitioning onto parts of the high-performance liquid chromatography (HPLC) instrument or environmental solids such as soil [42] or activated sludge [43] or any material used to conduct the study, e.g. vessels, tubes and other surfaces [44]. This effect may be ascribed to ionic and non-ionic interactions. As a consequence of this property, sterile controls should always be carried out simultaneously in order to differentiate between biotransformation processes and sorption.

Another effect of the low aqueous solubility of some of the compounds is volatilization, if the compounds exhibit high vapor pressure and low aqueous solubility at the same time, such as FTOH and other fluorotelomer-based biotransformation products. For instance, 8:2-FTOH exhibits caused a low boiling point of approximately 80°C, a vapor pressure of 3 Pa at 25°C [45] and poor water solubility of ca. 150 µg L⁻¹, which results in a relatively high water-air partitioning coefficient [46,47]. Furthermore, when dissolved in water, the tendency to sorb onto particles is very high [43], which was investigated in detail by Liu *et al.*, who found a log K_{OC} of 4.13 ± 0.16, but a log K_{DOC} value of 5.3 ± 0.29 and partially irreversible binding of 8:2-FTOH to DOC [45].

1.4 Sources and application of perfluorinated and polyfluorinated compounds

As a result of their unprecedented surface tension reduction and chemical stability, PFASs have been produced for more than 50 years [48] and have been used in various industrial, household and consumer applications. The fields of use range from aqueous firefighting foams (AFFF), inks, varnishes, leveling agents, lubricants and auxiliary chemicals in polymerization processes to applications in the semiconductor manufacturing, galvanic, leather, paper and textile industry

[49]. Several of the lower molecular weight PFASs, for instance FTOHs and N-EtFOSE are used as intermediate products for polymers, which is one of their main fields of application [48].

The use in these products renders unintentional and intentional emissions into the environment inevitable. Unintentional emissions may be caused by wash-off or volatilization, whereas intentional emissions are largely confined to usage of AFFF containing PFASs.

A rather complex source for several PFASs is biotransformation of other PFAS species. The most prominent examples are the degradation of 8:2-FTOH to PFOA and the transformation of N-EtFOSA to PFOS [50]. This subject will be discussed more thoroughly in chapter 1.6. The global fate of PFASs is further complicated by atmospheric degradation (photodegradation), which plays an important role for volatile PFASs, such as FTOHs, fluorotelomer olefins (FTO) and FOSEs [51-54].

1.5 Environmental occurrence, effects and regulation of PFASs

First hints on the widespread occurrence of fluorinated and perfluorinated molecules arose already in the 1960s, when Taves discovered “two forms of fluorine in human serum” by ashing and subsequent potentiometric analysis with a fluoride-selective electrode [55]. Nearly ten years later, Taves *et al.* were able to identify that the organically bound fluorine in human plasma was partially attributed to PFOA [56].

During that time, however, no powerful tool that allowed for sensitive and selective detection of these compounds was available. Gas chromatography coupled to MS (GC-MS), which was already on the market, did not meet these criteria, mostly due to the ionic structure of the majority of PFASs, which disallows volatilization required for GC-MS. This issue was solved only in the 1980s, when the group of John Fenn invented electrospray ionization (ESI) [57,58] technique based on previous work by Dole and co-workers [59].

With the invention and commercialization of these new techniques, sensitive analysis of PFASs was facilitated and soon led to the ubiquitous detection of several PFASs. Concerns began to arise when several PFASs, especially PFOS and PFOA, were not only detected in blood from directly exposed workers in PFAS manufacturing facilities [60], but ubiquitously in human blood around the world [61-63]. Concentrations were usually in the $\mu\text{g L}^{-1}$ range. Half-lives of several months up to years imply that PFAS concentrations in human blood only decline gradually [64,65]. The notorious persistence of PFASs is reflected by rather high concentrations even in remote areas such as the Arctic or Alaska, where they have been detected in polar bears, snow, ocean water and numerous other matrices [66-68]. Despite the phase-out of PFOS, it is still the PFAS occurring at highest concentrations in aquatic biota [68,69].

PFASs have also been detected in the water cycle. Usually, concentrations are in the low ng L^{-1} range, both in WWTP effluent, surface water, ground water, tap water and mineral water [70-

73]. These concentrations can be considered ubiquitous background levels. However, higher concentrations may be caused when point sources are present. In this case, concentrations in the $\mu\text{g L}^{-1}$ range have been detected [74,75], which may become a cause for concern.

When PFASs, especially acidic PFASs, enter mammalian organisms, they are concentrated in the blood circulation, where they are bound to serum proteins, especially albumin [76,77]. This is one of the key differences to legacy organic pollutants such as polychlorinated biphenyls, which are enriched in fatty tissues. This behavior is caused by the lipophobic and hydrophobic nature of PFASs and the ionic character of acidic PFASs.

The most intensively investigated toxic effect of PFASs is their peroxisome proliferator potential, which was already discovered in the 1980's [78-82]. Furthermore, decreased body weight [83,84], developmental effects [85,86], carcinogenicity [87,88] and immune system alterations [89,90], have been described, the latter ones may even occur at environmentally relevant concentrations [91].

As it fulfills the criteria 'persistent, bioaccumulative, toxic' (PBT) with the lowest half maximal effective concentrations (EC_{50}) of PFASs, it was added to Annex B of Stockholm Convention on persistent organic pollutants (POPs) in 2009 [92]. For Germany, mainly regulations for drinking water have been established, where a sum of PFOA and PFOS of $0.3 \mu\text{g L}^{-1}$ is accepted and $0.1 \mu\text{g L}^{-1}$ is considered a target value for the future. Only recently, PFOS was proposed to be added to the list of priority substances within the European Water Framework Directive [93,94].

It was shown in several studies that toxicity and ecotoxicity generally decreases with decreasing perfluoroalkyl chain length. Latała *et al.* found decreasing toxicity to different algae species, including green, blue and red algae [95]. Also toxicity to the bioluminescent bacterium *Vibrio fischeri* decreased significantly with declining perfluoroalkyl chain lengths [96]. The same trend could be demonstrated for saturated and unsaturated fluorotelomer acids [97]. Their toxicity towards the three algal species *Hyalella azteca*, *Chlorella vulgaris* and *Pseudokirchneriella subcapitata* generally decreased with decreasing chain length. None of these studies included perfluorobutanoic acid (PFBA) in the experimental plan. However, it becomes obvious that more attention should be paid on perfluoroalkyl substances with shorter chain lengths, as it is likely that novel fluorinated products will incorporate such short perfluoroalkyl chains. So far, only one study assessed the toxicity of perfluorobutanoic acid (PFBA) to an aquatic organism, i.e. zebrafish (*Danio rerio*) embryos [98]. The observed EC_{50} values and no observed effect concentrations (NOEC) suggest that PFBA is less toxic by at least one order of magnitude as compared with PFOA. Also in this study, PFOS was the most toxic compound among the four PFASs tested (PFOS, perfluorobutane sulfonate (PFBS), PFOA and PFBA).

1.6 Biotransformation of fluorinated compounds

Perfluorinated compounds have been proven to be non-biodegradable under aerobic conditions. In a study under sulfur-limiting conditions, the degradability of PFOS, 1*H*,1*H*,2*H*,2*H*-PFOS (6:2-fluorotelomersulfonate, 6:2-FTS), trifluoromethane sulfonate (TFMS), difluoromethane sulfonate (DFMS) and 2,2,2-trifluoroethane sulfonate (TFES) was investigated with respect to desulfonation and release of inorganic fluoride [99]. 6:2-FTS is used in AFFFs and has been proven to leach into groundwater upon application [100]. It was clearly shown that only those compounds bearing at least one hydrogen atom in α -position to the sulfonate group are desulfonated, namely 6:2-FTS, DFMS and TFES. Defluorination was only observed for 6:2-FTS and TFES. The TPs generated remain unknown. It is worth mentioning that sulfur-limiting conditions are by no means representative of environmental conditions, but if desulfonation under these extreme conditions does not occur, it is unlikely to be possible under environmental conditions.

Recently, the biodegradation of 6:2-FTS was studied in more thoroughly [101]. It was discovered that biotransformation proceeds very slowly and almost 70% of the initial 6:2-FTS concentration was detected after 90 days. The main stable TPs generated were perfluoropentanoic acid (PFPeA) and PFHxA at approximately 1%.

The thermodynamic aspect of defluorination has been assessed very thoroughly by Parsons *et al.* [102] comparing defluorination with other dehalogenation reactions. In conclusion, the implementation of long perfluorinated alkyl chains is very likely to result in a non-biodegradability of the compound, although defluorination is a thermodynamically favored reaction. If biotic transformations occur at all, they will cease in proximity to the perfluorinated moiety in the molecule leaving long-lived highly fluorinated TPs. It is stated that reductive defluorination – similarly to other reductive dehalogenations – is favorable under anaerobic conditions.

A number of highly fluorinated chemicals have been subjected to biodegradation studies. Among these, the group of fluorotelomer-based chemicals has attracted high scientific attention, which can be explained both due to their complex metabolism and their high production amounts. The most prominent fluorotelomer-based chemicals are fluorotelomer alcohols (FTOHs) and fluorotelomer olefins (FTOs), which are mainly used as chemical intermediates in the production of fluorinated polymers.

Biodegradation of FTOHs has been studied in soil, wastewater and mineral media amended with bacteria originating from different environmental compartments. The striking partitioning behavior of FTOHs complicates the understanding of the environmental fate of these compounds in several ways: Firstly, mass balance is difficult to achieve in laboratory experiments and this can only be remedied by working with closed systems, which, in turn, does

not represent environmental conditions. Secondly, owing to the high tendency to be volatilized, diverse atmospheric chemical reactions may occur, which may finally also lead to PFCAs [51-53]. Briefly, atmospheric chemical reactions of FTOHs with radicals do also lead to different PFCAs, thus, these reactions must be taken into account to evaluate the sources of PFCAs. In the following, microbial degradation of 8:2-FTOH is described in detail. The degradation of other FTOHs is likely to be similar, but not much effort has been put on these other chemicals.

In general, biodegradation of 8:2-FTOH is initiated by oxidation of the hydroxyl group to the respective aldehyde (8:2-FTAl) and to the carboxylic acid (8:2-FTA) (see Figure 3). The 8:2-FTA is then transformed to an unsaturated carboxylic acid (8:2-FTUA) by formal cleavage of hydrogen fluoride, representing the first step within the cycle of β -oxidation. Both FTA and FTUA of various chain lengths have been determined in low concentrations in environmental samples [103,104]. It appears that 8:2-FTUA can be further metabolized by several pathways. One gives rise to the 7:3-FTUA and then to the potentially persistent 7:3-FTA, which was first described in the literature by Wang *et al.* [105]. If this step can be confirmed, this would be one of the first reports on microbial defluorination [39]. Also PFHxA is generated via 7:3-FTUA by unknown metabolic pathways. PFHxA may crop up to approximately 4 mol% [42], albeit it was not detected in other studies.

Most importantly, also for environmental regulations, the metabolic conversion of 8:2-FTOH leads to PFOA, which was detected in all degradation studies of 8:2-FTOH performed so far. The elucidation of the metabolic pathway resulting in PFOA is still matter of ongoing research. While initial studies proposed β -oxidation of 8:2-FTA after activation to its CoA-derivative [106], latest studies suggest that 8:2-FTA is transformed to the transient TP 7:2-sFTOH, and finally to PFOA by an unknown pathway [42]. It has to be pointed out, that these studies were carried out under very different conditions (degradation study in defined mineral medium vs. study in soil), so it cannot be excluded that both mechanisms are possible. However, the pathway suggested by Wang *et al.* was corroborated by synthesizing a number of transient TPs and subjecting them to individual degradation tests in order to explicitly conclude the metabolic pathways.

The yield of PFOA ranged from 0.5 % [107] to 25 % [42] and is certainly dependent on the duration of the degradation tests. Later, yet another stable TP derived from 8:2-FTUA degradation, namely 2H-PFOA was discovered [42]. The detailed metabolic reactions have not been identified yet. Analogously to 8:2-FTOH, also 6:2-FTOH degradation has been scrutinized and lead to coherent results [108,109].

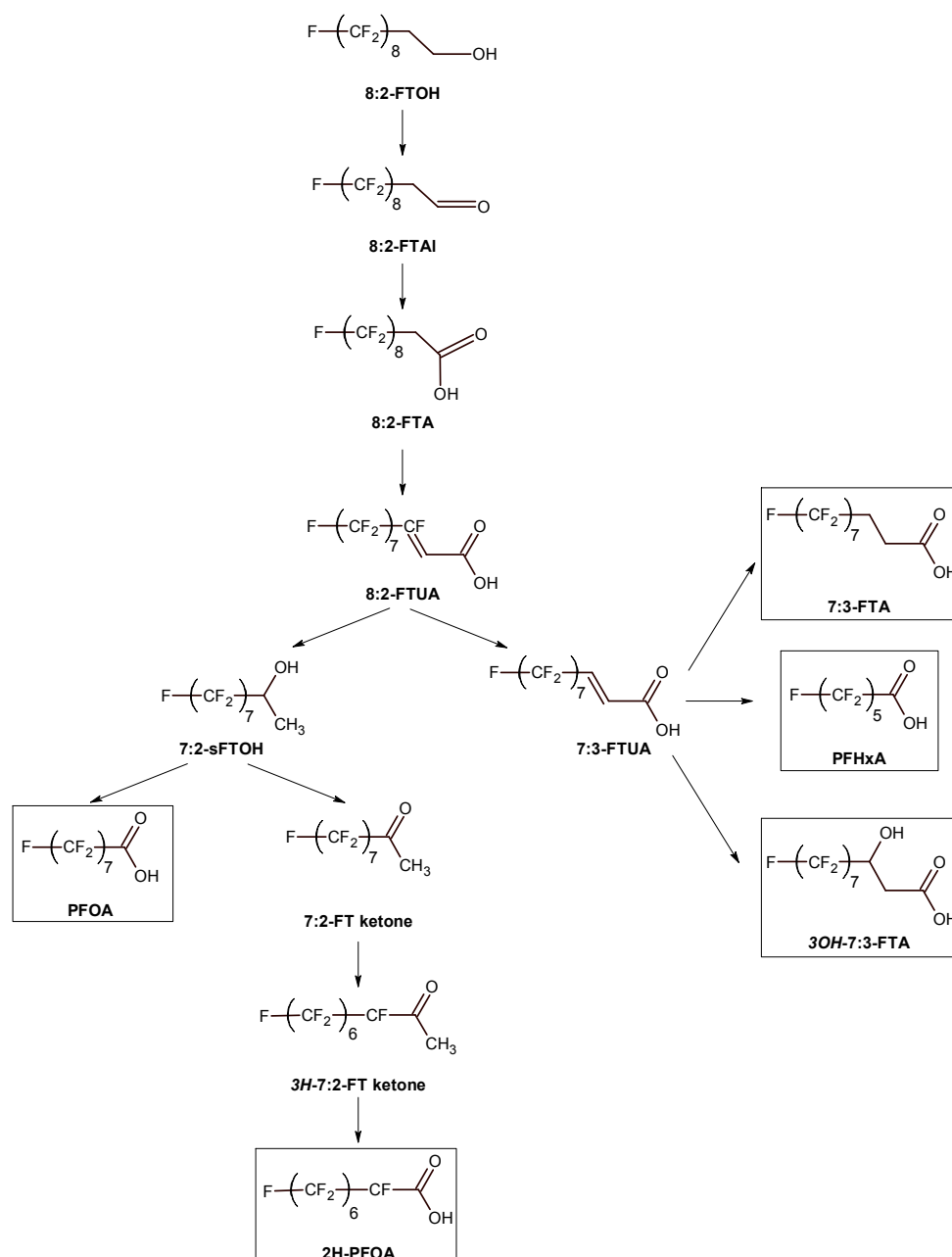


Figure 3: Biotransformation pathways of 8:2-FTOH as studied in soil by Wang *et al.* showing the partial transformation of 8:2-FTOH to PFOA. Figure reprinted with modifications from Ref. [42]. Dead-end TPs are tagged with rectangles.

Fluorotelomer ethoxylates (FTEO) are polyethoxylated fluorotelomer derivatives used mainly as additives in paints and coatings. Their degradation behavior has been briefly analyzed by Schröder, who detected carboxylic intermediates under aerobic conditions [110].

In a comparative study of compounds with low degree of fluorination, ω -substituted alkane-1-sulfonates were tested for biotransformation and mineralization potential [111-113]. The concept behind the study was based on implementation of fluorinated functional groups into inherently degradable alkane-1-sulfonates. These studies were carried out to elucidate which fluorinated functional groups were apt to undergo mineralization to fluoride and other inorganic and non-toxic TPs. It is evident that none of such functional groups can contain long-chained perfluoroalkyl chains.

Once such fluorinated functional groups were found, these should be implemented into newly designed fluorinated surfactants. The application-oriented advantages of PFASs are related to their perfluoroalkyl chain length. Short-chained functional groups cannot reach the peerless properties of long perfluoroalkyl chains. However, implementation of several such functional groups into one molecule is supposed to impart at least comparable properties. The principle design of such a novel fluorinated surfactant is depicted in Figure 4 b). Herein, the fluorinated functional group (green) is covalently bound to a biodegradable spacer (red). Several of these joint moieties are connected to a hydrocarbon backbone (blue). If surfactant properties are required, polar or ionic groups (R) can be attached to the hydrocarbon backbone.

The bond between the degradable spacer and the hydrocarbon backbone can be cleaved hydrolytically or enzymatically, e.g. an ester bond. This would allow for cleavage of the subunits (Figure 4 c), which are biodegraded releasing the fluorinated functional group. In an ideal case, this group is chemically instable or completely biodegradable leaving behind fluoride and other inorganic and non-harmful substances. If this is goal is not accessible, short-chained fluorinated organic TPs with better environmental properties can be tolerated. As outlined in chapter 1.5, toxicity of PFASs often decreases dramatically when the perfluoroalkyl chain is shortened.

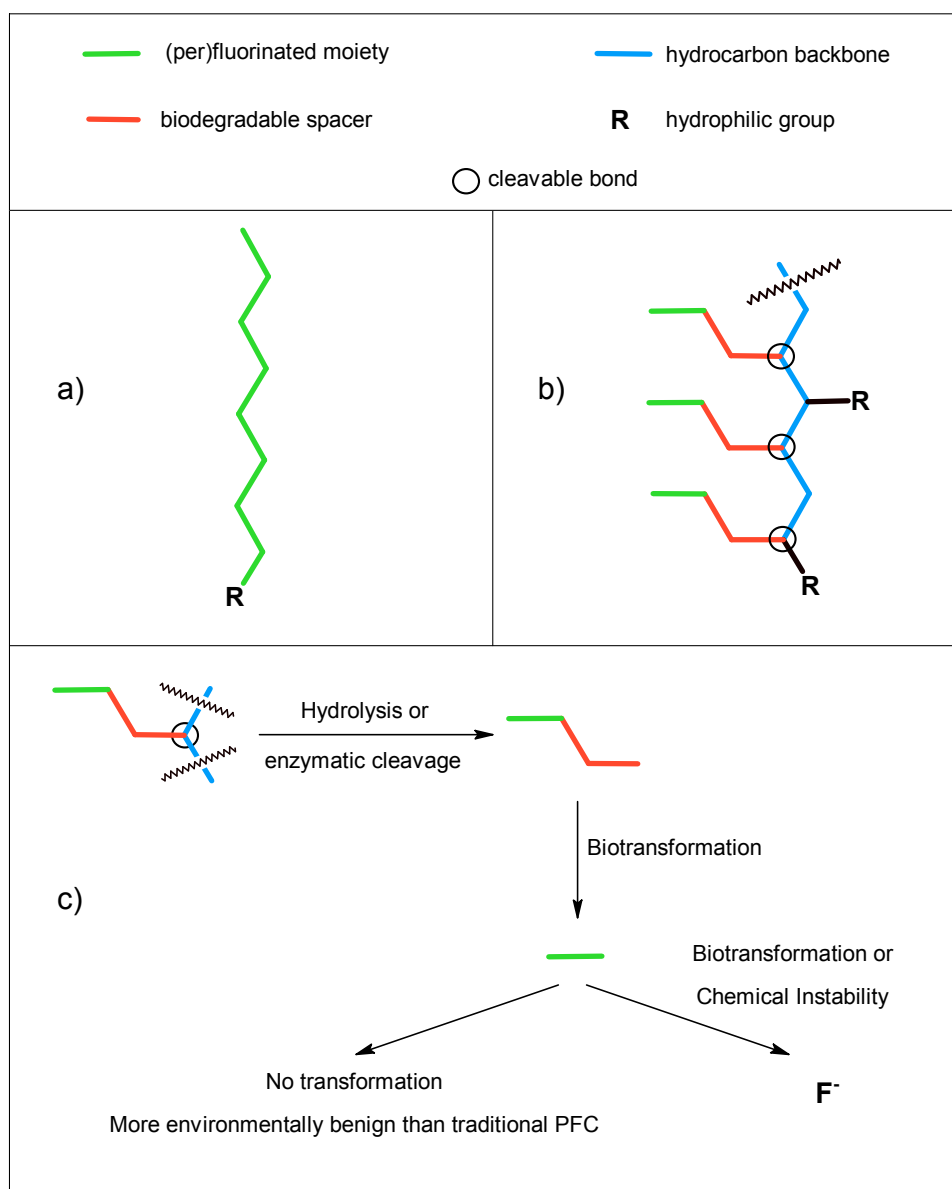


Figure 4: a) Design of traditional long-chained PFASs b) Schematic illustration of a novel PFAS c) Transformation pathway of novel PFASs via multi-step hydrolysis and biotransformation. For detailed explanation please consult text.

One of the functional groups studied was the trifluoromethyl (TFM) group. In this context, biotransformation of 10-(trifluoromethoxy)decane-1-sulfonate was investigated and it was proven that this compound is mineralized to an extent of 90% under aerobic conditions [111].

It was proposed that the biotransformation pathway ending up in inorganic fluoride involves the initial cleavage of the sulfonate group followed by ω -oxidation and stepwise scission of C_2 moieties in terms of β -oxidation results in the formation of trifluoromethanol (TFMeOH) (see Figure 5).

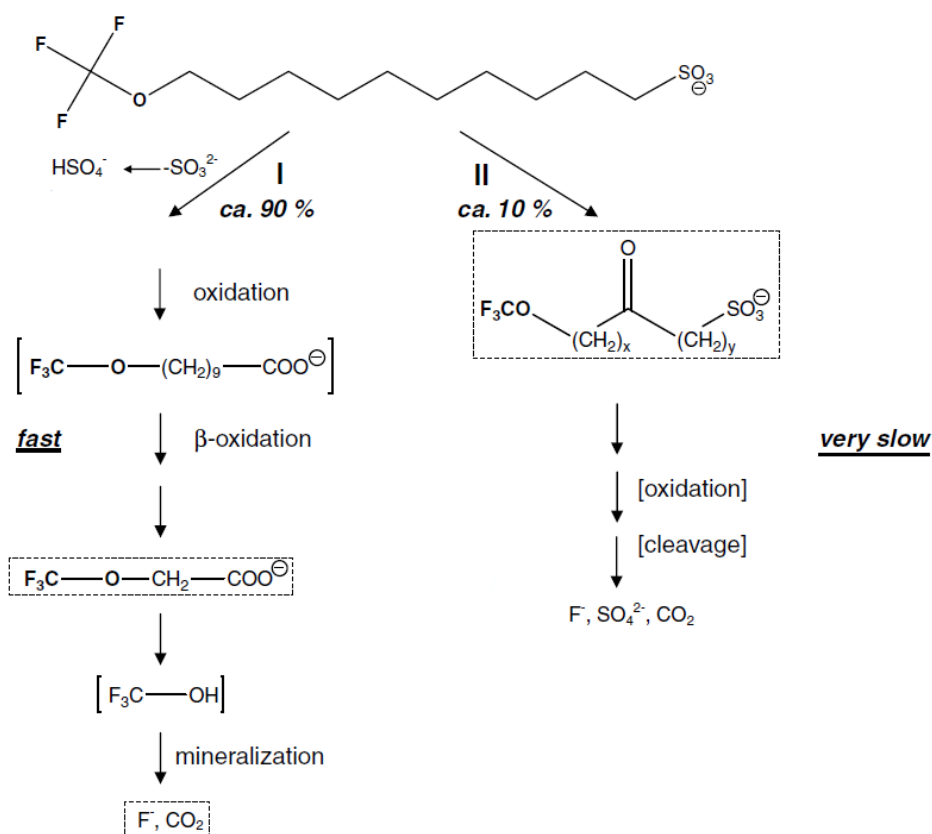


Figure 5: Biotransformation routes of the surfactant candidate 10-(trifluoromethoxy)decane-1-sulfonate. The left-sided pathway accounts for approximately 90% and yields inorganic fluoride. Taken from Ref. [111] with modifications.

TFMeOH is instable in water and reacts to carbonyl difluoride (COF_2) under release of HF [114]. Carbonyl difluoride is also instable in water and finally decays to HF and CO_2 [115]. Due to the results presented above, the TFM group was adjudged an appropriate functional group to be utilized in the development of novel fluorosurfactants.

A question which still remains to be answered is the role of highly fluorinated polymers. These polymers comprise perfluorinated polymers such as poly(tetrafluoroethylene) or perfluoropolyethers, fluorotelomer-based polymers such as acrylates, methacrylates and urethanes [116,117], and N-ethyl-perfluorooctane sulfonamidoethanol (N-EtFOSE) or N-methyl-perfluorooctane sulfonamidoethanol (N-MeFOSE)-based polymers, which are of the acrylate, urethane or adipate type [48].

The number of published work on degradation of polymers is still very scarce due to the complexity of this subject and difficulties involved in the experimental setup, since most polymers are water-insoluble, especially those which contain fluorine. The water-insolubility dramatically affects the time-scale of biodegradation and reproducible results are also difficult to obtain [118].

Russell *et al.* studied the biodegradation of a copolymer being constituted of fluorotelomer acrylate monomers, hydrocarbon acrylate monomers and dichloroethylene monomers [116]. The resulting polymer had a number average molecular weight of 40,000 Da and was incubated in aerobic soil for two years. Formation of PFOA and other 8:2-FTOH related TP's was observed, but it was shown by mass balance that this is the result of degradation of impurities present in the starting material. The perfluorinated alkyl chain might shield the ester group from esterases or other enzymes that might catalyze the decomposition of the ester to the respective FTOH and the remainder [119].

However, in another article describing the biodegradation of an acrylate-linked fluorotelomer-based polymer similar to the one Russell *et al.* investigated, it was shown that biodegradation of this polymer did occur releasing several well-known FTOH TP's [117]. Thereby different half-lives ranging between 870 – 1400 y were calculated. Assuming that biodegradation of such polymers is surface-mediated, the half-life of more finely grained commercial fluorotelomer-based polymers might be as low as 10 – 17 y. Chemical hydrolysis of this polymer type was not observed within a pH-range from 1.2 to 9 [120].

The findings upon polyfluorinated polymers are still contentious [119] and new data to confirm the non-degradability are urgently needed in order to assess the relevance of polymer biodegradation. Similarly to fluorotelomer-based polymers, N-EtFOSE and N-MeFOSE-based polymers might be enzymatically cleaved or hydrolyzed to N-EtFOSE and N-MeFOSE, respectively. The release of these chemicals would then result in PFOS formation. Unfortunately, no studies on biodegradation of such polymers have been published yet.

1.7 Objectives

PFASs exhibit several deleterious effects for humans and the environment which must be regarded and understood in an integral way. Only by interdisciplinary use of chemical analysis including trace analysis, biotransformation studies and mass spectrometric comprehension as well as toxicological assessment is it achievable to assess the environmental relevance of newly introduced chemicals. Therefore, the objectives of this PhD thesis were of versatile nature.

The first objective was to investigate the biotransformation behavior of a fluorotelomer-based compound, namely FTEO. Other fluorotelomer based compounds had been shown to exhibit complex biotransformation routes including partial defluorination. The detailed biotransformation route should be enlightened via HPLC-ESI-MS methods, which allows for simultaneous assessment of degradability for structurally similar compounds, such as commercial FTEO mixtures. Before biotransformation can be carried out, such a mixture must be characterized as to the degree of ethoxylation and the perfluoroalkyl chain length.

The significance of biotransformation products detected in the laboratory experiment should be determined by monitoring them in environmental samples. To allow for correct quantification, these TPs should be synthesized and characterized by hybrid triple quadrupole/linear ion trap (QqQ_{LIT}) MS and high-resolution MS as well as NMR spectroscopy. Traditional PFASs, such as PFOA and PFOS should also be included in the monitoring campaign so that a current picture of the PFAS concentrations in German WWTPs and surface waters is assessed.

Fluorinated surfactants with a shorter perfluoroalkyl chain may substitute long-chained PFASs in several applications, where the unparalleled chemical stability is not required. Fluorinated building blocks which could be released from the fluorinated surfactants by hydrolysis, should be investigated with respect to their potential to be mineralized. If no mineralization occurs, stable TPs should be identified by hyphenated MS techniques and their toxicity towards aqueous organisms be determined.

If possible, it should be aimed at conceiving chemical structural requirements that allow for complete mineralization. This would enable chemists to design new biodegradable fluorinated compounds and thus diminish the burden of environmental compartments in the future. Generalizable structural demands can be considered too ambitious due to the complexity of enzymatic reactions when compounds with different functional groups are regarded. Thus it was focused on specific functional groups, such as the TFM group.

Since numerous fluorinated substances were measured during this thesis by ESI-MS and collision-induced dissociation (CID) techniques, the rather scarce common knowledge on the fragmentation pathways should be extended. Different state-of-the-art mass spectrometric techniques should be used for this purpose including multi-stage MS and high-resolution MS. The knowledge obtained is not only of significance from a mass spectrometric point of view, but can deliver valuable information for environmental analytics. The newly gained knowledge can be applied during detection and identification of new environmental fluorinated pollutants. Whereas identification could be performed by comparing the fragmentation of compounds with the spectra presented in this thesis, detection could be possible, if substance-class specific fragmentation patterns are discovered, which could then be exploited by scan modes such as neutral loss scans or precursor ion scans on QqQ instruments.

2 Theory

2.1 Liquid chromatography

Chromatography describes a physico-chemical process, where a mixture of compounds is separated between a mobile and a stationary phase due to adsorption, partitioning or other physico-chemical effects. In combination with mass spectrometric methods, HPLC is usually carried out under reversed-phase (RP) conditions implying higher polarity of the mobile phase (eluent) as compared with the stationary phase. The principles behind chromatography and HPLC are considered familiar and hence, will not be explained in more detail [121].

Although modern MS, especially tandem mass spectrometers (MS/MS), achieve an unprecedented selectivity, chromatography may become crucial when working with complex matrices. Such matrices often have to be dealt with when performing biotransformation studies or trace analysis in contaminated matrices. Today, the separation step via HPLC when combined with MS/MS fulfills two major tasks: The most important is separation of analytes from highly concentrated matrix components, which can cause ion suppression during ESI [122-124]. The second task is separation of isomeric and thus isobaric components (although isobaric showing very different fragmentation patterns do not pose a significant problem). Especially structural isomers cannot be separated by MS only and in these cases, only chromatography or other separation techniques can help distinguish and resolve such structurally similar compounds.

Although some applications are still based on gas chromatography (GC) – MS (e.g. analysis of FTOHs by GC-chemical ionization (CI) – MS) most analyses for PFASs are performed using HPLC. The typical PFASs such as PFCAs and PFSAAs are non-volatile and therefore not suited for GC analysis without hazardous and time-consuming derivatization. Chromatographic separations of PFASs are routinely carried out by HPLC and exclusively under reversed-phase (RP) conditions [125]. Thus, PFASs are retained chiefly by their perfluorocarbon chain length, but of course, functional groups attached to that moiety also influence the chromatographic behavior. Improved chromatographic selectivity compared with common C₁₈ or C₈ phases can be achieved by special phases such as pentafluorophenyl (PFP) [126] or perfluorinated C₈ phases [42,110], which both provide better selectivity for highly fluorinated substances and, in the latter case, circumvented false-positive results as compared with RP-C₁₈ phases.

2.2 Mass Spectrometry

2.2.1 Application of mass spectrometry and definitions

Mass spectrometers represent instruments, which are capable of determining the mass-to-charge ratio (m/z) of charged particles [127]. As a result, they can be used in various applications and for numerous issues. They can be used either as a stand-alone instrument or coupled to other instruments, usually separation techniques such as chromatography or capillary electrophoresis.

Every MS consists of three main parts: an ion source, a mass analyzer and a detector. The ion source allows for ionization of neutral molecules and/or transfer of ions into the gas phase. The latter step is required since ions can only be separated by their m/z ratio if high vacuum conditions persist, which is the case in the mass analyzer. Detection of ions can be carried out spatially separated from the mass analyzer (e.g. with quadrupole instruments) or within the mass analyzer (e.g. with Fourier-transform ion cyclotron resonance MS).

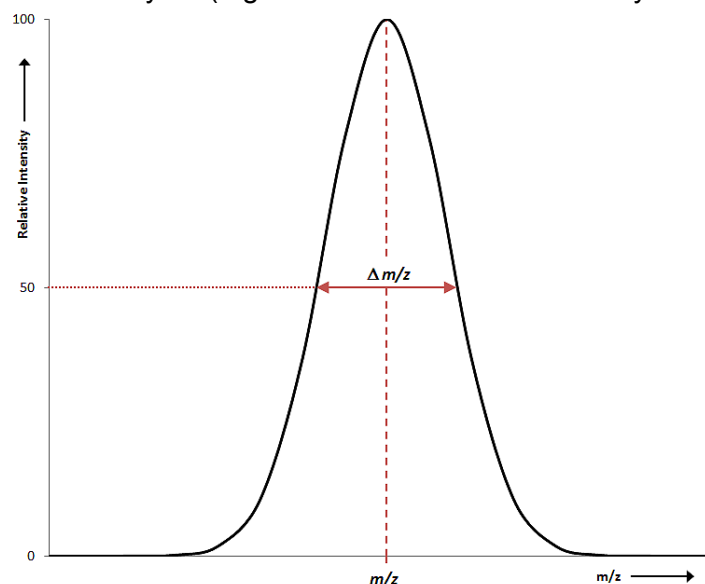


Figure 6: Definition of mass resolving power by the FWHM method

When quadrupole instrumentation is used, detection of the ions is carried out by electron multipliers, usually continuous electron multipliers with a horn-shaped design. These devices generate an electronic signal which is proportional to the impacts per time interval – at least this is true for a given dynamic range. Since understanding of the processes does not contribute significantly to the understanding of this thesis, it will not be discussed more thoroughly.

Depending on the setup used, different tasks may be solved by application of MS. When investigating unknown compounds, they can provide the nominal mass or the exact mass of an unknown compound or – if fragmentation is provoked – provide valuable information about the structure of the compound.

When coupled to other techniques, mass spectrometers serve as ultra-sensitive detectors, e.g. for environmental samples. They can exhibit unprecedented selectivity for target compounds and thus allow for analysis of trace compounds even in very complex matrices.

Two main characteristics of mass analyzers are the resolving power (often interchangeably used with the term “resolution”) and mass accuracy. Resolving power is defined as the quotient

of the measured mass and the peak width, often expressed as full width at half height (FWHH), as depicted in Figure 6.

Mass accuracy is expressed by the error of mass measurement

$$error\ (ppm) = \frac{m/z_{measured} - m/z_{theoretical}}{m/z_{theoretical}} \cdot 10^6$$

and is usually calculated in parts per million (ppm). Although not inherently linked to each other, high resolving power generally also implies high mass accuracy.

An important characteristic of a MS is the so-called duty cycle. It can be expressed as the percentage ratio of target ions that enter the MS and target ions which are effectively detected. The duty cycle plays a significant role as far as MS sensitivity is concerned.

2.2.2 Ion sources

When coupled to HPLC, the ion source has to fulfill several purposes. Besides the previously mentioned ionization and transfer of analytes into the gas phase, evaporation of the mobile phase is crucial to maintain vacuum in the mass analyzer. Ion sources compatible to HPLC are named atmospheric pressure ionization (API) methods since the ion source region is normally not under vacuum.

The most important API technique today is ESI, which allows for ionization and transfer into the gas phase of polar or ionic compounds and macromolecules up to molecular weights beyond 100 kDa. ESI-MS after LC has been routinely used ever since its commercialization [128].

The ESI technique was invented by the group of John Fenn [57,58] based on previous work by Dole and co-workers [59]. ESI can be operated in positive or negative polarity and produces protonated molecules, deprotonated molecules or adduct ions (with Na⁺, K⁺, NH₄⁺, Cl⁻, acetate, solvent clusters, etc.) by spraying a solution through an electrically charged capillary (see Figure 7). The droplets formed contain a net charge and are accelerated towards a counter-electrode. Their size diminishes by evaporation, which may be thermally assisted. When a certain charge density is reached (the so-called Rayleigh limit), the droplets disintegrate by coulombic repulsion releasing smaller droplets. This process is referred to as “Coulomb explosion”. Formation of the free ions is explained by two different models: the “ion evaporation model” (IEM) by Iribarne and Thomson [129,130] and the “charge residue model” (CRM) as proposed by Dole *et al.* [59]. Briefly, IEM suggests that ions are emitted from highly charged droplets into the gas phase, whereas with CRM, ions are generated by repeated and complete evaporation of solvent resulting in free ions in the gas phase.

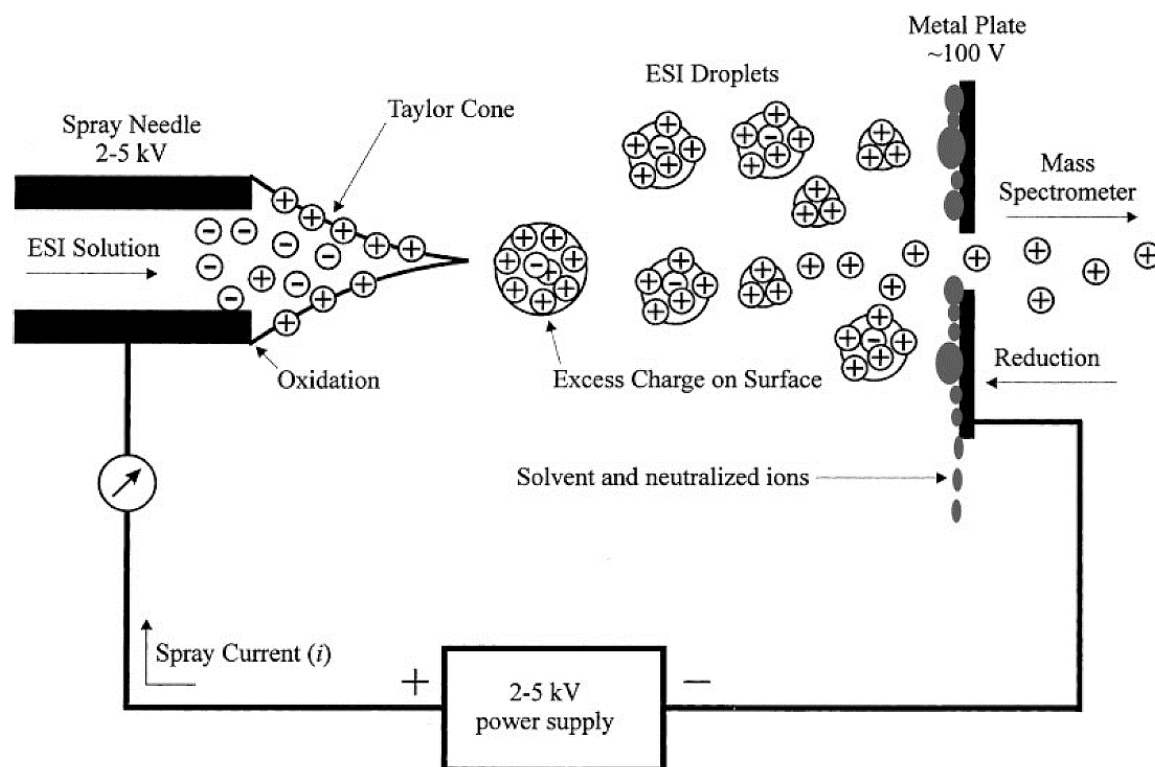
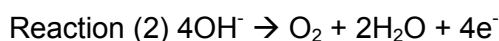


Figure 7: Basic setup and functionality of an ESI ion source and the ESI process; Reprinted from Ref. [131]

While IEM holds for small inorganic ions, ionization of macromolecules such as proteins seems to be better explained by CRM process. It is interesting that the ions observed in the gas phase, that is, those detected by the mass spectrometer, are not necessarily the same as those in solution [132]. This is only true for very stable ions, such as sodium ions. In the case of PFASs, transfer from the liquid to the gas phase possibly only occurs for anions of very strong acids, such as PFSA, but possibly not for PFCA and related compounds, which may have higher pK_a values (although discussed very controversially, see [133-135]). This may seem odd, but is a direct consequence of the differences between liquid-phase and gas-phase acidity and basicity, respectively. The specific mechanism of PFAS ionization has not been investigated in detail.

The ESI source represents a special form of an electrolytic cell [136]. In positive ESI polarity, the capillary is an anode, where oxidation occurs. Depending on the material of the capillary and the ions and solvents used, different reactions may occur, for example:



In Reaction (1), metal atoms (M) from the surface of the capillary are oxidized leaving behind metal ions and electrons. In Reaction (2), hydroxide ions present in the solvent are oxidized to molecular oxygen, water and electrons. Both reactions result in an excess charge, in this case cations. The electric circuit is closed by reduction of cations on the counter electrode. Some excellent reviews on the fundamentals of ESI have been published [131,132,137,138].

Other API techniques, such as atmospheric pressure photoionization (APPI) and atmospheric pressure chemical ionization (APCI) have been marginally applied. Although providing advantages over ESI, such as reduced matrix effects, APCI has been rarely applied for PFAS analysis. Analytes measured with APCI comprise various ethoxylated PFASs [110,139] and PFOA [140]. However, no investigations with respect to matrix effects were made in these papers.

2.2.3 Mass analyzers

The mass analyzer represents the heart of every MS. Its task is to separate a bulk of ions by their m/z ratio. This effect can be achieved by electronic or magnetic fields.

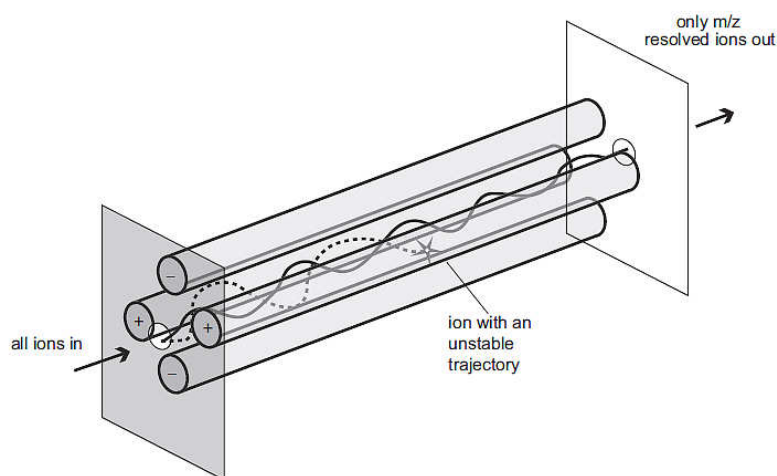


Figure 8: Simplified scheme of a quadrupole mass analyzer showing the trajectories of an ion with resonant m/z (passing the quadrupole) and a non-resonant ion (colliding with one of the quadrupole rods). Reprinted from Ref. [141]

The simplest and cheapest mass analyzer is a quadrupole, which consists of four metal rods, which are equidistantly spread around a central axis (see Figure 8). A positive direct current is applied to two opposing rods and a negative direct current to the remaining two rods. An alternating current, which is shifted by 180° between the two rod pairs, is added onto the direct current. Thus, the voltage can be expressed as

$$U_+(t) = +(U + V \cdot \sin(\omega t))$$

and

$$U_-(t) = -(U + V \cdot \sin(\omega t))$$

where $U_+(t)$ and $U_-(t)$ are the resulting voltages at the positively and negatively charged rods in function of the time, respectively. U represents the direct current, V is the amplitude of the alternating current and ω is its angular frequency.

A qualitative approach to the functionality of a quadrupole can be made as follows: Regarding positive ions and the rods with positive direct current, ions below a critical m/z ratio respond quickly to the alternating current and are distracted towards the rods when the rods temporarily change their polarity due to the high-frequency alternating current. Heavy ions however respond slowly and are not distracted. These rods with positive direct current represent a high-pass filter for cations.

The inverse behavior is true for rods with negative current. Ions with an m/z above a critical value are attracted by the rods because they respond slowly when the alternating current temporarily renders the rods positive for a brief moment. Light ions however are able to alter their trajectory away from the rods and thus do not collide with them. This means that rods with a negative direct current work as a low-pass filter for cations.

The two rod pairs can be regarded as a combination of a high-pass filter and a low-pass filter creating a band-pass filter of a certain band width. This band width represents the resolution of a quadrupole and is governed by the ratio of the direct current U and the alternating current V . The m/z position of the band-pass filter is adjusted by the magnitude of U and V and it represents the m/z ratio of an ion with a stable trajectory through the whole quadrupole, i.e. of an ion which can pass the quadrupole. Thus, a mass range may be scanned for by ramping of the voltages U and V while maintaining a constant U/V ratio [142]. A quantitative approach to describe a quadrupole can be made with the help of Mathieu's equation which results in stability diagrams of ions. Since this does not significantly contribute to the present thesis, it will not be explained in detail.

Quadrupole mass analyzers usually achieve mass resolving powers of approximately 1000 and can only determine the nominal m/z ratio of the ions because mass accuracy is usually in the range of 0.1 Da. Due to their robustness and low price, they are the most commonly used mass analyzers [143].

Quadrupoles can be operated in three modes: Single ion monitoring (SIM), scan and radio-frequency only (RF only). In SIM mode, the voltages remain at one distinct value so that only ions of one certain m/z ratio can pass. This implies a duty cycle of (nearly) 100%, since the target analytes are measured incessantly. However, also the temporally shifted alternating measurement of several distinct m/z values is referred to as SIM. In scan mode, voltages are varied constantly so that a range of m/z values can be measured allowing to record mass spectra. Since at any one time, only ions of one m/z ratio can pass the quadrupole and be detected, this implies much lower duty cycles in scan mode as compared with SIM mode. In fact, if only a small m/z range of 100 is scanned for, the duty cycle drops to 1% and inevitably causes lower sensitivity. On the downside, SIM can only be utilized only for target analysis.

Finally, in RF only mode, all ions can pass the quadrupole regardless of their m/z ratio, which plays an important role for ion optics and for multi-stage MS collision cells.

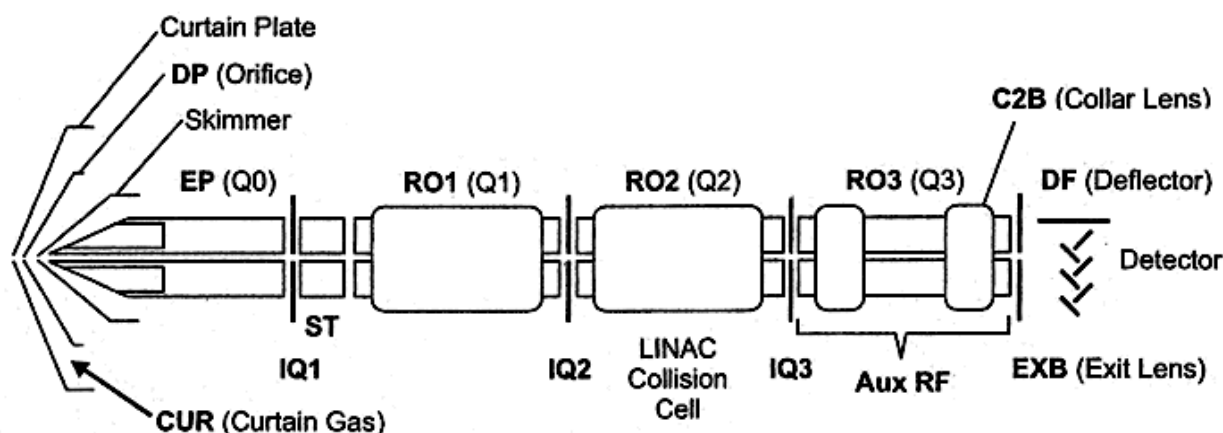


Figure 9: Setup of the Applied Biosystems 3200 Q Trap[®]; Reprinted from Ref. [144]

Single quadrupole MS instruments have been largely replaced with triple quadrupole instruments (QqQ) today, at least that is true for HPLC-MS. QqQ instruments consist of two quadrupoles (Q1 and Q3), which can be used for mass analysis, separated by a collision cell, which is basically a quadrupole (or hexa/octapole) that can be filled with an inert gas such as nitrogen or argon (see Figure 9). Q2 is always maintained in RF-only mode offering no m/z separation. By acceleration of the ions that pass the first quadrupole (so-called precursor ions), collision of these ions with the inert gas molecules or atoms can result in the formation of characteristic fragments, called product ions, which are then analyzed in the third quadrupole. This process is referred to as CID and represents the most frequently applied technique to provoke fragmentation in instruments applying API.

QqQ instruments are routinely used for trace analysis, since they are both very sensitive and selective due to multiple stage mass separation.

Recent advances include exchange of Q3 by a linear ion trap (LIT) [145].

An LIT can be described as a quadrupole to which an entrance lens and an exit lens are added. Direct current can be applied to these lenses generating an electrostatic field, which retains the ions within the trap. During the fill

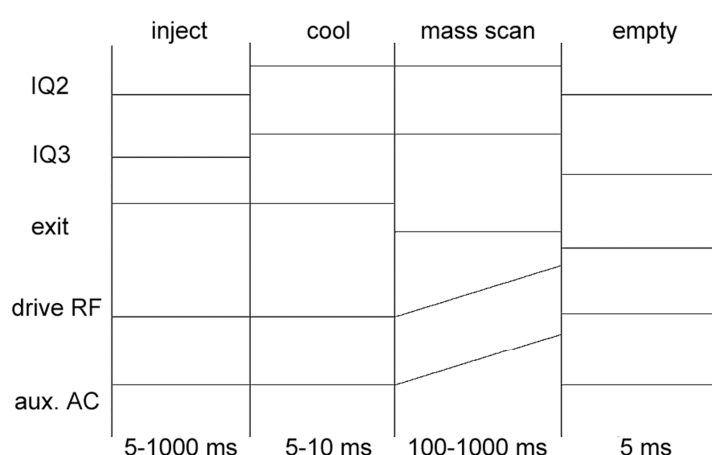


Figure 10: Schematic illustration of one LIT scan cycle; RF = radio frequency, AC = alternating current. Reprinted with modification from Ref. [145]. Compare with Figure 9.

time of a cycle (see Figure 10), the entrance lens IQ3 is open, and the exit lens EXB is closed. Afterwards, a potential is applied to the entrance lens, and the ions are allowed to cool, i.e. to decelerate, for a short time. The actual m/z separation is achieved by ramping the so-called ‘drive radio frequency’ and an auxiliary alternating current that is applied to the quadrupole rods in a quadrupolar fashion, while maintaining a direct current at the exit lens, which is of lower amplitude than during trapping. The radio frequency specifically excites ions of a certain m/z ratio and thus accelerates them axially allowing them to overcome the potential barrier of the exit lens, which finally makes them reach the detector.

In contrast to quadrupole scan mode, ions are trapped and ejected sequentially during a mass scan. Therefore, the duty cycle of LITs is much higher compared with quadrupole scans, where most of the ions are discharged and do not reach the detector. The duty cycle of a LIT can be estimated by the ratio of ion trap fill time and total cycle time and can be even increased by application of Q0 trapping during the mass scan.

The MS used for most of the analyses carried out in this study was an Applied Biosystems 3200 Q Trap MS (see Figure 9), which is a hybrid triple quadrupole/linear ion trap MS (QqQ_{LIT}). These instruments can also be used in “normal” quadrupole mode, offering the very same modes as QqQ instruments, but they may alternatively be operated in so-called ‘enhanced modes’ utilizing the Q3 as an LIT allowing for higher sensitivity, higher mass resolving power and MS³ scans. The mass-resolving power can be improved by slower mass scan rates. Although LITs cannot be considered high-resolution MS, they can easily outperform conventional quadrupole in terms mass-resolving power, reaching values of several thousands [145].

The versatility of these instruments is illustrated in Table 1, where the modes used in this study are summarized. The applications range from detection of unknowns (Q1MS, EMS, neutral loss scan, precursor scan) to sensitive target analysis (multiple-reaction monitoring, MRM) and structural elucidation by CID (product ion scan, enhanced product ion scan, MS³).

Table 1: Selected modes, which the Applied Biosystems 3200 Q Trap can be operated with. Please note that the names are adopted from Applied Biosystems software Analyst®

Mode	Q1	q2 Collision Gas	Q3	Exemplary Application
Q1MS	Scan	off	RF only	Complete Mass Spectrum
Q1MI	SIM	off	RF only	Analysis of compounds showing no fragmentation
Enhanced MS	RF only	off	LIT	Complete Mass Spectrum Higher sensitivity
MRM	SIM	on	SIM	Trace analysis / Analysis in complex matrices
Product Ion Scan	SIM	on	Scan	Structural elucidation / Investigation of fragmentation patterns
Enhanced Product Ion Scan	SIM	on	LIT	Structural elucidation / Investigation of fragmentation patterns
Precursor Ion Scan	SIM	on	Scan	Detection of unknown compounds
Neutral Loss Scan	Scan	on	Scan ^a	Detection of unknown compounds
MS ³	SIM	on	LIT/eject/excite/LIT	Structural elucidation / Investigation of fragmentation patterns

^a Fixed m/z difference between Q1 and Q3

Besides low-resolution MS, other analyzers are frequently used nowadays which achieve very high resolution and much higher mass accuracy. Among these, orbitrap MS has gained growing attention since its commercialization in 2005. An orbitrap consists of an outer electrode which is split in half by a ceramic ring and an inner spindle-like electrode [146]. The orbitrap is based on a rather ancient design called a Kingdon trap [147], which was further optimized by Knight *et al.* [148]. However, none of their instruments was able to determine m/z ratios, instead they used the devices for ion storage purposes.

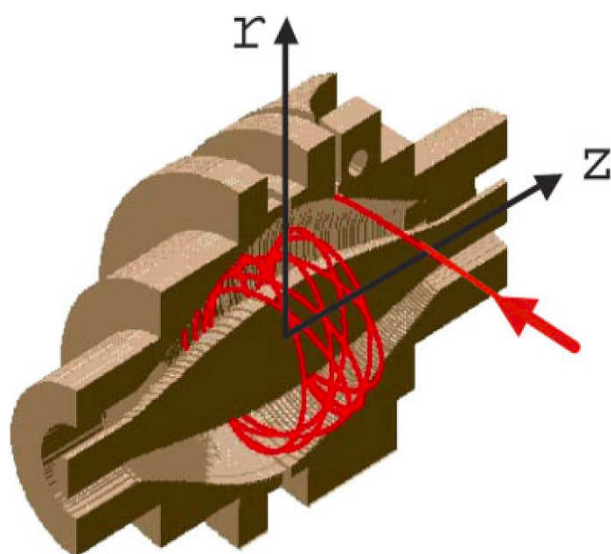


Figure 11: Schematic illustration of an orbitrap mass analyzer. Please notice that the frequency of oscillation along the z-axis is measured for m/z determination. Reprinted from Ref. [149].

In contrast to ion cyclotron resonance MS, which exhibits similar characteristics in terms of mass-resolving power and mass accuracy, no strong magnetic fields are required for orbitrap MS, which leads to less expensive maintenance of the instrument. Orbitrap MS exclusively makes use of electrostatic fields around the inner electrode. Ions are transferred into the orbitrap orthogonally to the z-axis (see Figure 11), and circulate around the inner electrode at a frequency, which is independent of their m/z ratio. However, ions also move back and forth along the z-axis.

The frequency of motion along the z-axis is given by the formula

$$\omega_z = \sqrt{k \cdot \frac{q}{m}}$$

where q is the charge, m is the mass and k is the field curvature, which is a constant for any orbitrap. It becomes obvious that the frequency of motion is inversely proportional to the square root of m/z .

In order to measure the frequency of motion and thus to determine the m/z ratio of the ions, an image current is recorded between the two halves of the outer electrode, which is amplified by differential amplification. Ions of one distinct m/z ratio produce a sine wave current. When ions of different m/z ratios are present, each of the ions will generate its own sine wave current, which in turn requires Fourier transformation of the data in order to calculate the independent m/z ratios. Orbitrap MS usually achieves mass-resolving powers of greater than 10^5 and mass accuracies of < 2 ppm when internal mass standards are used [149].

The high mass-resolving power and mass accuracy has rendered orbitrap MS widespread in analytical laboratories. Its main application fields are in the bioanalytics, especially proteomics, but also in other analytical sectors which deal with the detection and characterization of unknown compounds [150]. Use of orbitrap MS for analysis of PFAS has been restricted to the confirmation of novel TPs [109].

2.3 CID fragmentation of aliphatic fluorinated compounds

Most up to date MS/MS instruments make use of CID, sometimes referred to as collision(ally)-activated dissociation (CAD), to form product ions of the species investigated. This process utilizes inert gas, mostly nitrogen or argon, to provoke collisions with accelerated ions that will lead to characteristic product ions. Unlike fragmentation after electron impact (EI), CID generally produces even-electron product ions, i.e. ions with no unpaired electrons. This implies that neutral, non-radical species are generally cleaved off the precursor ions, often small organic or inorganic compounds, such as CO₂, HF, or H₂O. An informative review on the detailed processes during CID has been published by Levsen and Schwarz [151].

MS fragmentation of organic compounds is greatly influenced by the technique used. Fragmentation reactions occurring after EI are largely known and often follow distinct rules, such as α -cleavage or McLafferty rearrangement [152], which also hold for fragmentation of PFASs. For CID, such general pathways do not exist and fragmentation differs largely from what has been known for EI fragmentation. Attempts have been made to study characteristic product ions or losses from organic compound classes [153], but these generalized pathways do not hold for every compound. The different fragmentation routes are a logical consequence of the different ion species produced: EI-MS initially leads to high-energy radical cations, whereas the ESI process – which is the most common ionization technique prior to CID – leads to protonated or deprotonated molecules. When performing CID fragmentation with fluorinated compounds, unfortunately, there is no common fragmentation pathway that is significant for fluorine. Furthermore, odd reactions may occur in the presence of fluorine, which will be subject of this section. Due to the unique properties of fluorine, fragmentation pathways of fluorinated molecules may differ largely from their non-fluorinated counterparts.

Fragmentation of classic PFASs, such as PFOS and PFOA has been studied very thoroughly [126,154]. PFASs are mainly known to produce sulfur-containing ions, such as SO₃⁻ (m/z 80) and FSO₃⁻ (m/z 99). However, this is only one part of the story. Technical mixtures of PFOS contain a number of positional isomers and the formation of the FSO₃⁻ ion is by far less abundant for these isomers as compared with non-branched PFOS [126]. Besides the two sulfur-containing ions, product ions of linear PFOS comprise – albeit to a low extent – perfluoroalkyl carbanions C_mF_{2m+1}⁻ (the so-called ‘9-series’, since the m/z values end with ‘9’) as well as C_nF_{2n}SO₃⁻ radical anions (the so-called ‘0-series’) [126,155]. The latter ones are suspected to be generated by initial radical cleavage of a C-C-bond within the perfluoroalkyl chain and subsequent losses of tetrafluoroethene. The perfluoroalkyl carbanions are supposed to derive from initial loss of SO₃ and subsequent loss of perfluoroalkenes such as tetrafluoroethene, hexafluoropropene, and so forth [155]. Interestingly, Langlois and Oehme

found that the substitution site of trifluoromethyl-branched PFOS can be determined because of one missing '0-series'-ion in the spectrum, depending on the branching site [126].

Perfluorocarboxylate fragmentation is generally initiated by loss of CO_2 , leading to a perfluoroalkyl carbanion $\text{C}_m\text{F}_{2m+1}^-$, which is normally only encountered with aromatic carboxylic acids, but not often with aliphatic carboxylates [153]. This can be explained by stabilization of the negative charge by the proximity of the perfluoroalkyl chain or similar groups in terms of negative inductive effects.

Further fragmentation of perfluoroalkyl carbanions was studied very thoroughly by Arsenault *et al.* [154], who found that the initial formation of the respective $\text{C}_m\text{F}_{2m+1}^-$ ion is followed by fluorine atom migration and thus charge migration throughout the whole linear perfluoroalkyl chain. They rationalize this hypothesis by stating that the charge shift produces more stabilized secondary carbanions in contrast to the primary carbanions initially generated. Further fragmentation of these ions occurs by cleavage of different perfluoroalkenes. Similar fragmentation patterns are observed for fluorotelomer acid derivatives, which also include loss of CO_2 , and HF.

Interestingly, if only one hydrogen atom is present in a perfluorinated alkyl chain, the fragmentation pathway may be altered substantially in contrast to the perfluorinated molecule. Under those circumstances, loss of hydrogen fluoride is often observed. A reason for this may be the energetically favored loss of HF in comparison to, for instance, loss of F_2 , whose difference is energetically favored by $110 \text{ kcal mol}^{-1}$ compared with F_2 [155]. Compounds falling under this category are 6:2-fluorotelomer sulfonates (6:2-FTS) [100] and 2H-PFOS [155]. Analogous to PFOS fragmentation, 6:2-FTS delivers SO_3^- (m/z 80) and HSO_3^- (m/z 81) as product ions.

FTOHs may fragment by multiple loss of HF. However, FTOHs are very delicate species with respect to their ESI-MS performance. If only traces of organic anions, such as formiate or acetate are present, FTOHs will form adducts such as $[\text{M} + \text{formiate}]^-$ or $[\text{M} + \text{acetate}]^-$. Under exclusion of acetate or formiate salts, the deprotonated molecule is formed [156]. It was discovered that methanol (MeOH) favors its formation, whereas ACN inhibits it [157]. Additionally, addition of basic compounds such as ethanolamine can promote formation of the $[\text{M} - \text{H}]^-$ species [158]. Interestingly, it was discovered with the help of deuterated standards that the proton in vicinity to the perfluoroalkyl chain is cleaved off, not the hydroxyl proton, as one might expect. This again underlines the strong negative inductive effect of perfluoroalkyl groups. Upon deprotonation, FTOHs suffer loss of all hydrogen atoms, although being separated by several bonds. A characteristic ion of fluorotelomer-derived compounds seems to be the ion at m/z $x55$, where $x = 3$ for 8:2-fluorotelomer derivatives and $x = 4$ for 10:2-fluorotelomer derivatives and so forth. This ion was observed for fluorotelomer alcohols [156].

3 Results and discussion

3.1 Characterization of a commercial fluorotelomer ethoxylate mixture

3.1.1 ESI-MS

Technical surfactants are often composed of chemical mixtures of structurally similar compounds. The reason for this is chemical synthesis, which may not only lead to one structurally defined chemical or because natural educts are used, e.g. fatty acids, which naturally occur as mixtures and it would be time- and cost-intensive to purify them. Eventually, these surfactants are optimized for performance regardless of the actual chemical structure of the compounds.

The first task to be solved when examining biotransformation is to elucidate the chemical structure of the product under investigation. The biotransformation experiment was carried out with a commercial mixture named 'Zonyl FSH'. Based on the information given by the manufacturer, the active ingredient are fluorinated compounds with the general structure as presented in Figure 12, thus a nonionic structure, and the molecular weight is stated to be 650 Da. The fraction of active ingredient is 50%, the remainder being water and dipropylene glycol methyl ether at equal shares [159].

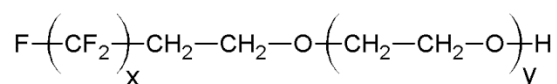


Figure 12: Structure and acronymization of FTEOs. The respective congeners will be acronymized x:2-FTEO_y

The active ingredient with the chemical formula is a derivative of FTOHs, which is probably reacted with ethylene oxide to form polyethoxylated FTOH. Following previous terminology of non-ionic surfactants like nonylphenol ethoxylates, these compounds will be termed fluorotelomer ethoxylates (FTEOs). The acronyms are based on FTOH acronyms, as presented in Figure 12. The x represents the number of perfluorinated carbon atoms, '2' signifies the two methylene groups and the 'y' indicates the degree of ethoxylation of the respective FTOH. Please notice that also FTOHs already contain one ethoxy group. Thus, FTOH would be FTEO₀.

The components of the Zonyl FSH mixture were studied in detail by measurements with ESI-MS. An ESI-MS full scan spectrum in positive mode is shown in Figure 13. This spectrum was recorded after dissolving Zonyl FSH in a mixture of H₂O and MeOH. Since FTEOs do not contain any highly acidic or basic functional groups, such as sulfonic acid groups or amino functions, adduct formation is the dominating type of ionization here.

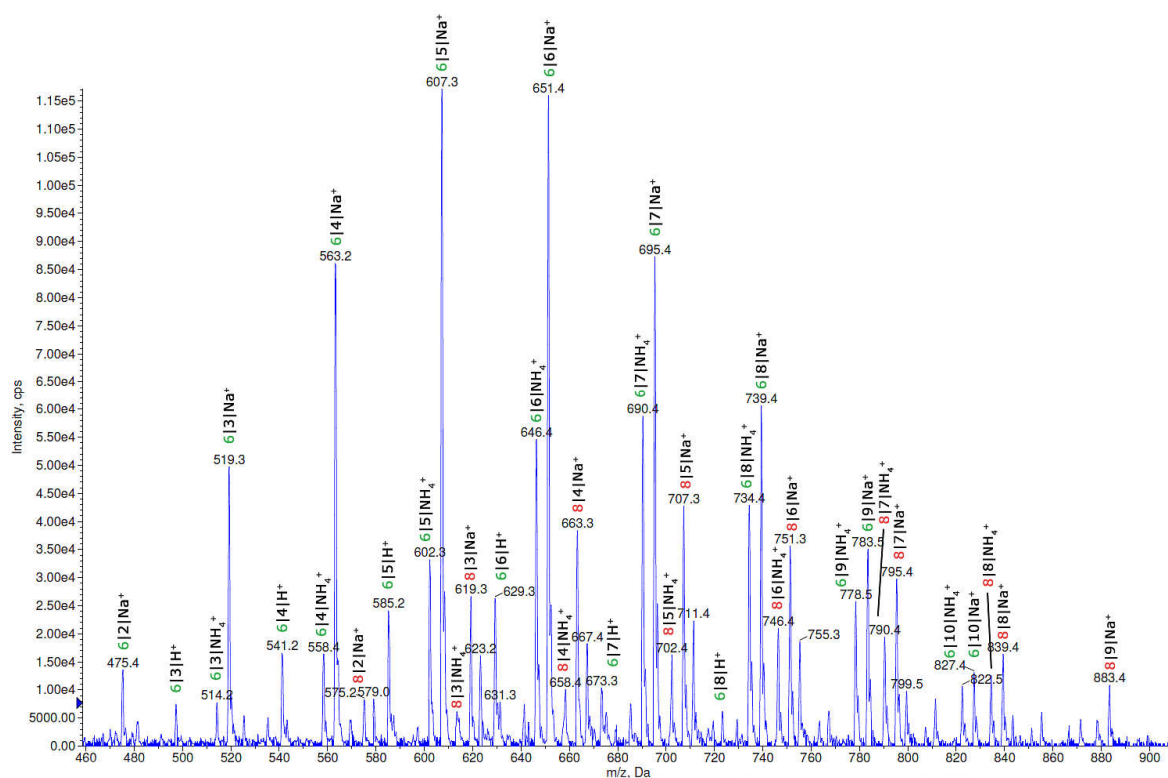
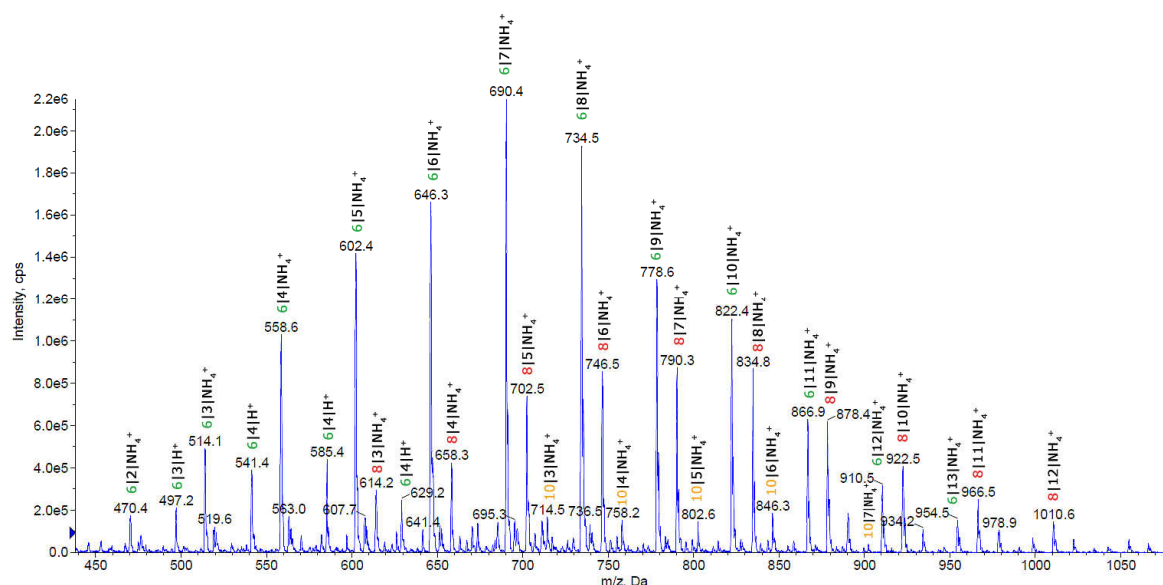


Figure 13: (+)ESI-MS Q1MS spectrum of 15 µg mL⁻¹ Zonyl FSH in H₂O/MeOH (1/1; V/V) . The denotation x|y|z signifies: x = number of perfluorinated carbon atoms, y = degree of ethoxylation, z = cation

Indeed, the resulting spectrum is qualified by a high number of peaks. Even at first glance several distributions with equidistant peaks of 44 Da are visible, which is characteristic of polyethoxylates [160], e.g. m/z 519, 563, 607 etc. By calculating potential m/z values for well-known adducts, e.g. H⁺, Na⁺, K⁺ and NH₄⁺, the peaks can be assigned to the respective compounds. As can be seen especially for the peaks with high intensities, ion species [M + H]⁺, [M + NH₄]⁺ and [M + Na]⁺ occur in this spectrum side-by-side with the sodium adducts showing greatest intensity for all species detected. Sodium cations are nearly ubiquitous and thus sodium adducts regularly appear in mass spectra even though no sodium has been added to the solution intentionally. Since the mass spectrum was recorded on a mass spectrometer which is often used in combination with HPLC and eluents containing ammonium acetate (NH₄OAc) or ammonium formate, ammonium can be hardly eliminated from this system. This is the reason why ammonium adducts occur in this spectrum. Proton adducts can result either from direct protonation of the FTEO by the constituents of the eluents, or by fragmentation of ammonium ions. This will be discussed more thoroughly in the course of this section.

The compounds detected with this method showed a perfluoroalkyl chain length of six and eight and a degree of ethoxylation from 2 to 11.

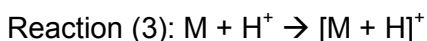
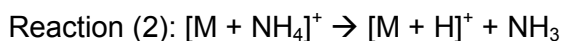
In order to generate a less complex spectrum, the same measurement was conducted with the addition of 5 mM NH₄OAc to the solvent. The resulting spectrum is shown in Figure 14.



3.1.3 Molecular weight distribution

It is well-known that molar responses in ESI can differ significantly even for structurally similar compounds [161]. Thus, it is not possible to assess the exact molecular distribution of the FTEO commercial mixture by means of ESI-MS. However, at least an estimation of the distribution can be made when comparing relative intensities in ESI. In order to minimize suppression effects, this estimation was done by LC-ESI/MS under isocratic HPLC conditions. If gradient elution had been chosen, ionization response would be further affected by the composition of the mobile phase when the compounds are eluted, which would further complicate comparison of the intensities.

MS of polyethoxylates using ammonium additives may involve the following processes



where M is the uncharged polyethoxylate and F represent fragments of M. Reaction (2) is initiated by CID. Thus, more vigorous collision will lead to higher degree of dissociation and thus lower the signal intensity of ammonium adducts. Inversely, too gentle collision will produce solvent ion clusters and thus decrease sensitivity for the ammonium adduct as well. The protonated molecules $[M + \text{H}]^+$ may be created both by reaction (3) and the combination of reaction (1) and (2). Reaction (4) represents the process which is intensified by higher declustering potentials (DP). At high DP settings, fragmentation of the molecule itself will occur, as represented by reaction (5).

In order to obtain more information about the processes occurring during CID of ammonium adducts and in order to assess the expressiveness of comparison of intensities of such compounds, the Zonyl FSH mixture was chromatographed under RP conditions and the MS operated at three different DP values, i.e. 10 V, 25 V and 40 V. As the name implies, DP is the voltage responsible for the acceleration of ions when colliding with the curtain gas, i.e. when declustering of the ions shall be achieved prior to entering the m/z separation stages (Reaction (4)). All measurements were carried out in triplicate in order to achieve higher significance of the results. For the following calculations, only congeners were used whose relative standard deviation for triplicate analysis was below 25%.

As can be seen in Figure 15 b), most of the congeners showed increased absolute signal intensities (as calculated by the HPLC-ESI/MS peak areas in SIM mode). Only compounds of

short perfluoroalkyl chain length and ethoxylate chain length showed a reduction in intensity. This is probably due to cleavage of ammonia from the ammonium adducts (reaction (2)). Longer chained compounds show a positive gain in intensity as a result of cleavage of solvent clusters (reaction (4)).

This different behavior of congeners at varying DP implies that – apart from different response factors during ESI – assessment of the molecular distribution in a polyethoxylate compound is also dependent on the MS settings.

This is also reflected in Figure 15 a), where the percentage gain in relative intensity is plotted for each compound. The relative intensities were calculated by dividing the peak area for a congener by the sum of all peak areas. It could be shown that again shorter chained compounds would be underestimated at higher DP values. Whereas for compounds with very low abundance the relative differences may be up to -60%, the results are in the 20% range for most of the compounds at higher abundance.

A correlation between the molecular weight and the gain in absolute intensity was established with the help of a second-order polynomial function (Figure 15 c), which showed a fairly high correlation with $R^2 = 0.73$. This behavior implies that in the range of approximately 400 Da to 550 Da, ammonium adducts tend to be fragmented to proton adducts and ammonia. In the range of 550 Da to 800 Da, a constant increase in the gain in sensitivity can be observed reaching ca. 60%, where the function then seems to reach a plateau (which is naturally not reflected by the quadratic function).

The contour plots expressing the percentage relative intensities of FTEO congeners in Zonyl FSH measured at different DP settings are illustrated in Figure 16. These plots clearly

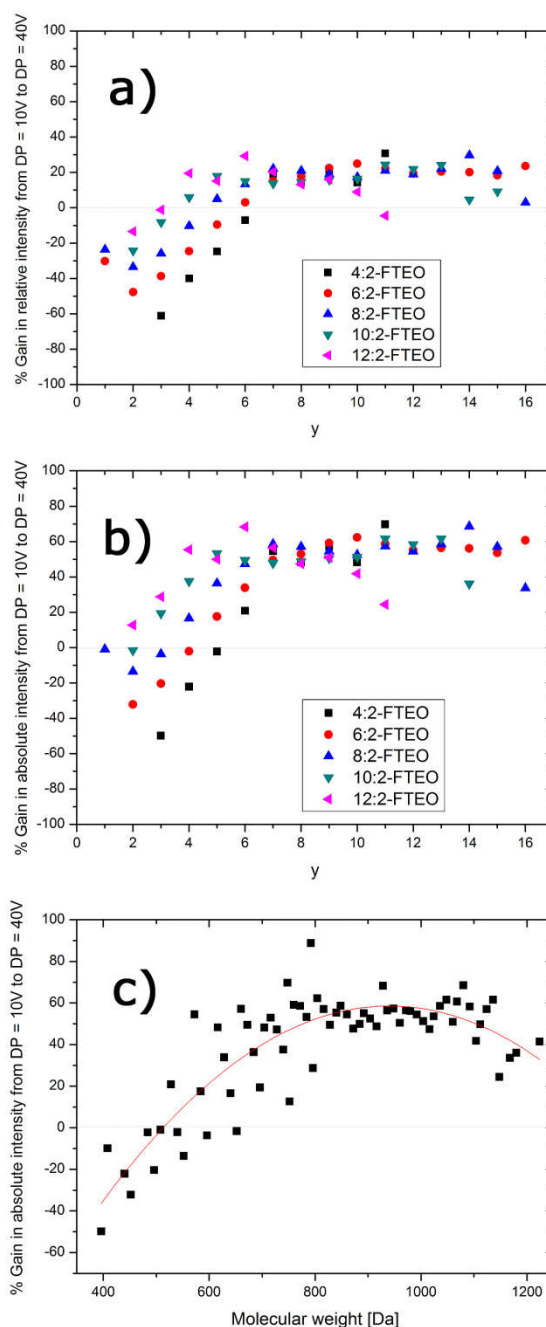


Figure 15: a) Percentage gain in relative intensity of FTEO ammonium adducts b) Percentage gain in absolute intensity of FTEO ammonium adducts c) Percentage gain in absolute intensity of FTEO ammonium adducts in function of the molecular weight of the respective congener

demonstrate that a maximum in intensity is always reached around 6:2-FTEO₅ to 6:2-FTEO₇, regardless of the DP value set. While the red area, which reflects the maximum abundance at 10%, is reduced from DP = 10 V to DP = 25 V, the two contour plots at DP = 25 V and DP = 40 V are nearly identical suggesting no major differences in the CID fragmentation of ammonium adducts between these values.

While the similarity between the measurements does not necessarily imply transferability from

relative intensities to molar distributions, it could yet be shown that the relative intensities indeed do represent an approximation of molar distribution in this case. When summing the relative intensities of FTEO ethoxymers with the same perfluoroalkyl chain lengths, 6:2-FTEOs account for approximately 57%, whereas the fraction of 8:2-FTEO is approximately 33%. This ratio (2.3) is comparable to the ratio of 6:2-FTOH to 8:2-FTOH detected by quantitative measurement in Zonyl FSH, which is ca. 1.7. Interestingly, it is also possible to measure FTEOs as their respective deprotonated molecule, if no ammonium-based modifier is present. This is in accordance with the findings of Berger *et al.* [156], who found the same phenomenon for FTOHs. However, signal intensities were several orders of magnitude lower than for ammonium or proton adducts in positive polarity. Details about deprotonated FTEO are discussed in chapter 3.2.2.

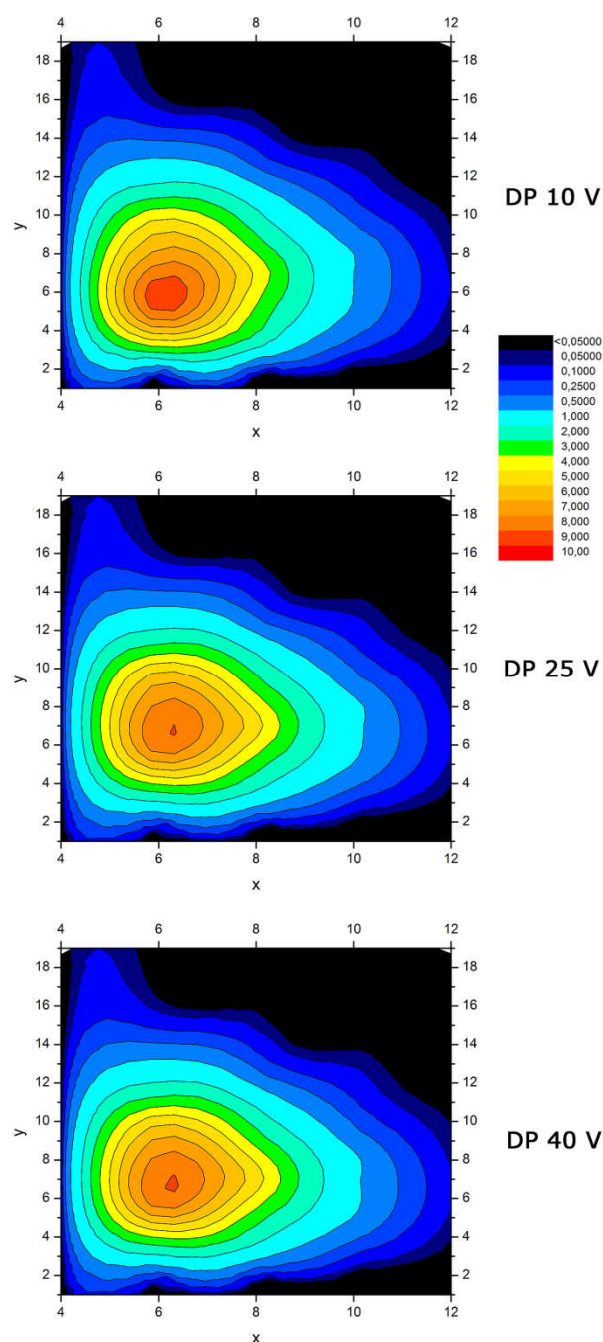


Figure 16: Relative molar intensities of FTEOs in technical mixture Zonyl FSH at DPs of 10 V (top), 25 V (middle) and 40 V (bottom).

3.1.4 Semiquantitative determination of FTEO

In order to assess the temporal course of FTEO and its TPs, a method based on RP-HPLC and ESI-MS was developed. Just like the biodegradation experiment, also analysis may suffer from adsorption effects, especially when long perfluoroalkyl chains and high aqueous content is considered (data not shown). This can be circumvented by dissolving the samples in at least 50% of organic solvent, either ACN or MeOH.

Since the signal intensity of protonated and sodiated molecules is greatly influenced by the sodium concentration in the eluents or in HPLC tubes, it was decided to use ammonium adducts of FTEO for semi-quantitative SIM or MRM methods. In order to maximize the reproducibility of the measurement, an internal standard should be used. This internal standard must be measured in positive mode - because FTEOs are measured in positive mode - and should also form ammonium adducts. In an ideal way, it should also have the same or similar retention time as the analytes in LC.

Three compounds were tested as potential internal standards: nonylphenol diethoxylate (NPEO₂), poly(ethyleneglycol)-6 (PEG-6) and atrazine, which does not form ammonium adducts. 16 measurements were carried out on three subsequent days and the relative standard deviation (RSD) was calculated for the ratio of the signal of all FTEO and the potential internal standard. NPEO₂ showed by far the best results with a percentage RSD of 1.6%, followed by PEG-6 (RSD = 5.7%) and atrazine (10.8%). The difference between NPEO₂ and PEG-6 can be explained by the greatly different retention times in HPLC. Since PEG-6 does not contain any non-polar backbone, it elutes very early, unlike NPEO₂ and all FTEOs. Atrazine, which was measured as the protonated molecule, cannot overcome fluctuations in ammonium concentration and therefore gives rise to higher deviations. Thus, NPEO₂ was chosen as the internal standard for all further semiquantitative measurements of FTEO and also of FTEOC, when measured as the ammonium adduct.

Since RP-HPLC was chosen as the chromatographic separation prior to MS, retention times of FTEO and FTEOC were mainly affected by the perfluoroalkyl chain length (see Figure 17 a)), which represents the non-polar moiety of these molecules. In fact, the ethoxylate chain length can be regarded as rather 'neutral' with respect to the interactions with the stationary phase, implying nearly coelution of all ethoxymers with one perfluoroalkyl chain length. Slight reduction of retention time can be observed with each ethoxylate group added to the molecule (Figure 17 b)).

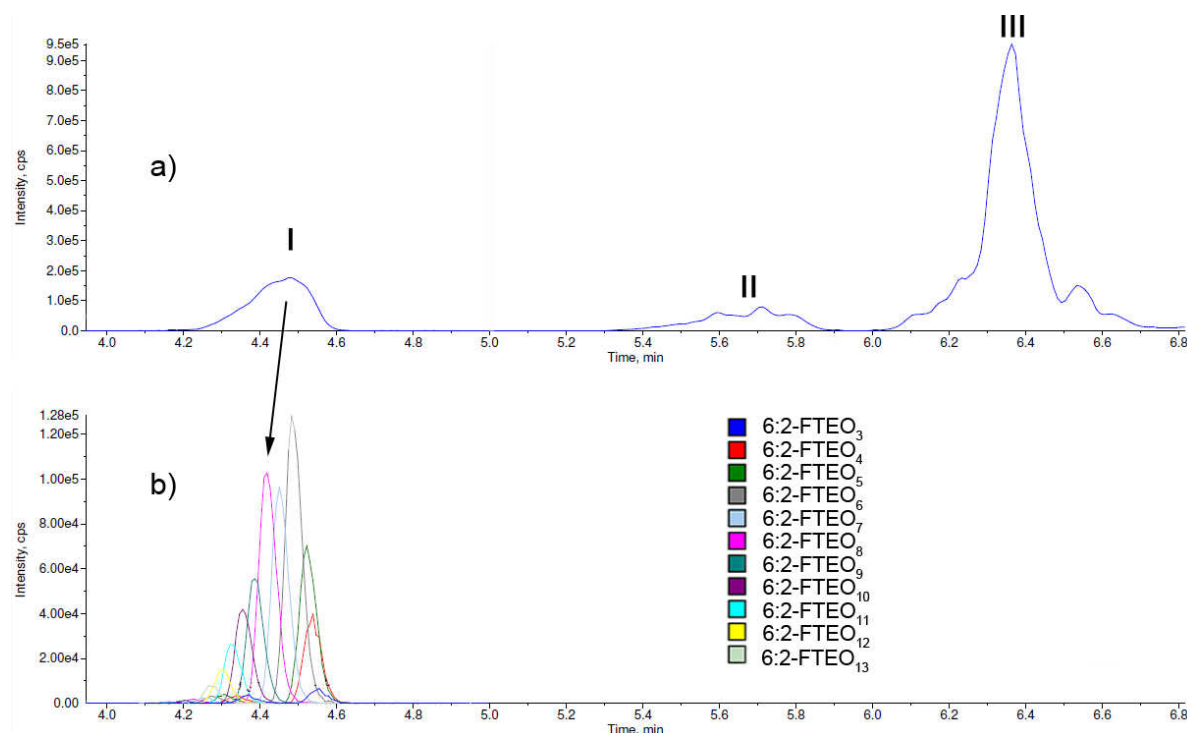


Figure 17: HPLC-(+)-ESI-MS/MS chromatogram of 750 ng Zonyl FSH mL⁻¹ a) Total ion chromatogram (TIC) showing I: 6:2-FTEO II: 8:2-FTEO and III NPEO₂ b) Extracted ion chromatograms of 6:2-FTEO congeners reflecting the poor resolution of ethoxymers of the same perfluoroalkyl chain length

The NPEO₂ used as the internal standard was from a technical mixture. Since different nonyl isomers are present in this mixture, the chromatographic peak of NPEO₂ appears as a very broad and non-Gauss-shaped peak. However, this had no negative implications for semi-quantitative measurement of FTEO.

For 10:2-FTEOs, no reliable method could be developed, because the signal intensities for these congeners were tremendously reduced within several hours. Thus, these were not included in further biotransformation experiments of FTEO.

3.1.5 Conclusion

The characterization of commercial fluorosurfactant mixtures via HPLC and MS techniques was successfully carried out up to a level where the distribution of distinct congeners of FTEO can be assessed. The qualitative approach via ESI-MS and HPLC-ESI-MS allows for detection of different cationic ion species of FETO, such as proton, sodium and ammonium adducts.

ESI-MS cannot describe the exact distribution by comparison of peak intensities due to molecular response changes caused by MS settings, such as acceleration voltages, or the solvent used. The influence of the DP, which accelerates solvent clusters towards a stream of nitrogen gas on signal intensity of FTEO ammonium adducts was quantified. It was shown that

high molecular weight FTEOs show increased intensities at higher DP settings, whereas the intensity of lower molecular weight FTEOs is reduced. The velocity of low molecular weight compounds is supposed to be higher than that of their larger counterparts, leading to fragmentation of low molecular weight FTEO. High molecular weight FTEO however profit from more pronounced declustering which in turn means higher signal intensities of the free FTEO ammonium adducts.

Including an internal standard for the semiquantitative determination of FTEOs via HPLC-ESI-MS resulted in high method reproducibility for 6:2-FTEOs and 8:2-FTEOs. For 10:2-FTEOs, signal intensities dropped within several hours, which is ascribed to adsorption onto the HPLC glass walls.

3.2 CID fragmentation of FTEO and its TPs

3.2.1 Fragmentation of cationic species

Collision induced dissociation of FTEO congeners can be easily induced from their respective ammonium adduct, which is useful to perform structural analyses, as ammonium adducts generally can be transformed to protonated molecules by CID. These protonated molecules may then further fragment to provide structural information. This is not possible with sodium adducts, which only cleave off the charged sodium ion upon CID leaving behind a neutral molecule.

CID of ammonium adducts of FTEO leads to several series of ions differing by 44 Da (Figure 18). First, loss of ammonia yields the protonated molecule, which decays by multiple cleavage of C_2H_4O , generating a series of oxonium ions. Interestingly, at some point, loss of water occurs, yielding a carbenium ion which is stabilized by conjugation with an ether function. Thereupon, sequential loss of 44 Da leads to shorter carbenium ions. The importance of conjugation by the ether function is displayed by the fact that none of these carbenium ions is observed below m/z 391 for 6:2-FTEOs. If further cleavage of 44 Da occurred, no oxygen could account for the mesomeric stabilization.

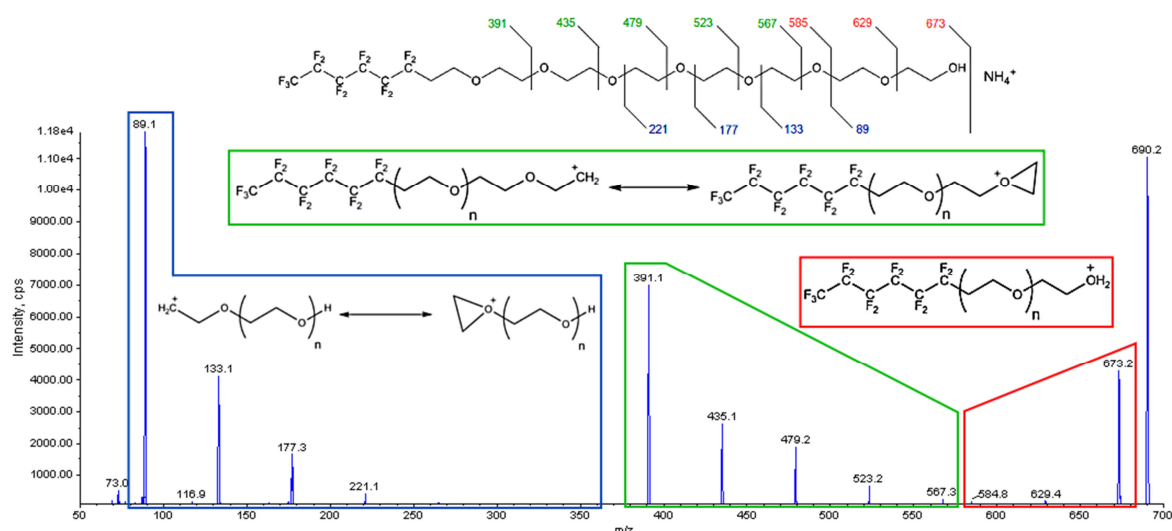


Figure 18: (+)ESI-MS/MS product ion spectrum of 6:2-FTEO₇ (m/z 690) and tentative structural assignment of the product ions. The spectrum was recorded by syringe pump infusion of a solution containing approximately 500 ng mL⁻¹ total FTEO in H₂O/ACN + 5 mM NH₄OAc

A third series of product ions is depicted in blue, representing carbenium ions that do not carry the perfluoroalkyl chain, but represent the well-known series of ions for PEG and its derivatives at m/z 89 + 44n [160].

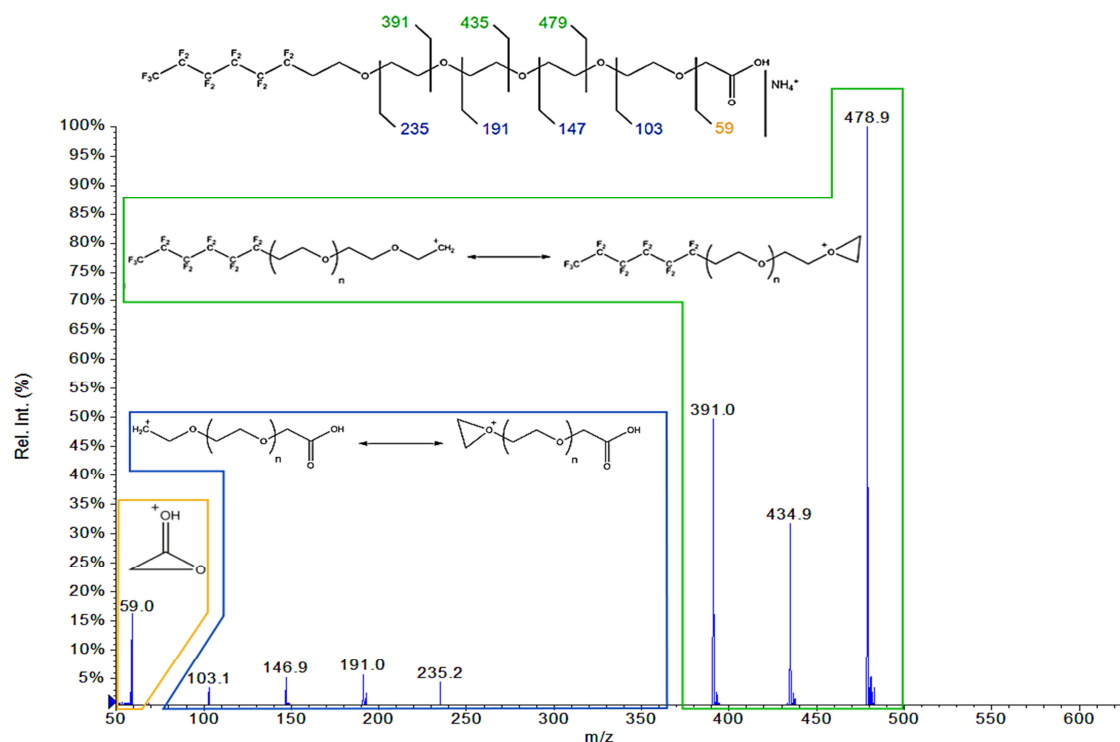


Figure 19: (+)ESI-MS/MS product ion spectrum of the ammonium adduct of 6:2-FTEO₅C (m/z 616) and tentative structural assignment of the product ions

The fragmentation pattern of ammonium adducts of FTEOCs in positive polarity is very similar to those observed for FTEO (see Figure 19).

In contrast to FTEO fragmentation, no oxonium ion series is formed from FTEOC. By loss of the terminal acetic acid function, the same series of carbenium ions is generated by multiple sequential loss of C_2H_4O as found for FTEO.

3.2.2 Fragmentation of anionic species

As already mentioned, it is also possible to measure FTEO in negative mode, if no ammonium is present. The product ion spectra differ greatly from those of proton and ammonium adducts, respectively, which can be considered a common phenomenon. Enhanced product ion spectra of 8:2-FTEO₇ and 8:2-FTOH are presented in Figure 20.

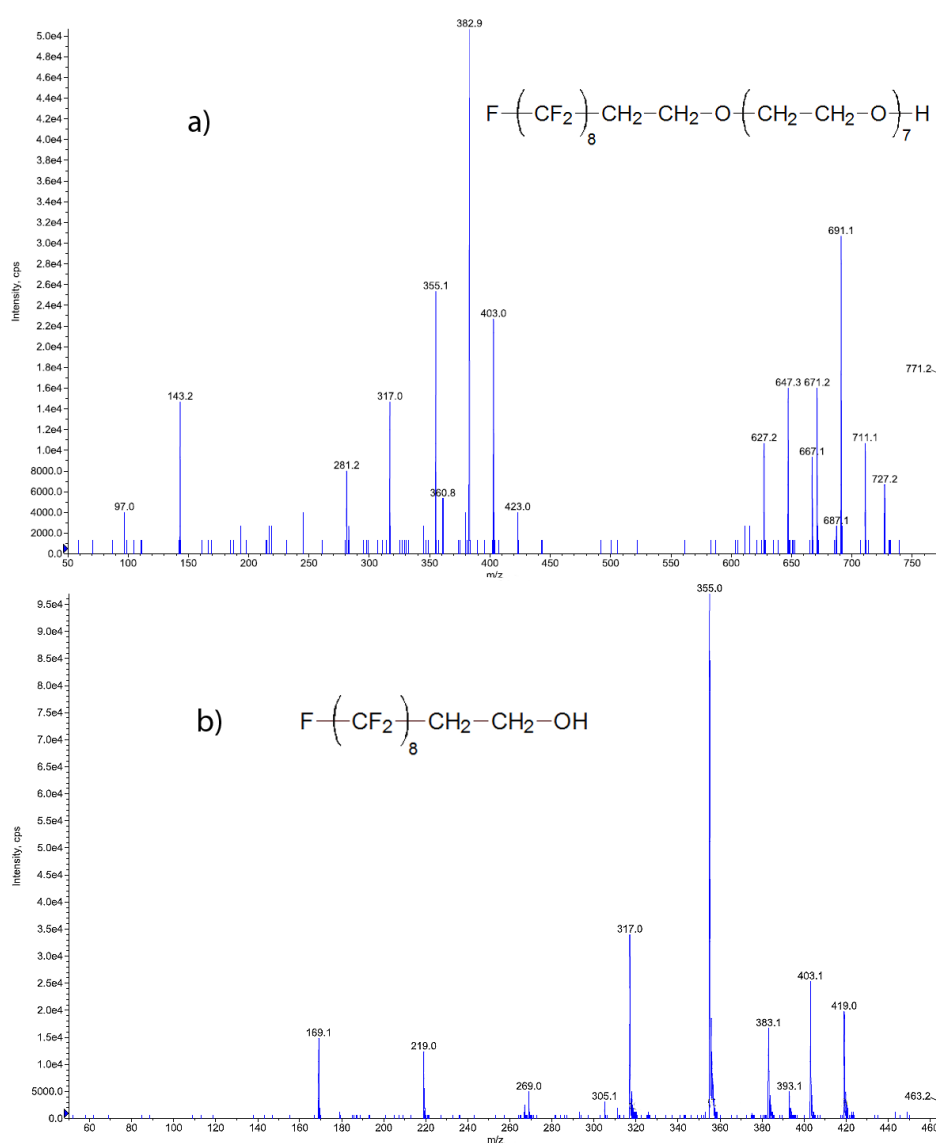


Figure 20: (-)ESI-MS/MS enhanced product ion spectra of a) 8:2-FTEO₇ b) 8:2-FTOH and the corresponding structural formulae

It becomes obvious that FTEOs show a CID fragmentation behavior which is partially similar to their respective parent FTOH. Since the fragmentation pattern of 6:2-based compounds and 8:2-based compounds is coherent, spectra will be shown exclusively for 8:2-based compounds.

There are two clusters of product ions in the spectra of FTEOs, one being located below m/z 450, the other one lies above m/z 600. The pattern at higher m/z values originates from multiple loss of C_2H_4O and HF from the precursor ion (see Figure 21). Interestingly, the carbanion species dominate the spectrum in the higher m/z range, although the negative charge located at the carbon atoms cannot be stabilized by neighboring groups, as shown in Figure 18 for the analogous 6:2-FTEO after positive ionization.

The pattern at lower masses is representative of the fluorotelomer chain. The latter statement becomes obvious when compared with the respective FTOH spectrum. The product ions at m/z 403, 383, 355 and 317 occur both in 8:2-FTEO and 8:2-FTOH product ion spectra and it was thus hypothesized that these ions are characteristic of fluorotelomer compounds.

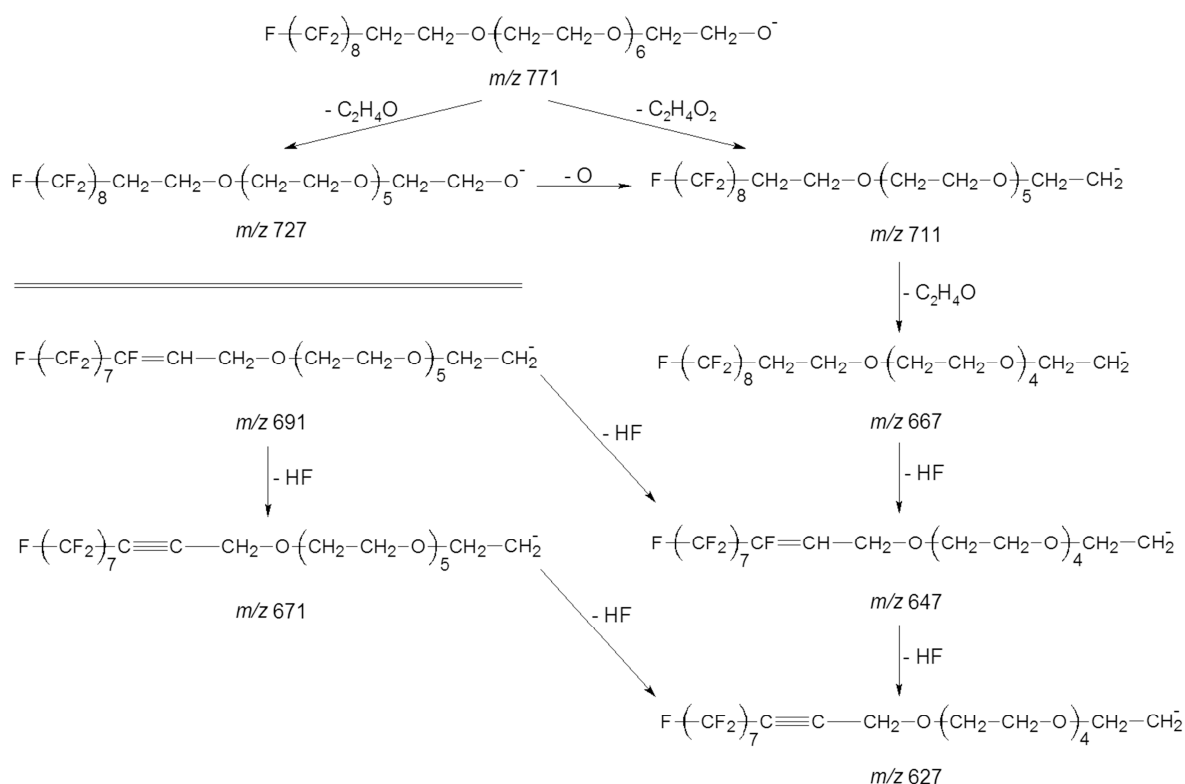


Figure 21: Proposed fragmentation pathway of 8:2-FTEO₇ after negative ESI. The associated product ion spectrum is shown in Figure 20.

The nature of the lower mass pattern was subjected to more detailed investigation. In order to do so, the synthesized short-chained FTEOCs 6:2-FTEO₁C and 8:2-FTEO₁C were measured by QqLIT and high-resolution MS on an orbitrap MS. The latter measurement allows for determination of the accurate mass of the ions and thus, to determine the sum formulae of the

product ions. The orbitrap MS and enhanced product ion spectrum of a QqLIT of 8:2-FTEO₁C are shown in Figure 22 and the summarized measured masses, theoretical masses, errors, proposed sum formulae and corrected ring and double bond equivalents (RDBE) of the product ions are presented in Table 2.

Corrected RDBEs are calculated by the formula

$$\text{corrected RDBE} = C - \frac{H}{2} - \frac{F}{2} + 0.5$$

where C is the number of carbon atoms, H is the number of hydrogen atoms and F is the number of fluorine atoms. As the measured species are anions, the RDBE has to be increased by 0.5 to assess the true number of rings and double bonds.

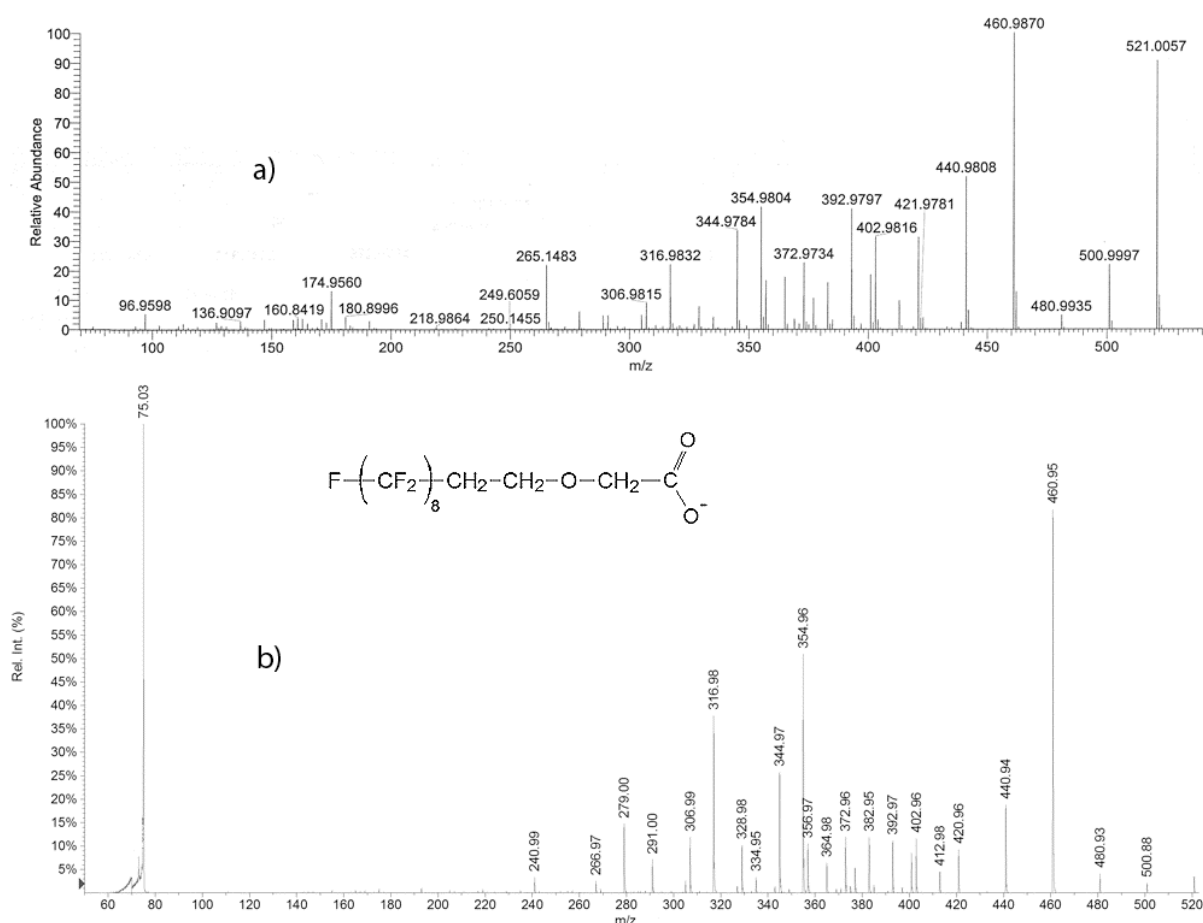


Figure 22: (-)ESI-MS/MS spectra of 8:2-FTEO₁C measured on a) orbitrap b) QqLIT (enhanced product ion)

The indicative masses of the 8:2-fluorotelomer structure – *m/z* 403, 383, 355 and 317 – also appear in the spectrum of this compound. Their suggested sum formulae are coherent with previously proposed formulae for 8:2-FTOH by Berger *et al.* [156]. Whereas it was proven that FTOH deprotonation occurs at the methylene group in adjacencies to the perfluoroalkyl chain, this seems highly unlikely for FTEOCs, which carry the carboxylic acid function and are believed

to be deprotonated at this very functional group. Thus, it is astonishing that FTEOCs and FTOHs partly generate the same product ions.

Numerous other product ions are observed for 8:2-FTEO₁C. The enhanced product ion spectrum of 8:2-FTEO₁C (Figure 22 b) shows one large peak, which does not occur in the orbitrap spectrum, that is the product ion at m/z 75 representing HO-CH₂-COO⁻. The orbitrap is not capable of measuring such low-mass product ions when rather high-mass precursor ions are fragmented.

Table 2: Measured m/z versus theoretical m/z of orbitrap MS measurement of 6:2-FTEO₁C and 8:2-FTEO₁C. Elemental compositions are proposed based on lowest errors and corrected ring and double bond equivalents are given. For further information, please see text.

	measured m/z	theoretical m/z	Error [ppm]	Elemental Composition	corrected RDBE
8:2-FTEO ₁ C	521.0057	521.0051	1.15	C ₁₂ H ₆ O ₃ F ₁₇ ⁻	1
	500.9997	500.9989	1.60	C ₁₂ H ₅ O ₃ F ₁₆ ⁻	2
	480.9935	480.9926	1.87	C ₁₂ H ₄ O ₃ F ₁₅ ⁻	3
	460.9870	460.9864	1.30	C ₁₂ H ₃ O ₃ F ₁₄ ⁻	4
	440.9808	440.9801	1.59	C ₁₂ H ₂ O ₃ F ₁₃ ⁻	5
	420.9746	420.9740	1.43	C ₁₂ H ₂ O ₃ F ₁₂ ⁻	6
	402.9816	402.9809	1.74	C ₁₀ HOF ₁₄ ⁻	3
	400.9684	400.9677	1.75	C ₁₂ O ₃ F ₁₁ ⁻	7
	392.9797	392.9790	1.78	C ₁₁ HO ₂ F ₁₂ ⁻	5
	382.9753	382.9747	1.57	C ₁₀ OF ₁₃ ⁻	4
	372.9734	372.9728	1.61	C ₁₁ O ₂ F ₁₁ ⁻	6
	364.9846	364.9841	1.37	C ₁₀ HOF ₁₂ ⁻	4
	356.9786	356.9779	1.96	C ₁₁ OF ₁₁ ⁻	6
	354.9803	354.9798	1.41	C ₉ F ₁₃ ⁻	3
	344.9784	344.9779	1.45	C ₁₀ OF ₁₁ ⁻	5
	328.9834	328.9830	1.22	C ₁₀ F ₁₁ ⁻	5
	316.9832	316.9830	0.63	C ₉ F ₁₁ ⁻	4
	306.9815	306.9811	1.30	C ₁₀ OF ₉ ⁻	6
	278.9864	278.9862	0.72	C ₉ F ₉ ⁻	5
6:2-FTEO ₁ C	421.0118	421.012	-0.48	C ₁₀ H ₆ O ₃ F ₁₃ ⁻	1
	401.0056	401.0053	0.75	C ₁₀ H ₅ O ₃ F ₁₂ ⁻	2
	380.9994	380.9990	1.05	C ₁₀ H ₄ O ₃ F ₁₁ ⁻	3
	360.9931	360.9928	0.83	C ₁₀ H ₃ O ₃ F ₁₀ ⁻	4
	340.9868	340.9866	0.59	C ₁₀ H ₂ O ₃ F ₉ ⁻	5
	320.9804	320.9803	0.31	C ₁₀ HO ₃ F ₈ ⁻	6
	312.9920	312.9917	0.96	C ₉ H ₂ O ₂ F ₉ ⁻	4
	302.9874	302.9873	0.33	C ₈ HOF ₁₀ ⁻	3
	300.9743	300.9741	0.66	C ₁₀ O ₃ F ₇ ⁻	7
	292.9855	292.9854	0.34	C ₉ HO ₂ F ₈ ⁻	5
	282.9812	282.9811	0.35	C ₈ OF ₉ ⁻	4
	272.9794	272.9792	0.73	C ₉ O ₂ F ₇ ⁻	6
	264.9907	264.9905	0.75	C ₈ HOF ₈ ⁻	4
	256.9844	256.9843	0.39	C ₉ OF ₇ ⁻	6
	254.9863	254.9862	0.39	C ₇ F ₉ ⁻	3
	244.9844	244.9843	0.41	C ₈ OF ₇ ⁻	5
	228.9894	228.9894	0.00	C ₈ F ₇ ⁻	5
	216.9893	216.9894	-0.46	C ₇ F ₇ ⁻	4
	206.9875	206.9875	0.00	C ₈ OF ₅ ⁻	6
	178.9924	178.9926	-1.12	C ₇ F ₅ ⁻	5
	166.9924	166.9926	-1.20	C ₆ F ₅ ⁻	4

As can be seen, a sum formula could be determined for most product ions detected and the errors were < 2 ppm, often even < 1 ppm.

More detailed information was gathered by recording MS³ scans of all product ions of 8:2-FTEO₁C and 6:2-FTEO₁C using the QqLIT instrument. With the help of this mode, fragmentation pathways can be elucidated since the sequence of fragmentations can be unscrambled, which is not possible with MS/MS methods. To visualize the results, the fragmentation scheme as well as the sum formulae and the nominal masses of the product ions of 8:2-FTEO₁C are presented in Figure 23.

The findings suggest two major fragmentation routes. The pathways I and II are directly connected to each other and product ions are exclusively formed by abstraction of CO or HF, except for the very last fragmentation step, where difluorocarbene, CF₂, is cleaved off. This whole fragmentation pathway is restricted to FTEO₁C fragmentation and cannot be generalized for other fluorotelomer-based compounds. Pathway III shares several product ions with 8:2-FTOH and FTEO fragmentation (see Figure 20).

The latter pathway is induced from m/z 481 by loss of C₂H₃O₂F. It is striking that this fragmentation pathway can only be triggered from the product ion with m/z 481 (or higher mass product ions), but not from those with lower m/z like m/z 461. This is conspicuous because one would expect that, for instance, m/z 461 could also be transformed to the product ion at m/z 383, but this was excluded by the MS³ measurement. The second peculiarity of the FTOH-based fragmentation pathway is that the fluorocarbon anion at m/z 317 is generated from m/z 383 by loss of carbonyl difluoride, but not from m/z 355. This would be theoretically possible by cleavage of molecular fluorine (F₂). This observation suggests a rearrangement of m/z 383 to m/z 317.

Interestingly, the two fragmentation pathways I and III coalesce in the product ion at m/z 317, although no link between these two routes occurs prior to m/z 317. However, it cannot be verified if both pathways virtually concur into the very same product ion or in two isomeric ions. Since this ion only has one successive product ion at m/z 267, this could be a hint that only one isomeric form of m/z 317 is present.

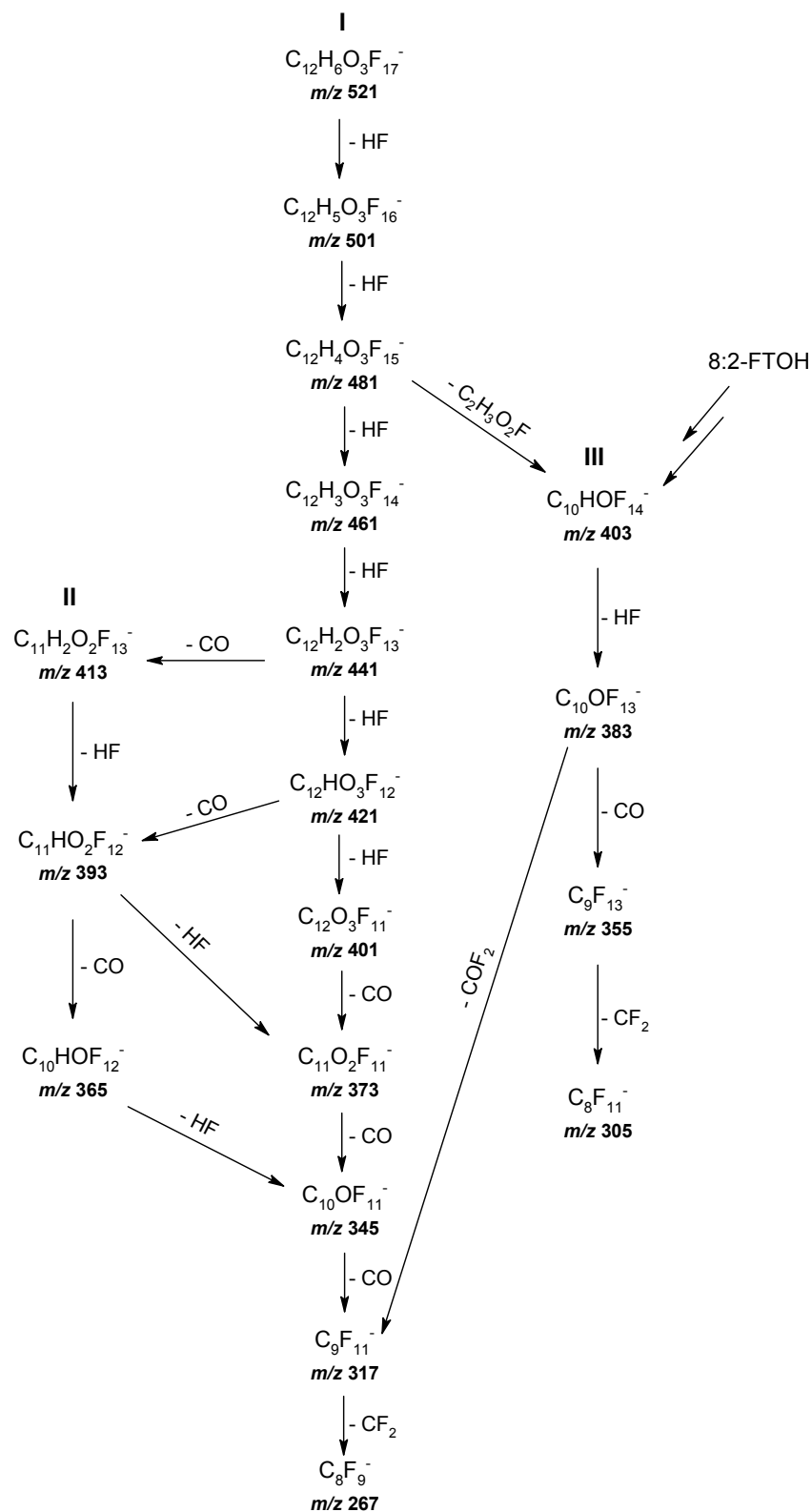


Figure 23: CID Fragmentation scheme of 8:2-FTEO₁C as measured by MS³ scans using QqLIT-MS. The sum formulae were determined with the help of orbitrap MS. 8:2-FTOH is added to this figure to denote the similarity in fragmentation.

Taking into account the information given in Table 2 about corrected RDBE values and sum formulae, it turns out that some of the structures of the fragments are very likely to be cyclic. Whereas the first losses of HF could be readily explained by abstraction of neighboring hydrogen and fluorine atoms and concerted double bond formation, the same cannot be stated for further reactions. Already the third loss of HF must either have resulted from HF abstraction of distant hydrogen and fluorine atoms, or rearrangement in form of hydrogen or fluorine migration must have taken place. In the first case, cyclization seems a likely explanation, whereas the second suggestion could give rise to linear, unsaturated molecules.

However, for fragments such as m/z 401 containing seven RDBEs, a cyclic structure seems by far more likely, because otherwise, the very labile cumulative double bonds would have to be formed. This product ion consists of 12 carbon atoms and is generated from deprotonated 8:2-FTEO₁C by sequential loss of six molecules of HF.

The exact structures cannot be determined without the help of sophisticated computational modeling methods such as density-functional theory based calculations. Another very valuable tool would be exchange of certain hydrogen atoms by deuterium, for instance by synthesizing mass-labeled FTEO₁C based on the synthetic route presented in Figure 33, by using mass-labeled bromoacetic acid or mass-labeled FTOHs. In this way, one could determine the order of HF cleavage (in case deuterium-labeled educts are used), or the sequence of CO abstraction (if ¹³C-labeled educts are used). All of these methods are very complex and costly and the results would not yield further information relevant for this work, thus they were not carried out.

A tentative suggestion for the fragmentation route of FTOH-based product ions of 8:2-FTEO₁C is given in Figure 24, starting with the common fragment at m/z 403. This fragment cleaves off HF under simultaneous fluorine migration leading to a new double bond, which increases the number of conjugated double bonds and thus, the mesomeric system. Thereupon, either decay of carbonyl difluoride or of CO occurs, leading to the product ions at m/z 317 or m/z 355. The latter one undergoes alkyl chain shortening by loss of difluorocarbene. This is probably achieved by abstraction of the terminal CF₂ group and migration of the fluorine atom previously attached to this CF₂ group.

The formation of conjugated double bonds and the stability of the leaving groups HF and CO are assumed to be the major driving forces for all fragmentation reactions of 8:2-FTEO₁C.

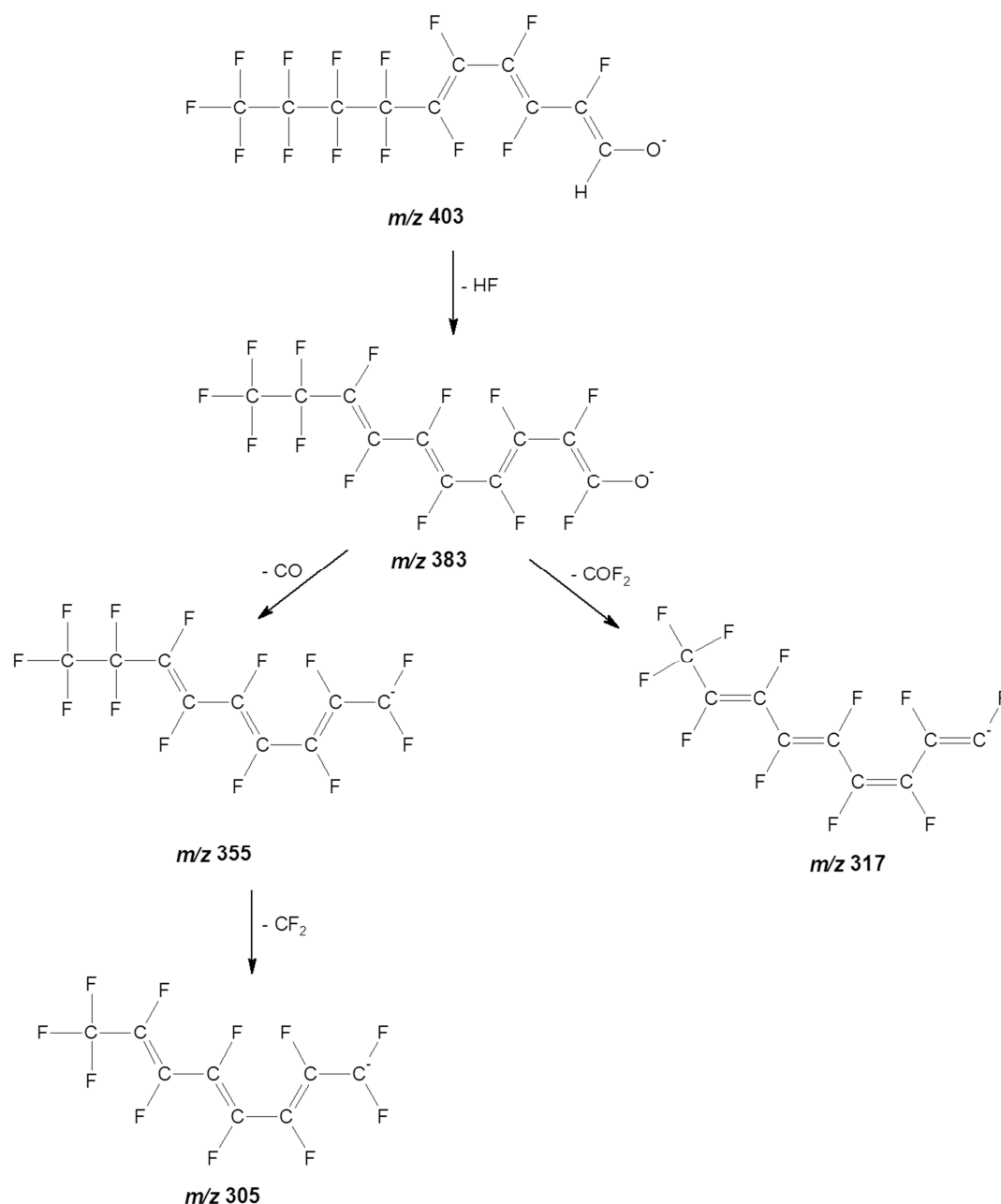


Figure 24: Tentative fragmentation pathway of FTOH-related product ions of 8:2-FTEO₁C. Several rearrangements occur during fragmentation.

Even though the structures could not be pinpointed, the investigations resulted in several findings of interest for the analytical community, but also for environmental purposes. It can be concluded that CID fragmentation pathways of polyfluorinated compounds, i.e. those which are not perfluorinated, generally suffer loss of HF, which serves both as a stable leaving group and leads to stable fragments if several molecules of HF can be cleaved off, leading to conjugated double bonds. This hypothesis should be scrutinized by computational methods.

Most importantly, the investigation shows that fluorotelomer-based compounds are likely to yield several product ions, if it is possible to measure these compounds in form of their deprotonated

molecule. This can be made use of when searching for novel environmental contaminants with the help of tandem MS that allow for precursor ion scans. The product ions presented in Figure 24 are suited for this purpose, except for m/z 305, which usually occurred at low intensities. Neutral loss scans for 20 Da can also be used to detect unknown PFASs, since the mass of 20 Da can only be achieved by combination of hydrogen and fluorine. However, this method would be suited for compounds containing these elements in general, whereas the precursor scans of m/z 403, 383, 355 and 317 are specifically related to fluorotelomer-based compounds.

3.2.3 Conclusion

Combination of MS techniques using different mass analyzers enabled the detailed investigation of fragmentation pathways of several fluorotelomer-based compounds. Whereas QqLIT-MS turned out to be a valuable tool for identifying the order of fragmentations due to the possibility of MS³ scans, the high mass accuracy and mass resolving power of orbitrap MS could be used to determine the sum formulae of product ions.

In this way, a general CID fragmentation pathway of deprotonated molecules of fluorotelomer-based compounds was observed and the product ions involved were identified in terms of their sum formulae and order of fragmentation. The exact structures of these characteristic product ions could not be revealed, but conclusive suggestions were made. These characteristic fragments can be made use of by subjecting them to precursor ion scans in environmental samples or consumer products analysis to detect unknown fluorinated compounds.

FTEO and FTEOC fragmentation after positive ESI showed fragmentations similar to other oligoethoxylates as well as product ions characteristic of the fluorotelomer chain.

3.3 Biotransformation of a commercial fluorotelomer ethoxylate mixture

3.3.1 FTOH residues in the commercial mixture

The crude commercial mixture was analyzed for residual unreacted 6:2-FTOH and 8:2-FTOH. HPLC-(-)ESI-MS/MS analysis showed that the 6:2-FTOH content was 0.54% and 8:2-FTOH content was 0.29% (see Figure 25).

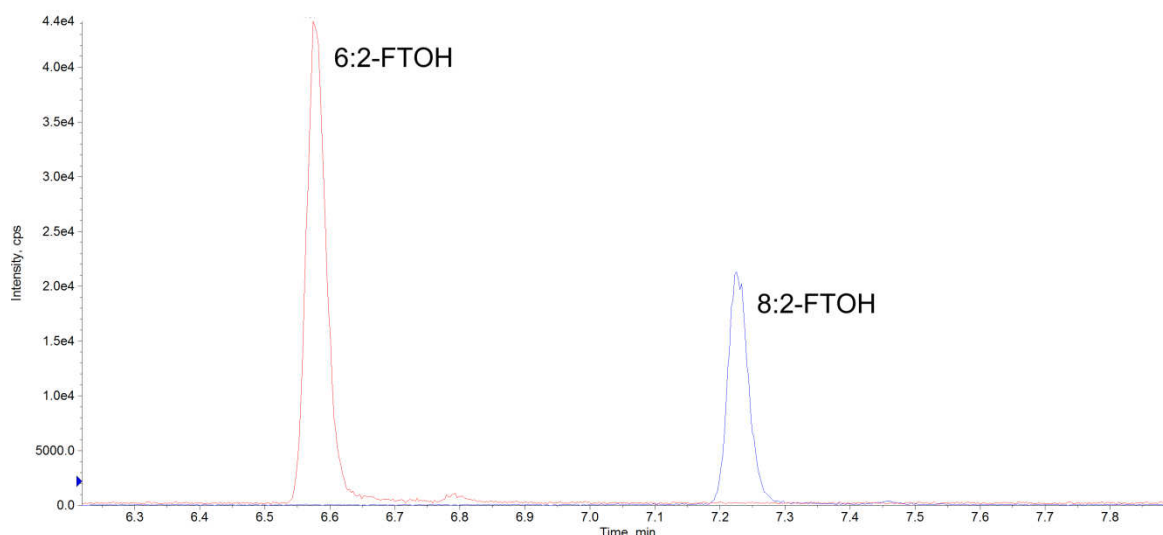


Figure 25: HPLC-(-)ESI-MS/MS XICs for 6:2-FTOH (red, m/z 423 \rightarrow 59) and 8:2-FTOH (blue, m/z 523 \rightarrow 59) of a solution containing $10 \mu\text{g mL}^{-1}$ Zonyl FSH

These results are in the range of those reported by Dinglasan-Panlilio and Mabury [162], who found 1.03 % for a different commercial FTEO product (Zonyl FSO-100). However, they used a completely different method (purging FTOH out of the raw material capturing volatilized FTOH on cartridges) and calculated the FTOH content as % of dry weight, which was not performed in the present study.

3.3.2 Generation of perfluorocarboxylic acids by biotransformation

The residual FTOHs in the commercial mixture represent a significant source of PFCAs by microbial transformation as proved in several studies [42,106,163]. On the other side, ultimate ethoxylate shortening of FTEOs would theoretically end up in FTOHs rendering FTEOs a potential source of PFCAs.

Monitoring of PFHxA and PFOA during the biodegradation experiment revealed that approximately 4.3 nM of PFHxA and even less PFOA (ca. 0.2 nM) was formed within 48 days. This corresponds to a 2.5% molar conversion of 6:2-FTOH to PFHxA and 0.3% molar conversion of 8:2-FTOH to PFOA. These values are coherent with previous studies.

An additional biodegradation test was carried out with 8:2-FTOH under the same conditions as for Zonyl FSH. This test was performed in order to evaluate potential loss of FTOH and volatile

TPs by aerating the bottles. Since no new information was gathered during that study, data is not shown here. These results suggest that FTEOs were not degraded to PFCAs, but to other unknown TP. This issue will be discussed in chapter 3.3.4.

3.3.3 Primary degradation vs. adsorption

As described in the experimental section, FTEOs were expected to exhibit strong adsorptive behavior, thus sterilized control experiments were inevitable to obtain reliable results. Figure 26 contrasts elimination of FTEOs in non-sterilized and sterilized degradation medium with respect to the fluorotelomer chain length. As expected, congeners featuring longer perfluorinated alkyl chains show increased adsorption rates as opposed to shorter perfluorinated chains. Moreover, adsorption decreases with longer polyethoxylate chain length, thus, in general adsorption decreases with higher hydrophilicity.

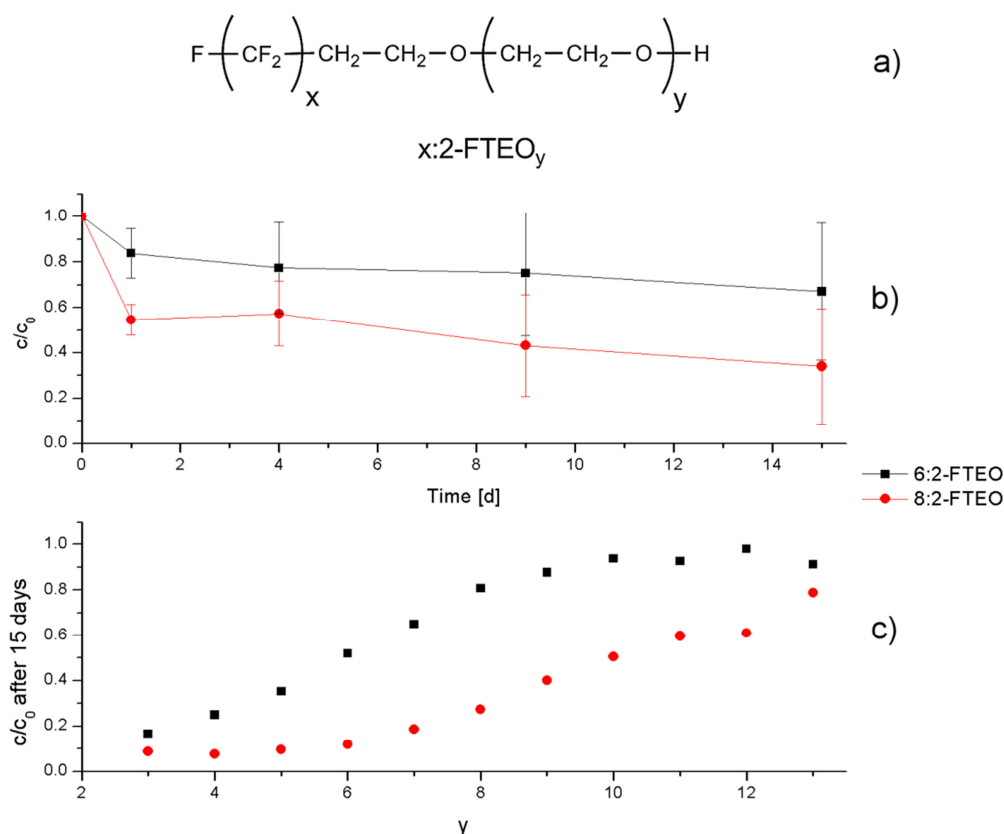


Figure 26: a) Structural formula and acronyms of FTEOs b) Adsorption of FTEOs in sterilized controls. Please notice that the error bars do not represent standard deviation of multiple experiments but standard deviation of c/c_0 of different ethoxymers as further illustrated in c) Dependency of ethoxylate chain length on adsorption of FTEOs in sterilized controls after 15 d

In contrast to the sterilized controls, no FTEOs were detectable in the non-sterile biodegradation experiment after three days (Figure 27). Although a considerable fraction may have been sorbed to glass or particles, comparison to the sterilized experiment proves that biotransformation had occurred. The steeper curve for 8:2-FTEOs may be attributable to their more pronounced adsorption. In general, the longer ethoxylates showed slower elimination as compared with shorter homologues.

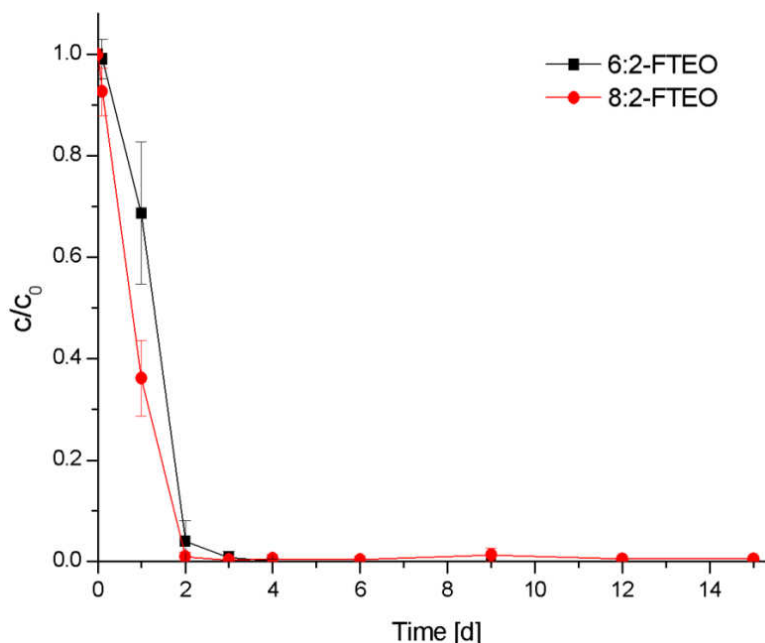


Figure 27: Biodegradation of FTEOs expressed as concentration divided by initial concentration. Please notice that the error bars represent standard deviation for different ethoxymers.

The rapid biotransformation rate is rather striking for fluorinated molecules, but is typical for polyethoxylates, such as alcohol ethoxylates [164] and nonylphenol ethoxylates [165]. This is attributable to the well biodegradable polyethoxylate chain [166,167].

As to the metabolic pathway of FTEOs, only the carboxylate species were detected. However, it is supposed that biotransformation starts with an oxidation to the respective aldehyde followed by a second oxidation to the carboxylate, analogous to polyethylene glycol biodegradation. Since aldehydes are very reactive species, their fast oxidation to FTEOCs may have disallowed analytical detection. The ether bond is assumed to be cleaved by an enzyme called diglycolic acid dehydrogenase, which oxidizes the carbon in α -position to the carboxylic acid function and subsequently cleaves off glycosylate leaving a polyethoxylate shortened by one ethoxylate group [168].

3.3.4 Temporal evolution of FTEOC

As shown in Figure 28, FTEOCs were generated without a significant lag phase. The long FTEOC ($y > 8$) were nearly completely degraded within 18 days. It is assumed that ethoxylate shortening transforms the longer chained FTEOC to shorter-chained FTEO, which are then reoxidized to the respective FTEOC.

In stark contrast, the intensities for shorter FTEOC remained constant after approximately 20 days. A steady state, in which the reaction rates of generation and shortening of a specific congener are equal, is very unlikely, because in this case the FTEO_1C compounds should be degraded as well. Thus, it is concluded that the shorter FTEOCs were not further degraded, even within a 48 days period. In fact, concentration of FTEO_yC with $y < 9$ remained stable once generated.

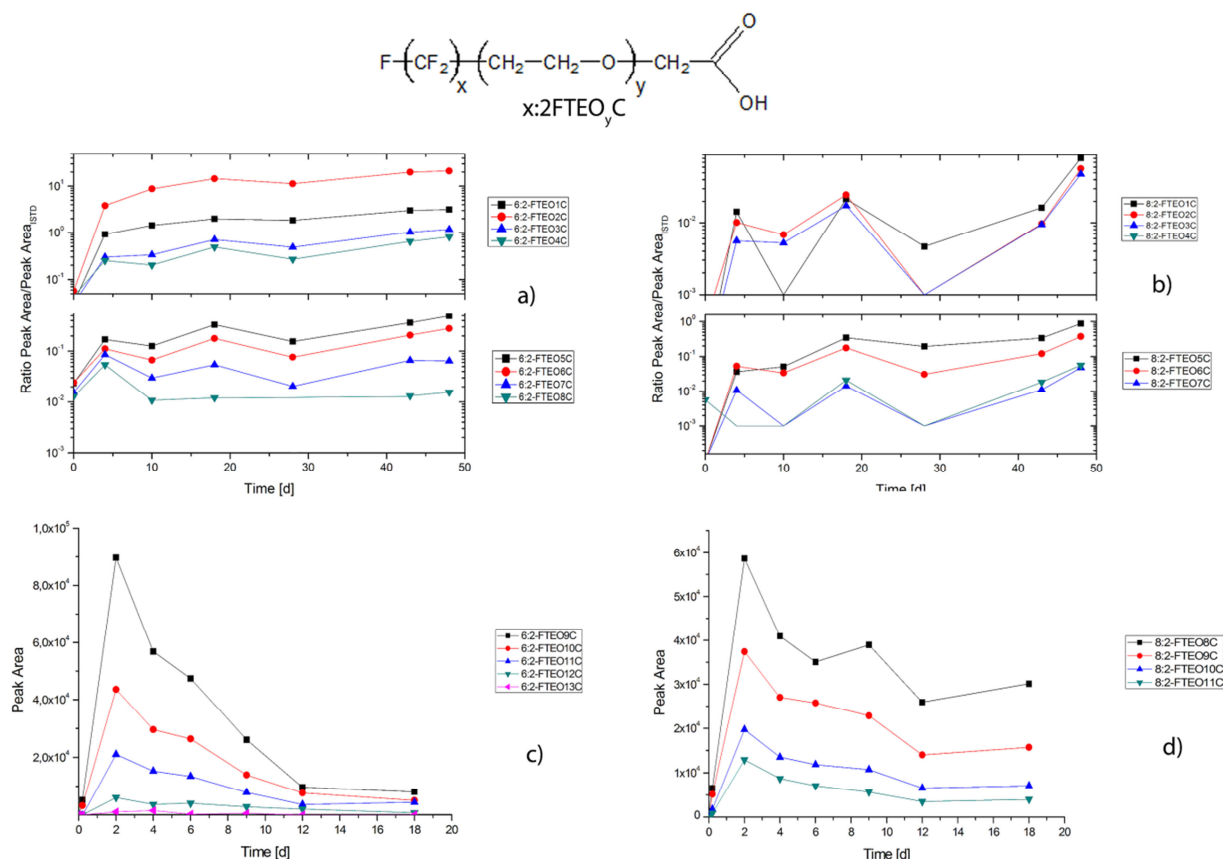


Figure 28: Temporal evolution of FTEOCs a) Peak are ratios of 6:2-FTEO₁₋₈C b) 8:2-FTEO₁₋₇C c) 6:2-FTEO₉₋₁₃C d) 8:2-FTEO₈₋₁₁C; please notice the logarithmic scale in a) and b) as well as different x-axis scales in a)/b) compared with c)/d); for further information see experimental section.

The unforeseen stability of these compounds under the given conditions is possibly caused by prevalence of perfluorocarbon chain in the lower ethoxylated molecules. This proximity of the perfluoroalkyl group might decrease the binding potential of the substrate to the active center, since the perfluoroalkyl group is both hydrophilic and hydrophobic. Similar effects of fluorinated

functional groups were observed in several other studies carried out in our laboratory [112,113]. These findings might suggest that FTEO degradation does not immediately contribute to the PFCA burden in the environment. However, it needs to be pointed out that this study was a short-term study compared with other studies that have been carried out e.g. for 8:2-FTOH in soils [42]. Nonetheless, further measurements confirming the findings were performed, which will be discussed in the following section.

3.4 Biotransformation of fractionated long-chained fluorotelomer ethoxylates

3.4.1 Two-dimensional fractionation of technical fluorotelomer ethoxylate mixture

The biotransformation experiment conducted with a technical mixture of FTEO was impeded by the presence of residual unreacted FTOHs, which lead to the formation of PFCAs during the biotransformation process.

Attempts were made to fractionate the technical mixture to as pure as possible congeners so as to investigate the fate of only one congener – preferably free of FTOHs – in a biotransformation study. In this way, it would be ultimately possible to tell apart whether the formation of PFCAs, as seen in chapter 3.3.2, is attributed only to biotransformation of residual FTOHs, or whether a part of the FTEOs is also converted to PFCAs.

In order to do so, the technical mixture was chromatographed two-dimensionally. First, the congeners were separated according to their perfluorocarbon chain length by reversed-phase column chromatography, and thereupon, the fraction containing the 8:2-FTEOs was separated under normal-phase conditions in order to separate the ethoxymers from each other (see 6.1.5.).

Even though quantification and semi-quantification across congeners is not entirely reliable when using ESI [161] due to different response factors during ionization, the relative amounts of the homologues were estimated in this manner. It is assumed that the response factors are comparable for *long-chained* ethoxymers of similar EO chain length. In this case, the distribution was calculated based on ammonium adducts of FTEO. These are presumed to be generated by chelation of the ammonium adduct by the oxygen bridges of the EO chain. Minor differences of the EO chain length are unlikely to cause major differences in the affinity to the ammonium ion and thus, in the response factor of the ethoxylates.

The fraction used for biotransformation study contained mainly 8:2-FTEO₁₄ (33.1%) and 8:2-FTEO₁₅ (60.6%) as well as minor amounts of 8:2-FTEO₁₆ (2.7%). 8:2-FTEO₆₋₁₃ were also present with contents of less than 1%. Importantly, no 8:2-FTOH could be detected in the fraction with a limit of detection (LOD) of 0.01% with respect to FTEO.

An ideal separation, i.e. fractions consisting of one ethoxymers only, could not be achieved, which is due to the relatively poor resolution of column chromatography and the pronounced similarity of the ethoxymers with high degree of ethoxylation. However, fractionation yielded a product which met the desired criteria of preferably long EO chains and a lack of any FTOH.

3.4.2 Primary degradation and adsorption

Three different experiments were carried out to study the biotransformation behavior of the fractionated FTEO, which differ mainly in the aeration frequency and technique of aeration. The most relevant parameters are summarized in Table 3.

Table 3: Summarized parameters for biotransformation experiments of fractionated FTEO

Acronym	Material	Aeration	Capturing of volatile TPs
'PP1'	PP	Regularly (1-5 d)	No
'PP2'	PP	Never	No
'G'	Glass	Regularly (1-5 d)	Yes

As expected, adsorption was significant in all experiments, even though the compounds mainly contained long EO chains. The course of the FTEO in the sterilized and non-sterilized experiments is visualized in Figure 29. After 40 days, adsorption accounted for approximately 75% in 'G' and 90% in 'PP1', respectively. Volatilization of these high molecular weight compounds is supposedly negligible. Despite the high degree of adsorption, biotransformation could be proven unambiguously, since no FTEOs were detectable after 37 d in both experiments.

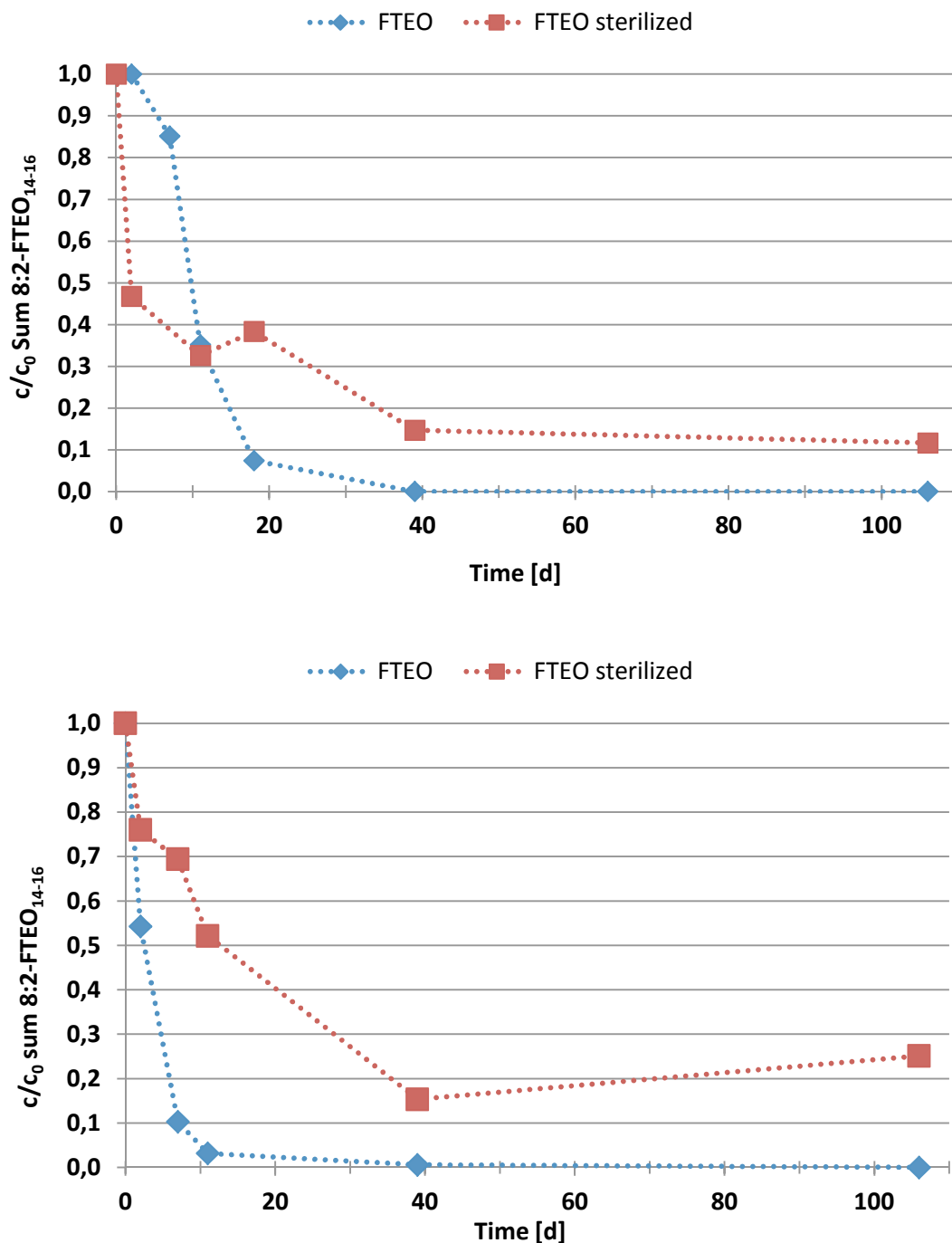


Figure 29: Course of FTEO in experiment 'PP1' (top) and 'G' (bottom) expressed as concentration of the sum of FTEO₁₄₋₁₆ divided by the sum of initial concentrations

Percentage adsorption was much more pronounced as compared with the previous experiment conducted with the technical FTEO mixture. In this experiment, adsorption of the 8:2-FTEO with the longest EO chain which was measured semi-quantitatively – 8:2-FTEO₁₃ – accounted for approximately 20%. Two effects may be the reason for this observation: Firstly, this can be explained by the different concentrations used in this experiment ($0.5 \mu\text{g FTEO mL}^{-1}$) and the one carried out with technical FTEO ($\beta = 5.7 \mu\text{g FTEO mL}^{-1}$). Secondly, the percentage of the

long-chained FTEO in the technical mixture is very low, whereas these are the only compounds present in the fractionated FTEO. Adsorption can only take place on distinct adsorption sites. Therefore, different compounds – also different FTEO congeners – will compete for these sites. Thus, adsorption of long-chained FTEO could be suppressed in the experiment with technical FTEO due to pronounced competition with other congeners.

Compared with the previous experiment, biotransformation was much slower. Likewise, this may be reasoned with reduced concentration as well as the fact that FTEO was added to the vessels in form of a methanolic solution. MeOH concentration was approximately 0.07% or 17.6 mM, which is five orders of magnitudes higher than the FTEO concentration. Thus, microorganisms are likely to consume MeOH as a first source of energy and carbon before attacking FTEOs.

3.4.3 Formation of transformation products

As explained previously, the main goal of this biotransformation experiment was the unambiguous clarification whether FTEOs may be degraded to PFCAs, which could not be proven with the experiment, in which technical grade FTEOs were used due to FTOH contamination.

Contrarily to the biotransformation experiment with the technical FTEO mixture (see chapter 3.3), PFOA formation was observed herein, as demonstrated in Figure 30. Whereas in the assays with regular aeration, only 1.4% and 2.4% conversion of FTEOs to PFOA was observed, PFOA concentration accounted for 6.5% conversion of FTEOs in the experiment with no regular aeration. These results are comparable with other studies on biotransformation of fluorotelomer-based compounds resulting in PFCAs, although 6.5% can be considered a rather high value.

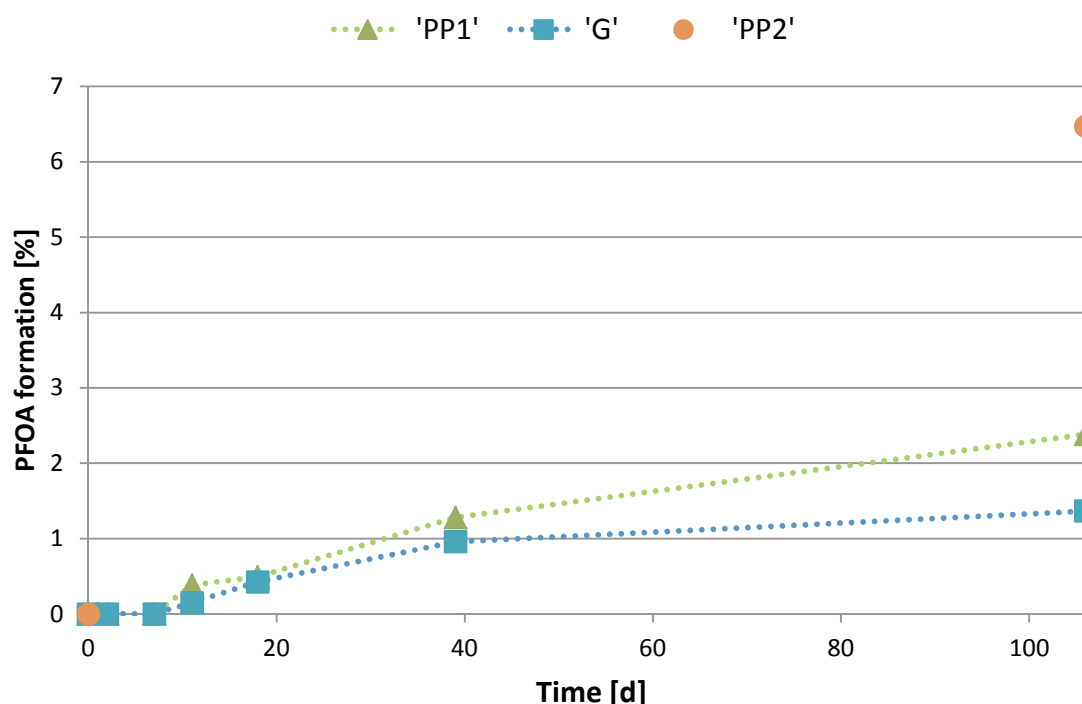


Figure 30: PFOA formation in three different biotransformation experiments with fractionated long-chained FTEOs. Formation is expressed as molar % conversion of FTEO. Please notice that in experiment 'PP2', only two points are present, since the tube was not opened until day 105.

The pronounced generation of PFOA in the closed-bottle experiment 'PP2' can be easily explained, since there are no losses of potential volatile TPs such as 8:2-FTOH, thus the entire 8:2-FTOH is available for biotransformation. The other two experiments may suffer from losses of volatile TPs in solution during aeration, which are then trapped on SPE cartridges in experiment 'G'. Unfortunately, no trapped FTOH could be detected in this test, which can be ascribed to the comparably high LOD of 8:2-FTOH (ca. 6 ng/cartridge). More effort should be put on this subject, e.g. longer sampling intervals for the cartridge leading to more enrichment of 8:2-FTOH above its LOD.

There is at least a hint that biotransformation of the FTEOs followed the FTOH transformation scheme, as depicted in Figure 3. In the samples after 106 d, 2H-PFOA (see Figure 31) was detected in MRM mode. No signal was obtained in sterile and control experiments. To confirm the identity of 2H-PFOA, the sample from 'PP2' experiment was concentrated 20-fold and studied by QqLIT-MS. The resulting enhanced product ion spectrum is shown in Figure 31.

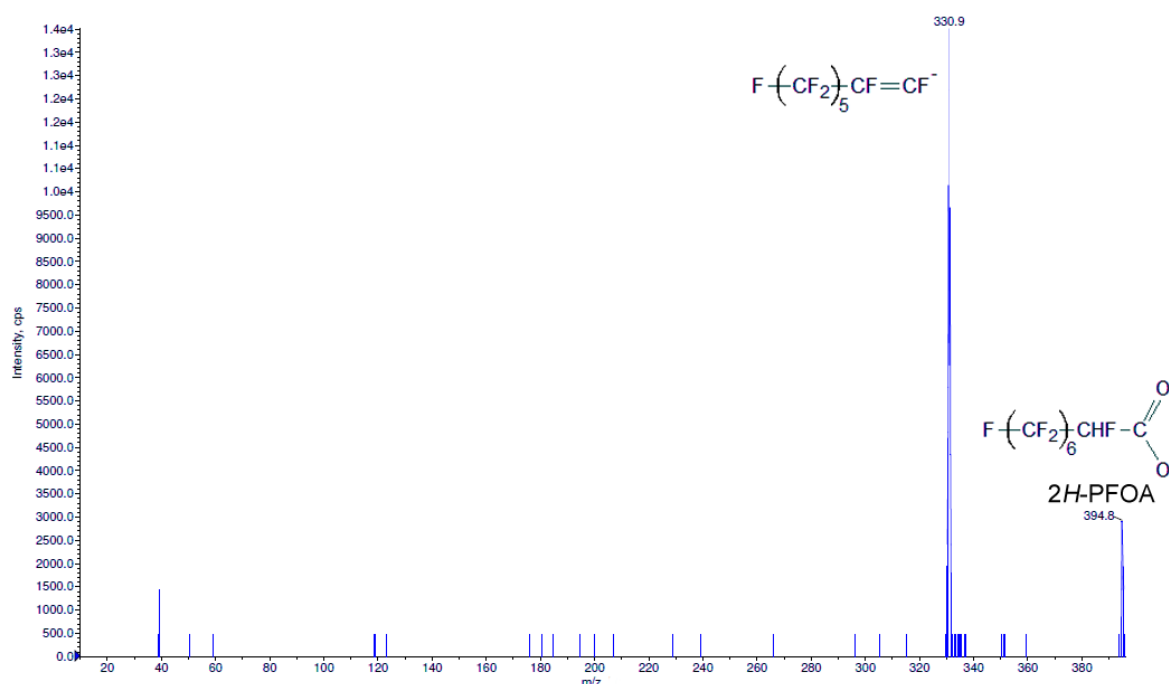


Figure 31: HPLC-ESI-MS/MS enhanced product ion spectrum of 2H-PFOA (m/z 395) and structural assignment of the product ions in a sample of 'PP2' experiment after 106 days. The sample had been previously enriched 20-fold by SPE.

Fragmentation of 2H-PFOA only yields the product ion at m/z 331 resulting from loss of HF and CO_2 from the precursor ion. Whereas this fragmentation pattern itself is not expressive, it is exactly what has been found by Wang et al. in previous studies [42]. Interestingly, the formation of an $[\text{M}-\text{H}-\text{CO}_2]^-$ ion seems to be suppressed here and only by cleavage of further HF and consequent formation of a terminal double bond, stability is high enough to allow for monitoring of the product ion.

Interestingly, only long-chained FTEOCs were detected in this experiment and no accumulation of short-chained FTEOC like 8:2-FTEOC₁C was observed, as shown in 3.3.4. These FTEOCs were measured as their ammonium adducts in positive ESI and thus, NPEO₂ could be used as the internal standard here. In fact, only 8:2-FTEOC₁₃₋₁₅C could be measured above their LOD (see Figure 32). These FTEOCs are directly derived from the FTEOs which were used in this experiment.

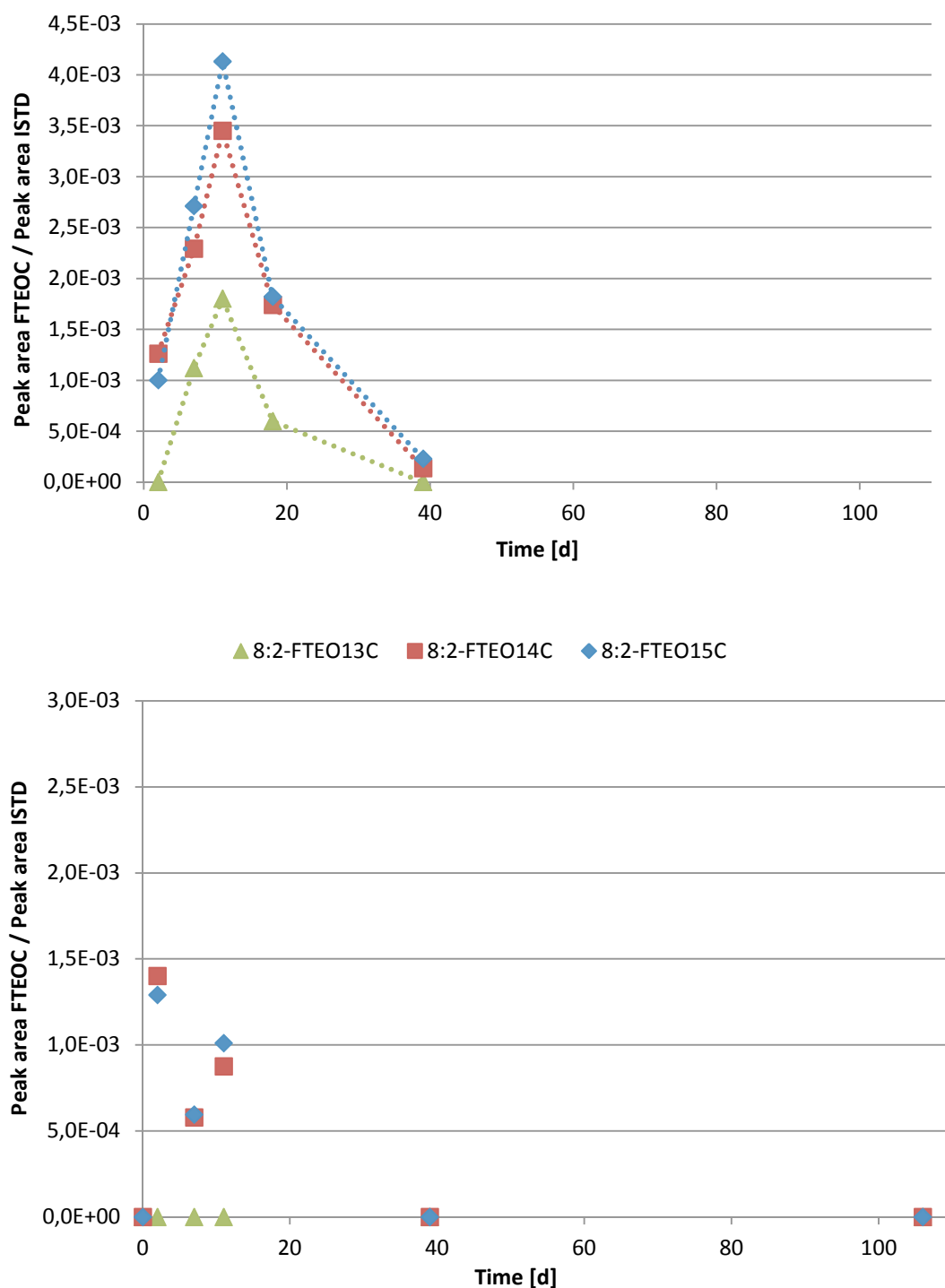


Figure 32: Temporal course of 8:2-FTEO₁₃₋₁₅C in experiment 'PP1' (top) and 'G' (bottom) expressed as the peak area ratio of the respective FTEOC and the internal standard NPEO₂

In experiment "PP1" the maximum intensity of the signal intensities is reached after 11 days, whereas in 'G', the maximum is attained after a duration of 20 days. It is worth noticing that the course of the FTEOCs is coherent with each other implying no visible dependency of the TPs in a way that one TP is generated from the other one.

This implies either very rapid transformation rates and no release of these FTEOCs or a different biotransformation pathway with cleavage in proximity to the perfluoroalkyl chain. The reasons for the complete biodegradation reaching the dead-end TP PFOA are not entirely clear, but one reason may be the relatively high concentration of these TPs in the assay with technical FTEO (see 3.30). This might have led to intoxication of the microorganisms by the carboxylic acid TPs and thus hamper further metabolic activities. Another explanation might be the inocula used in the different experiments. Although taken from the same source (but at a different time), differences in the microorganisms cannot be prevented unless microbiological purification steps and confirmation of the species present are performed. A further reason might be the use of MeOH to dissolve the fractionated FTEO, which may lead to reinforced growth of one or several species being able to degrade FTEOC to FTOH and thus PFOA.

3.4.4 Conclusion

The biotransformation of FTEOs was investigated with two different approaches. The first experiment revealed biotransformation to the respective carboxylate and further shortening by cleavage of the ethoxylate groups is supposed to occur. For carboxylates with a short ethoxylate chain, no further biotransformation occurs rendering them recalcitrant in the experiment.

In stark contrast, in a series of other experiment carried out with previously fractionated 8:2-FTEO₁₄₋₁₆, pronounced formation of PFOA was observed, particularly in a closed-bottle test, where a molar conversion of 6.5% was measured after 105 d. The FTEOCs associated with the test compounds were detected and it was shown that these are transformed. However, no short-chained FTEOCs were detected which suggests that the biotransformation route is different from the abovementioned one. The exact route remains unknown, but one of the known TPs of 8:2-FTOH, namely 2H-PFOA, was detected and its presence confirmed by mass spectrometric fragmentation analysis.

3.5 Monitoring of PFASs in environmental samples

3.5.1 Synthesis of standards

The stability of long-chained FTEOCs in the biodegradation experiment of the technical FTEO mixture suggests that these compounds may be present in environmental compartments. Waste water treatment plants receiving industrial waste water are a well-known entry path of organic pollutants into natural compartments [4,8]. Therefore, a selective and sensitive method was developed based on solid phase extraction (SPE) on weak anion exchanger and HPLC-ESI-MS/MS. In order to provide quantitative data, 6:2-FTEO₁C and 8:2-FTEO₁C were successfully

synthesized by Williamson etherification of the respective FTOH and bromoacetic acid (Figure 33) to be used as standards.

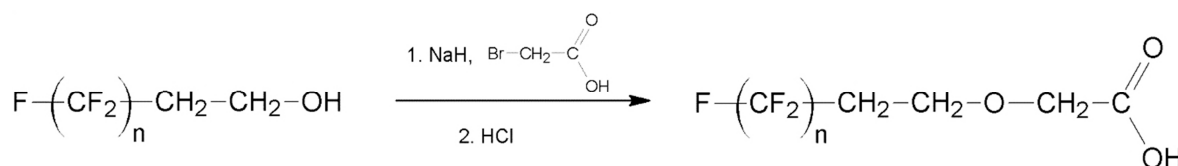


Figure 33: Synthetic route to FTEO₁C; n = 6,8

In principle, higher ethoxylated FTEOCs can be synthesized in the same manner by subsequent extension (etherification with bromoacetic acid) and reduction with LiAlH₄. However, this procedure is highly laborious and particularly complex when considering clean-up of mixtures of fluorinated compounds. Even clean-up of the crude FTEO₁C products was complex since common procedures such as column chromatography failed due to irreversible adsorption to the stationary phase. As a consequence, synthesis of higher ethoxylated FTEOCs was not performed.

3.5.2 Monitoring of FTEO₁Cs and classic PFASs in environmental samples

A method based on solid-phase extraction (SPE) on polymeric sorbent exhibiting weak anion-exchanger properties was developed for FTEO₁Cs, PFCAs and PFSA. Quantitation via HPLC-ESI-MS/MS suffered from strong memory effects in the instrument, especially for 8:2-FTEO₁C, which apparently sorbed to parts in the HPLC system and desorbed at higher organic solvent fraction. This entailed blank values of several ng mL⁻¹ and complicated quantification tremendously. In contrast, 6:2-FTEO₁C was much less problematic showing no or carryover.

The regularly measured PFCAs and PFSA were also included in this study in order to obtain an overview of the PFAS contamination of Hessian WWTP effluents and polluted river waters. These WWTP effluent samples were two-week mixed samples, the surface water samples were grab samples. All samples were from the state of Hesse, Germany. The method developed was valid for the matrix investigated showing high recoveries for nearly all compounds investigated (see Annex, Table 21). Unfortunately, PFBA and PFPeA could not be included in this monitoring campaign at that time due to very low recoveries, which can be explained by the high polarity of PFBA leading to weak retention on RP materials. Furthermore, broad chromatographic peak shapes implying low peak heights are a result of the high polarity. All this prevented reliable measurement in these rather contaminated matrices.

The main problem arises by the fact that for long-chained PFASs, high content of organic solvent in the storage HPLC vials is necessary to overcome pronounced adsorption of the analytes. Thus, the analytes were reconstituted in a mixture of water and MeOH at equal shares. This in turn is problematic for compounds with low retention times in HPLC. These

compounds are poorly retained in the beginning of the HPLC gradient, when dissolved in mixtures with higher organic solvent fraction than that in the initial mobile phase. When only PFBA is measured, this problem can be easily circumvented by dissolving the sample in water only, because in contrast to long-chained PFCAs and PFSAAs, PFBA does not show adsorption to the HPLC vials (data not shown).

The data obtained are summarized in Table 4 underlining the ubiquitous detection of PFASs. Several compounds, namely PFHxA, PFHeA, PFOA, PFBS, PFHxS and PFOS were detected in all of the samples. The novel TPs 6:2-FTEO₁C and 8:2-FTEO₁C were measured above the LOQ in one WWTP sample, where 8:2-FTEO₁C was the compound of highest concentration with 51 ng L⁻¹, and 6:2-FTEO₁C was measured at 15 ng L⁻¹. Apart from WWTP-14, 6:2-FTEO₁C was detected in two samples and 8:2-FTEO₁C was detected in another sample below their respective LOQ.

Table 4: PFAS concentrations measured in selected WWTP effluents and river waters; concentrations in ng L⁻¹

Location	Type of Water	6:2-FTE ₁ OC	8:2-FTEO ₁ C	PFHxA	PFHeA	PFOA	PFNA	PFDA	PFBS	PFHxS	PFOS	PFDS	Sum PFAS
River-1	River	n.d.	n.d.	20.3	7.1	19.6	2.0	2.8	32.7	35.0	159	<LOQ	278
River-2	River	n.d.	n.d.	40.3	11.1	23.5	2.2	2.9	72.0	290	320	0.575	762
River-3	River	<LOQ	n.d.	9.0	4.6	9.9	1.3	1.2	5.6	21.3	29.7	n.d.	83
River-4	River	n.d.	n.d.	2.0	1.7	3.0	<LOQ	n.d.	1.4	0.9	2.2	n.d.	11
WWTP-1	WTPP effluent	n.d.	n.d.	11.1	3.8	19.7	1.5	1.6	4.3	1.8	3.0	n.d.	47
WWTP-2	WTPP effluent	n.d.	n.d.	12.9	6.4	13.4	4.3	2.1	4.9	3.1	13.7	n.d.	61
WWTP-3	WTPP effluent	n.d.	n.d.	4.8	2.2	7.0	0.9	<LOQ	1.3	1.4	1.7	n.d.	19
WWTP-4	WTPP effluent	n.d.	n.d.	3.1	2.6	6.8	0.8	<LOQ	1.4	5.2	4.2	n.d.	24
WWTP-5	WTPP effluent	n.d.	n.d.	23.3	6.7	24.7	3.1	4.8	1.2	0.8	1.4	n.d.	66
WWTP-6	WTPP effluent	n.d.	n.d.	3.7	2.4	7.3	1.0	<LOQ	1.2	1.6	5.5	<LOQ	23
WWTP-7	WTPP effluent	n.d.	n.d.	5.5	1.8	6.9	0.7	1.7	2.0	2.7	3.3	<LOQ	24
WWTP-8	WTPP effluent	n.d.	n.d.	6.8	3.2	10.9	1.2	1.9	0.7	1.3	6.7	n.d.	33
WWTP-9	WTPP effluent	n.d.	n.d.	3.6	1.8	6.9	0.9	2.0	0.5	2.2	32.6	n.d.	50
WWTP-10	WTPP effluent	n.d.	n.d.	5.7	3.5	7.0	1.3	1.2	1.8	2.2	2.9	n.d.	26
WWTP-11	WTPP effluent	n.d.	n.d.	3.1	2.2	6.9	0.5	<LOQ	2.8	6.2	2.6	<LOQ	24
WWTP-12	WTPP effluent	n.d.	n.d.	3.3	1.2	7.1	0.5	<LOQ	3.2	1.9	2.5	n.d.	20
WWTP-13	WTPP effluent	n.d.	n.d.	2.5	1.5	6.1	0.8	n.d.	1.4	1.4	1.2	n.d.	15
WWTP-14	WTPP effluent	15.1	51	15.9	8.5	30.6	2.3	11.8	3.4	5.0	2.7	n.d.	146
WWTP-15	WTPP effluent	n.d.	<LOQ	4.5	1.9	7.4	0.7	n.d.	1.3	2.1	1.8	n.d.	20
WWTP-16	WTPP effluent	n.d.	n.d.	5.2	2.5	10.3	1.9	2.2	1.6	3.7	14.8	n.d.	42
WWTP-17	WTPP effluent	<LOQ	n.d.	8.3	4.0	7.9	1.0	<LOQ	3.1	1.2	1.5	n.d.	27

n.d. = not detected

<LOQ = lower than limit of quantification

As mentioned before, higher ethoxylated FTEOC show more pronounced response in positive ESI polarity and were thus analyzed in a different method. Validation of this method was not performed since no standards were available or synthesized. In the sample WWTP-14, higher ethoxylated FTEOCs were detected as well, namely 8:2-FTEO₄₋₈C (see Figure 34). Retention times matched those found in samples from the biodegradation test, and the transitions $[M + NH_4]^+ \rightarrow m/z$ 491 and $[M + NH_4]^+ \rightarrow m/z$ 579 were monitored to confirm the identity of the compounds present.

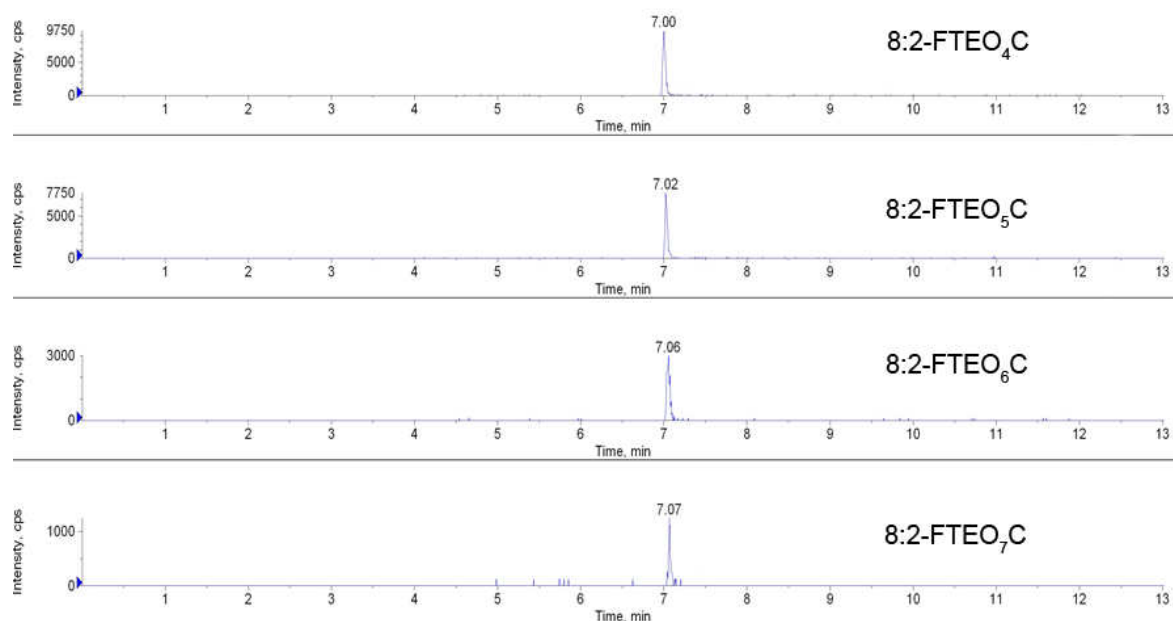


Figure 34: LC-(+)-ESI-MS/MS XICs for 8:2-FTEO₄₋₇C in sample from WWTP-14; measured in MRM mode monitoring the transitions for $[M + NH_4]^+ \rightarrow m/z$ 491

As far as WWTP samples are concerned, summed up concentrations of PFASs were in the two-digit $ng\ L^{-1}$ range, except for the sample for WWTP-14, where high concentrations of 8:2-FTEO₁C made the concentrations exceed the $100\ ng\ L^{-1}$ level. Except for three samples, PFOA occurred at highest concentrations. Linear correlation showed fairly high coefficients of determination between concentrations of C₆-C₉ PFCAs, as depicted in Table 5. For all other combinations of compounds, no such statistically significant correlation could be found. For PFOA and PFOS, correlation was extremely low with $R^2 = 0.04$. These correlations may give a hint that the origins for PFCA pollution may be derived from conjoint sources, whereas different sources may be the reason for PFSA pollution. Also correlations among PFASs do not show any statistically significant correlation.

Table 5: Linear coefficient of determination (R^2) between concentrations of PFHxA, PFHpA, PFOA and PFNA in WWTP samples

	PFHpA	PFOA	PFNA
PFHxA	0.77	0.76	0.58
PFHpA		0.75	0.61
PFOA			0.36

The lowest of all PFAS concentrations with only 11 ng L⁻¹ total PFASs were detected in one surface water sample. Other river samples showed high concentrations with up to 762 ng L⁻¹, which was mainly caused by high concentrations of PFHxS and PFOS. These surface waters are known to be fed with high fraction of industrial wastewaters.

In order to validate the results, they were verified by interlaboratory comparison with a certified method (Gellrich, internal communication), which had successfully participated in interlaboratory tests for PFAS analysis. Results generally differed not more than 20%.

3.5.3 Conclusion

The presence of 6:2-FTEO₁C and 8:2-FTEO₁C, two previously detected TPs from FTEO biotransformation, should be investigated in environmental samples by SPE and HPLC-ESI-MS/MS. Analytical standards were synthesized from 6:2-FTOH and 8:2-FTOH by Williamson etherification.

A monitoring study in 17 WWTP samples and 4 surface water samples showed one positive finding above the respective LOQs for both compounds as well as three detections below the LOQ. Furthermore, higher FTEOCs were detected in one sample, but could not be quantified due to a lack of analytical standard. The low number of positive samples suggests that FTEOCs indeed may be transformed, as shown in chapter 3.4.

Classic PFASs, such as PFCAs and PFSAAs were also included in the monitoring campaign and their nearly ubiquitous presence was confirmed. Whereas the sum of PFAS concentrations most WWTP samples was in the range of 15-150 ng L⁻¹, high concentrations up to 762 ng L⁻¹ were measured in a polluted river sample. Statistical analysis revealed high linear correlation factors for the concentrations of PFHxA, PFHpA, PFOA and PFNA, but no high correlation between any other compound pair.

3.6 Biotransformation of novel fluorosurfactant building blocks

3.6.1 3-(Trifluoromethoxy)-1-propanol

3-(Trifluoromethoxy)propan-1-ol (TFMPrOH, see Figure 35) is a novel TFM-based building block designed to be used in innovative fluorosurfactants. In order to discover whether it is appropriate as an environmentally friendly building block for higher molecular weight fluorosurfactants, its biodegradation potential was studied.

Initially, a method for the parent compound TFMPrOH was aimed at. Thus, a method based on HPLC-ESI/MS should be established. Its mass spectrometric behavior was studied by MS/MS and it could be shown that it forms a proton adduct at m/z 145. CID fragmentation leads to the trifluoromethoxy cation at m/z 85 and the trifluoromethyl(methylen)oxonium ion at m/z 99 (see Figure 35). Surprisingly, no cleavage of water was observed.

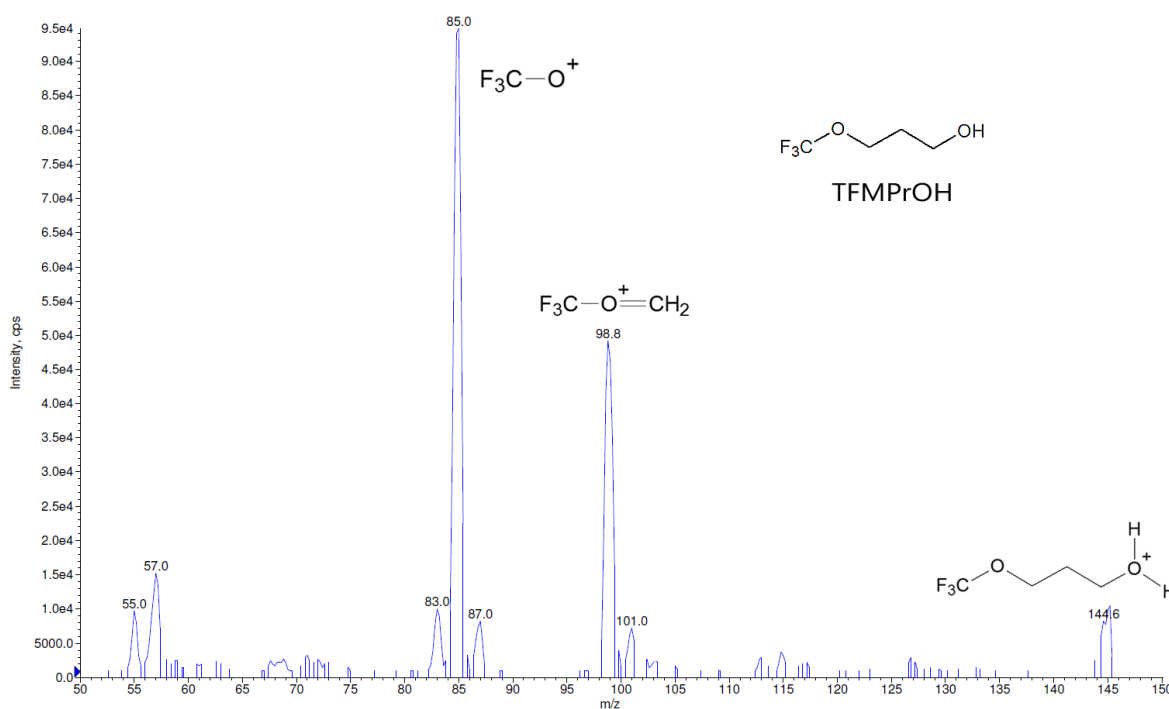


Figure 35: (+)ESI-MS/MS product ion spectrum of TFMPrOH and proposed structures of the product ions

Even though mass spectrometric signals were observed for TFMPrOH, the study of biotransformation suffered from the incapability of measuring the initial compound by HPLC-ESI-MS. The reason for this could be suppression of the very weakly basic aliphatic hydroxyl group due to early elution from the HPLC and ion suppression effects. Also GC-EI/MS was tested as a commonly applied method for volatile analytes, but no signal of the initial compound was observed either.

Thus, focus was set on TPs, mainly on acidic ones, since alcohols are commonly transformed to acids under aerobic conditions. Since TFM-substituted compounds had been previously

measured in our laboratory [111], negative ion CID fragmentation of compounds bearing this functional group were known. Fragmentation usually yielded the trifluoromethanolate anion at m/z 85. In such cases, precursor ion scans can give valuable information about unknown compounds. As shown in Figure 36, a compound with an m/z ratio of 157 could be detected.

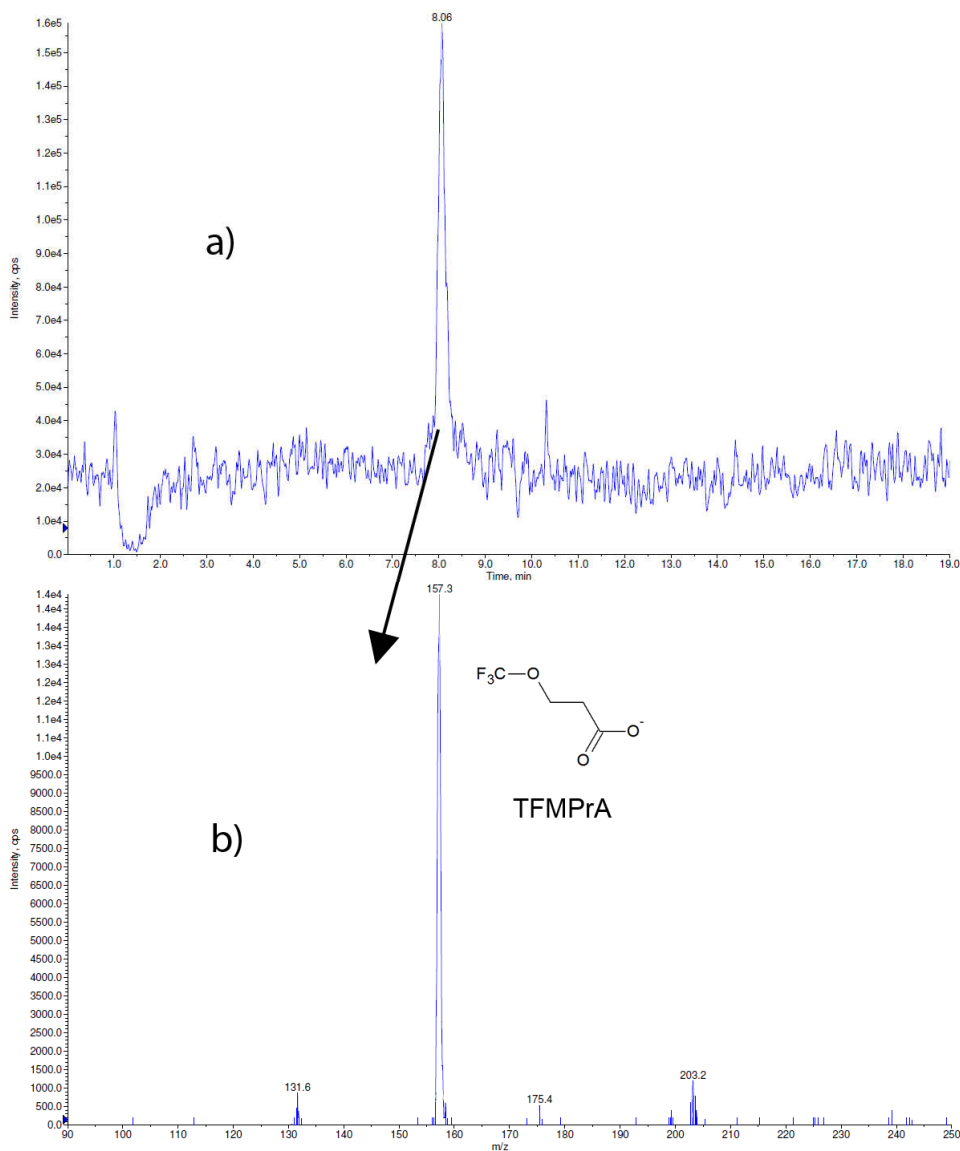


Figure 36: HPLC(-)ESI-MS/MS precursor ion scan of a TFMPPrOH biodegradation sample after seven days a) TIC b) precursor ion spectrum at 8.1 min suggesting the presence of TFMPPrA (m/z 157)

The molecular mass of 158 Da (m/z 157 in negative ESI polarity) suggests an ω -oxidized TP, namely 3-trifluoromethoxypropionic acid (TFMPPrA). Furthermore, a second TP at m/z 129 was detected (data not shown), which suggests the presence of trifluoromethyl carbonate (TFMC). Their structure was verified by 'enhanced product ion scans' using the LIT (see Figure 37).

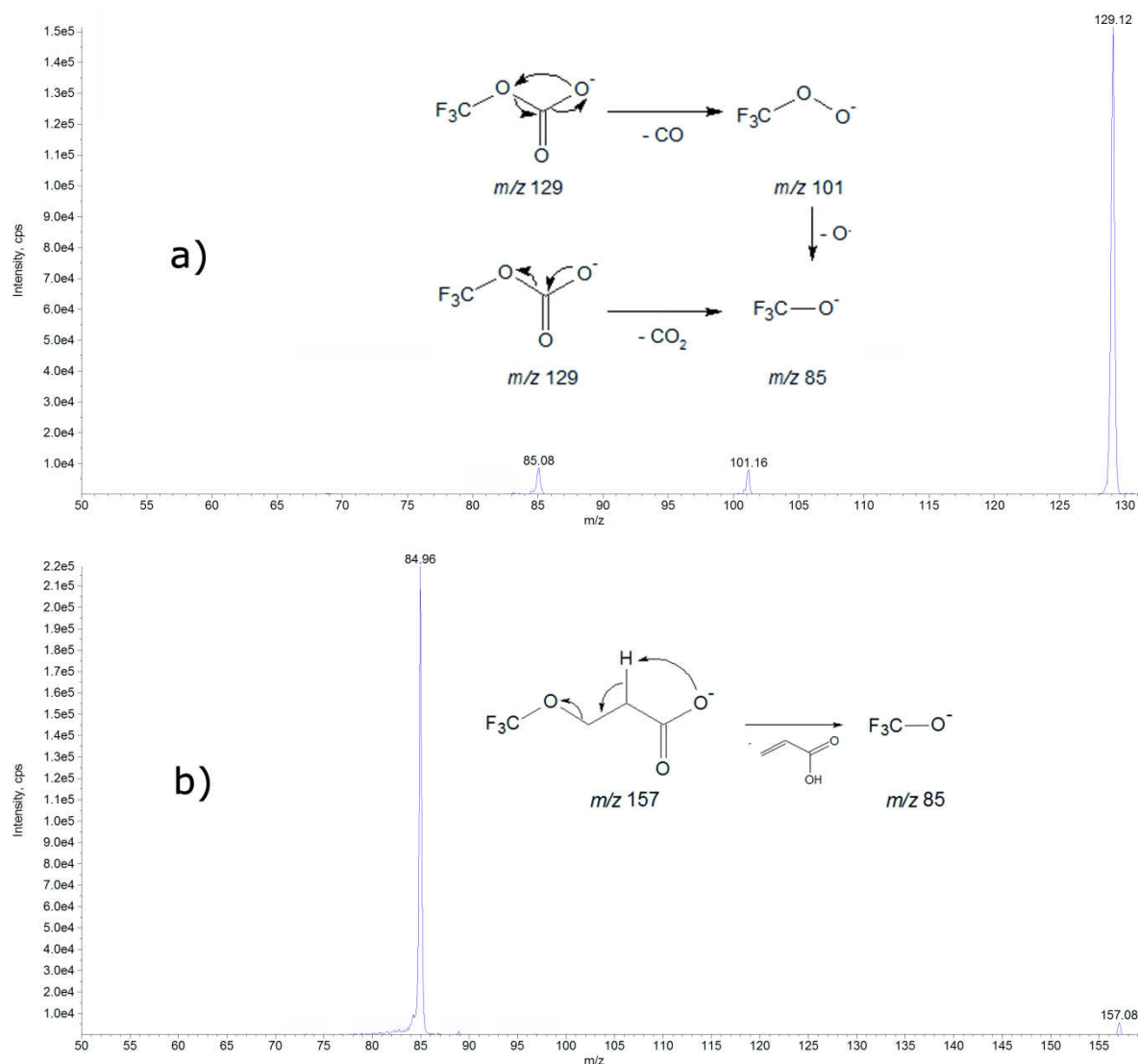


Figure 37: HPLC-ESI-MS/MS enhanced product ion spectrum of a) TFMC and b) TFMPra. Tentative fragmentation pathways are presented

Both molecules yield the trifluoromethanolate ion at m/z 85, which had been known from previous measurements [111]. This is generated by loss of carbon dioxide (in case of TFMC) and acrylic acid (in case of TFMPra), respectively. TFMC further leads to the trifluoromethyl peroxide anion at m/z 101, which could not be generated from TFMPra or any other substance containing the TFM moiety. The reason for this might be accounted for by the mechanism of formation, which is tentatively explained by a concerted rearrangement of the free carboxylic oxygen atom to the esterified oxygen atom under simultaneous cleavage of carbon monoxide.

Although the trifluoromethanolate ion can be formed directly from TFMC by cleavage of carbon dioxide, as explained above, cleavage of atomic oxygen from the trifluoromethyl peroxide anion might also contribute to the signal obtained for trifluoromethanolate. The signal intensities for product ions of TFMC are very low and could not be substantially increased by increasing the

collision energy (CE). This is an odd behavior and might be due to the formation of lower-mass product ions, whose m/z ratio is below the instrumental cut-off mass at m/z 50.

The temporal evolution of the two TPs detected was investigated in SIM mode and is presented in Figure 38.

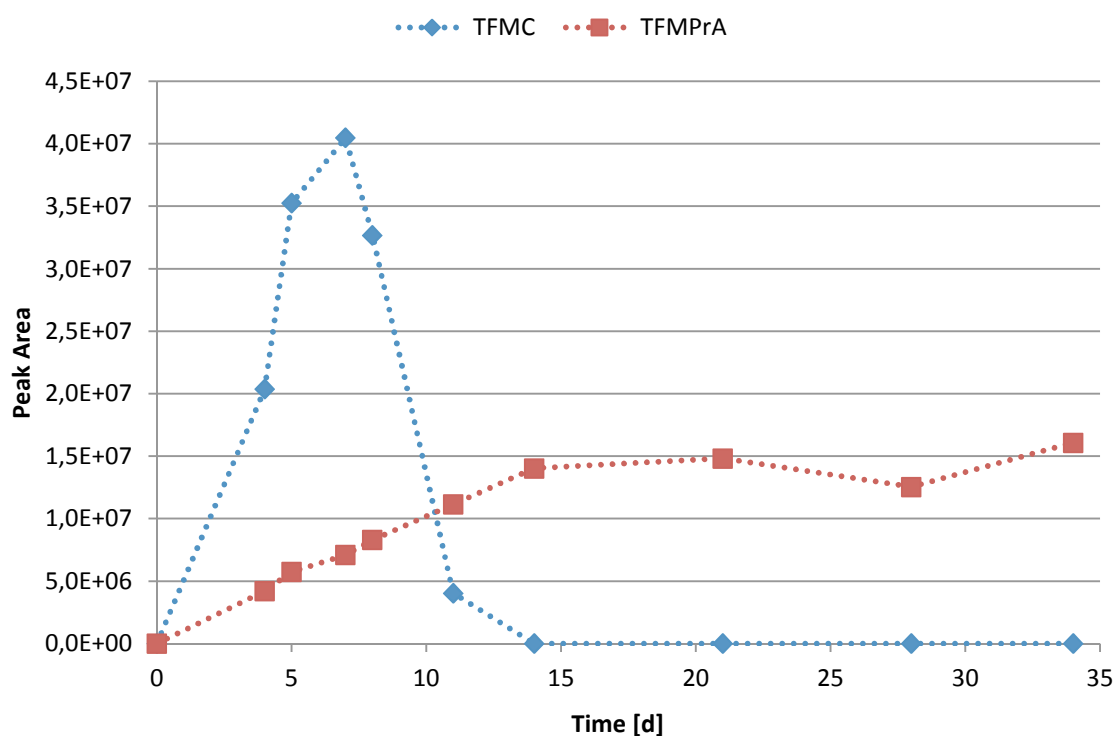


Figure 38: Temporal evolution of TFMPROH metabolites TFMPPrA and TFMC

As described in the experimental section, the assay was kept closed for the first four days to prevent volatilization of TFMPROH or volatile TPs. Therefore, no data points are available for this time period. Both TFMC and TFMPPrA showed a rapid increase in peak area. Whereas TFMC reached a maximum after seven days and was then completely metabolized showing no signal anymore after 14 days, TFMPPrA reached a plateau just at this time point. Even after 34 days, no decline was observed suggesting stability of this TP.

This is rather striking since so far, it was assumed that longer ω -TFM substituted alkanolic acids were degraded by β -oxidation until free unstable TFMeOH is generated [111]. The stability of TFMPPrA was also verified by different fluoride measurements, as depicted in Table 6. Besides free inorganic fluoride, fluoride was also measured after UV decomposition of organic compounds, and after filtration and UV decomposition. This is a very valuable method to affirm results obtained from organic analysis, such as LC-ESI-MS, and to determine the percentage of biotransformation pathways in case of multiple pathways [112].

Table 6: Fluoride determination in TFMP_{Pr}OH biodegradation samples after 77 days

	$\beta(\text{F}^-)$ [mg L ⁻¹]	Fluoride [% theoretical]
Inorganic	0.75	19.3
After filtration and UV decomposition	4.5	116
After UV decomposition of the whole sample	4.54	117

Herein, fluoride measurement after UV decomposition yielded 4.54 mg L⁻¹, which is ca. 17% higher than the theoretical value, as calculated based on the initially spiked test compound. This value can be explained by evaporation of the biodegradation medium, which was kept at room temperature and aerated regularly, which contributes to evaporation of water. Assumed that only biotransformation of TFMCA can lead to inorganic fluoride and that this pathway yields 100% fluoride, it accounts for $0.75/4.54 = 16.5\%$.

The tentative biotransformation pathway is presented in Figure 39. The first pathway is likely achieved by ω -oxidation of the hydroxyl group to the carboxylate group yielding TFMP_{Pr}OH, probably via the short-lived aldehyde.

It must be highlighted that the pathway leading to TFMC and inorganic fluoride is highly speculative, since no intermediate TPs were detected. However, it can be stated that no link between TFMP_{Pr}A and the second pathway can be established, since the HPLC-MS signal of TFMP_{Pr}A remains constant. Thus, a second reaction to TFMP_{Pr}OH must have occurred. The detection of TFMC must have been preceded by an insertion of an oxygen atom into the alkyl chain. A possible but unproven explanation is given as follows:

A likely reaction would be the in-chain oxidation of the alkyl chain in proximity to the TFM group yielding the hemiacetal **I** (Figure 39), which can be oxidized to the ester **II**. A Bayer-Villiger-oxidation-like reaction, that is an insertion of an oxygen atom leading to the 3-hydroxypropyl trifluoromethyl carbonate **III**. Ester hydrolysis leads to TFMC, which subsequently decays to TFMeOH and thus finally yields fluoride and carbon dioxide [111,114,115].

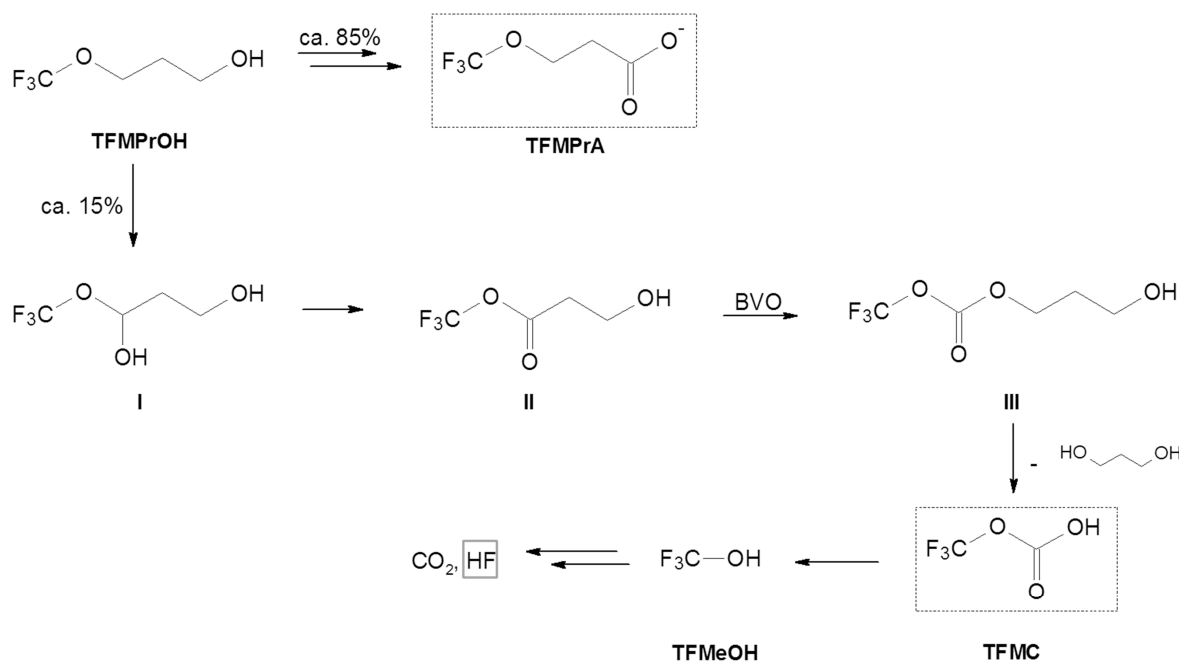


Figure 39: Proposed biotransformation pathways of TFMPPrOH; BVO = Bayer-Villiger oxidation. The dotted rectangles indicate the TPs identified by HPLC-ESI-MS/MS

As the ω -oxidation pathway apparently proceeds much more rapidly, the 3-(trifluoromethoxy)propoxy group does not seem to be a good candidate for environmentally friendly substitutes of PFASs assuming that in potential fluorosurfactants, the 3-(trifluoromethoxy)propoxy group is cleaved off as TFMPPrOH. Whereas at least approximately 15% of the organically bound fluorine can be released as inorganic fluoride, the long-term fate and effects of the remaining TFMPPrA are questionable and cannot be assessed without further laborious studies.

3.6.2 6-(Trifluoromethoxy)-1-hexanol

Biodegradation of a building block with considerable structural similarity to TFMPPrOH was investigated in a different experiment. The substance under investigation is 6-(trifluoromethoxy)hexan-1-ol (TFMHxOH, see Figure 40). Herein, the similarities and differences between these two compounds with respect to biotransformation should be scrutinized.

TFMHxOH biotransformation was initially investigated by the temporal assessment of the test compound itself. In this case it was possible by measuring the protonated molecule $[\text{M} + \text{H}]^+$ in positive ESI mode.

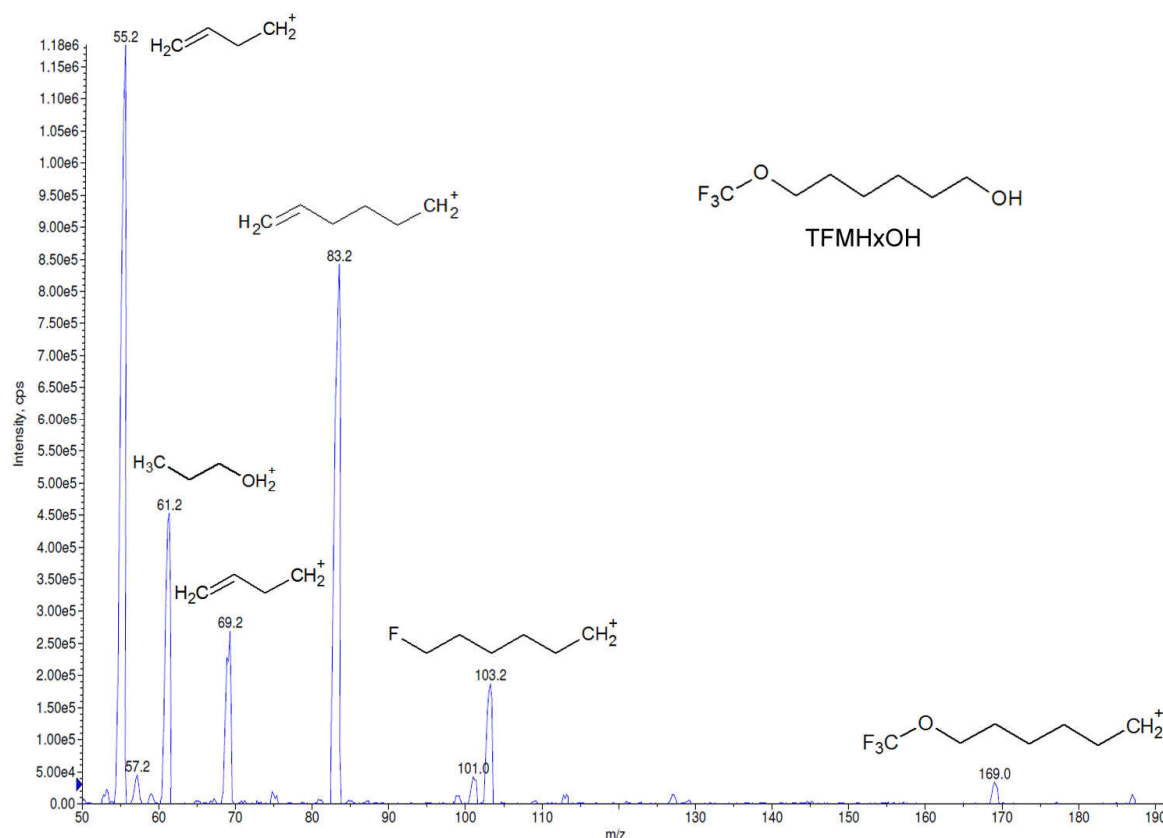


Figure 40: (+)-ESI-MS/MS CID enhanced product ion spectrum of TFMHxOH and tentative assignment of chemical structures

Fragmentation is initiated by loss of water which is characteristic of alcohol fragmentation from protonated molecules. This results in a carbenium ion species, which further decays by loss of the TFM group in form of TFM₂OH leading to an unsaturated carbenium ion at m/z 83. Cleavage of ethane results in the unsaturated carbenium ion at m/z 55. These two ions were used as transitions for MRM during HPLC-MS measurement.

A different fragmentation pathway of the carbenium ion at m/z 169 leads to the formation of the product ion at m/z 103. The proposed fragmentation pathway is shown schematically in Figure 41. It is proposed that fragmentation involves a rearrangement where a fluorine atom of the trifluoromethyl group migrates to the methylene group in α -position to the ether bridge, while carbonyl difluoride is concertedly cleaved off. The carbenium ion at m/z 83 can also be generated through loss of HF from m/z 103.

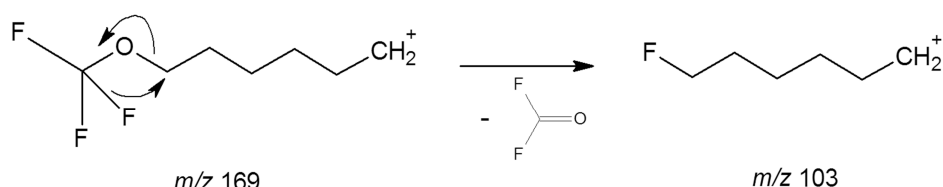


Figure 41: Proposed fragmentation mechanism of the carbenium ion at m/z 169 deriving from TFMHxOH. Fragmentation is achieved by cleaving off carbonyl difluoride to form the fragment at m/z 103. This process represents a fluorine migration

The assay suffers from loss of TFMHxOH also in the sterilized experiment. This can be reasoned by a mixture of volatilization and adsorption to glassware or particles present in the inoculum. Yet, the reduction in concentration of TFMHxOH proceeds more rapidly in the active assay indicating biotransformation. Complete primary transformation was achieved after 11 days.

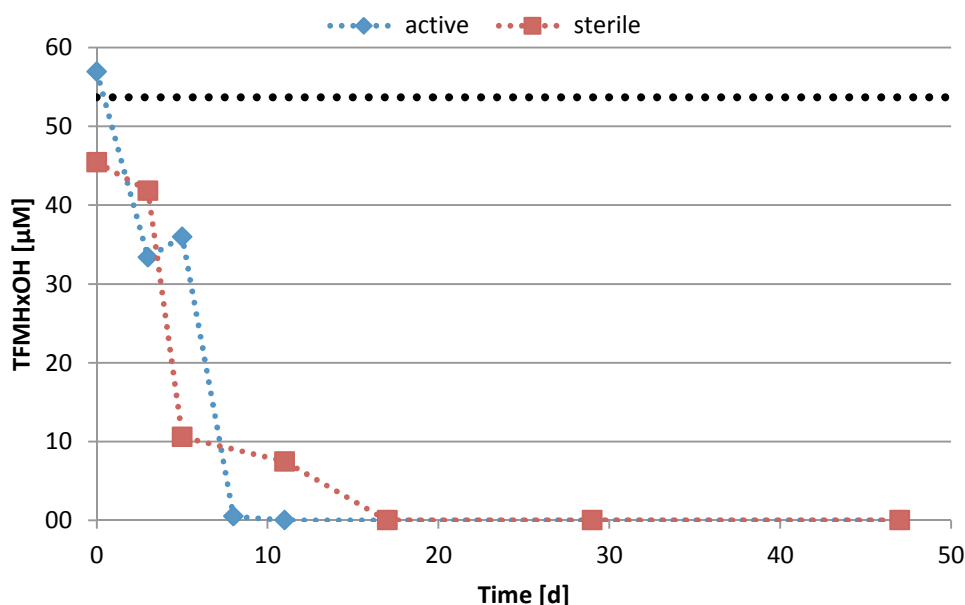


Figure 42: Temporal evolution of TFMHxOH in active and sterile biodegradation assays. The black dotted line indicates the theoretical initial TFMHxOH concentration

Similarly to the biodegradation assay of TFMPROH, two acidic TPs were detected for TFMHxOH as well, in this case 6-(trifluoromethoxy)hexanoic acid (TFMHxA) and again TFMC.

The identity of TFMHxA was verified by performing product ion scans (see Figure 43). Besides the common trifluoromethanolate anion at m/z 85, a second product ion at m/z 113 was observed, which represents an ω -unsaturated alkenoic acid anion. This ion results from cleavage of neutral TFMeOH from the precursor ion. This ion species had also been detected in measurements of Peschka *et al.* when examining 10-(trifluoromethoxy)decane-1-sulfonate [111].

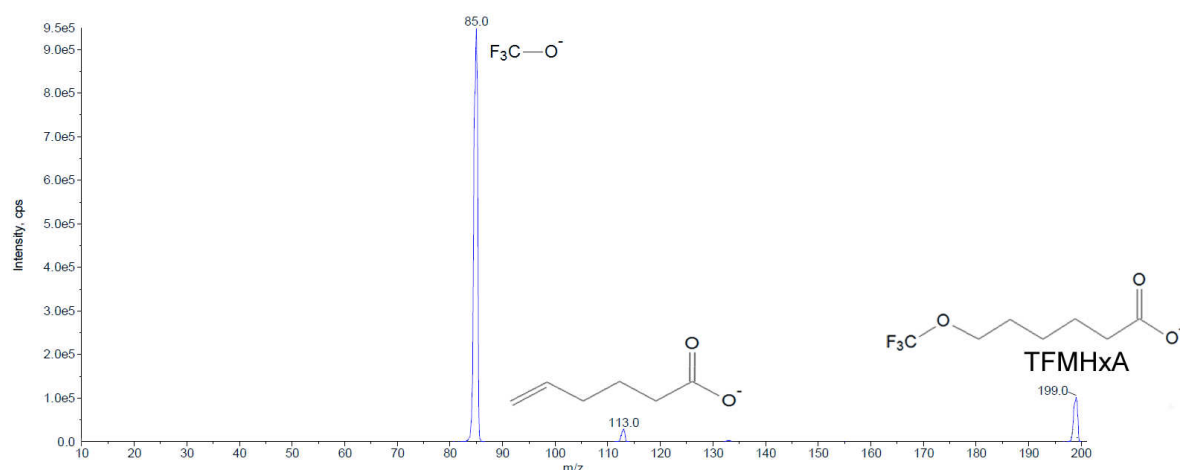


Figure 43: (-)-ESI-MS/MS product ion scan of TFMHxA and proposed structures of the product ions.

Both compounds were generated rapidly with TFMC showing a maximum after only four days and no signal after 11 days, as shown in Figure 44. TFMHxA showed its maximum concentration after five days and - in stark contrast to TFMPPrA – was completely degraded afterwards showing complete degradation also after 11 days. The main difference between the degradation between TFMPPrOH and TFMHxOH, however, is a very high degree of defluorination, which represents almost 100% of the theoretical value.

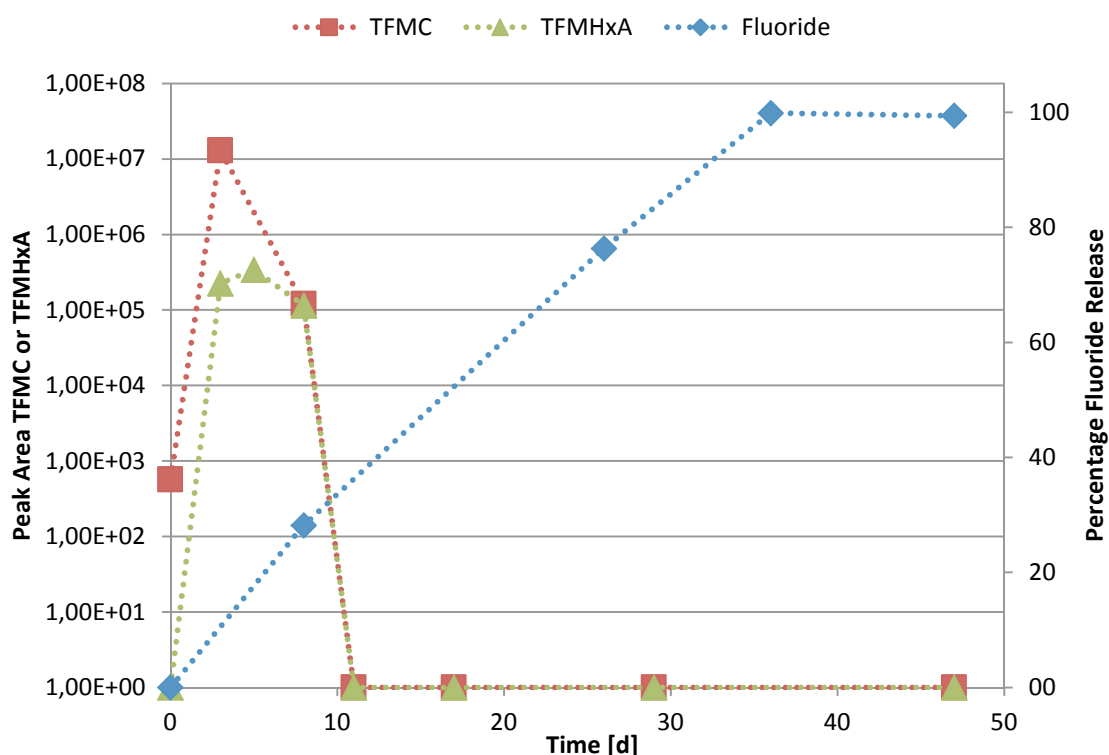


Figure 44: Temporal evolution of TFMHxOH TPs TFMC and TFMHxA (Please note the logarithmic scale) and percentage fluoride release.

This difference in mineralization yield between TFMP_{Pr}OH and TFMH_xOH cannot be entirely explained, because no further TPs were detected in the course of this experiment. Thus, the degradation pathways presented here are speculative (see Figure 45). It is assumed that TFMH_xOH is oxidized in a similar manner as TFMP_{Pr}OH, leading to TFMH_xA. Unlike TFMP_{Pr}A, TFMH_xA is further metabolized, as suggested in Figure 45.

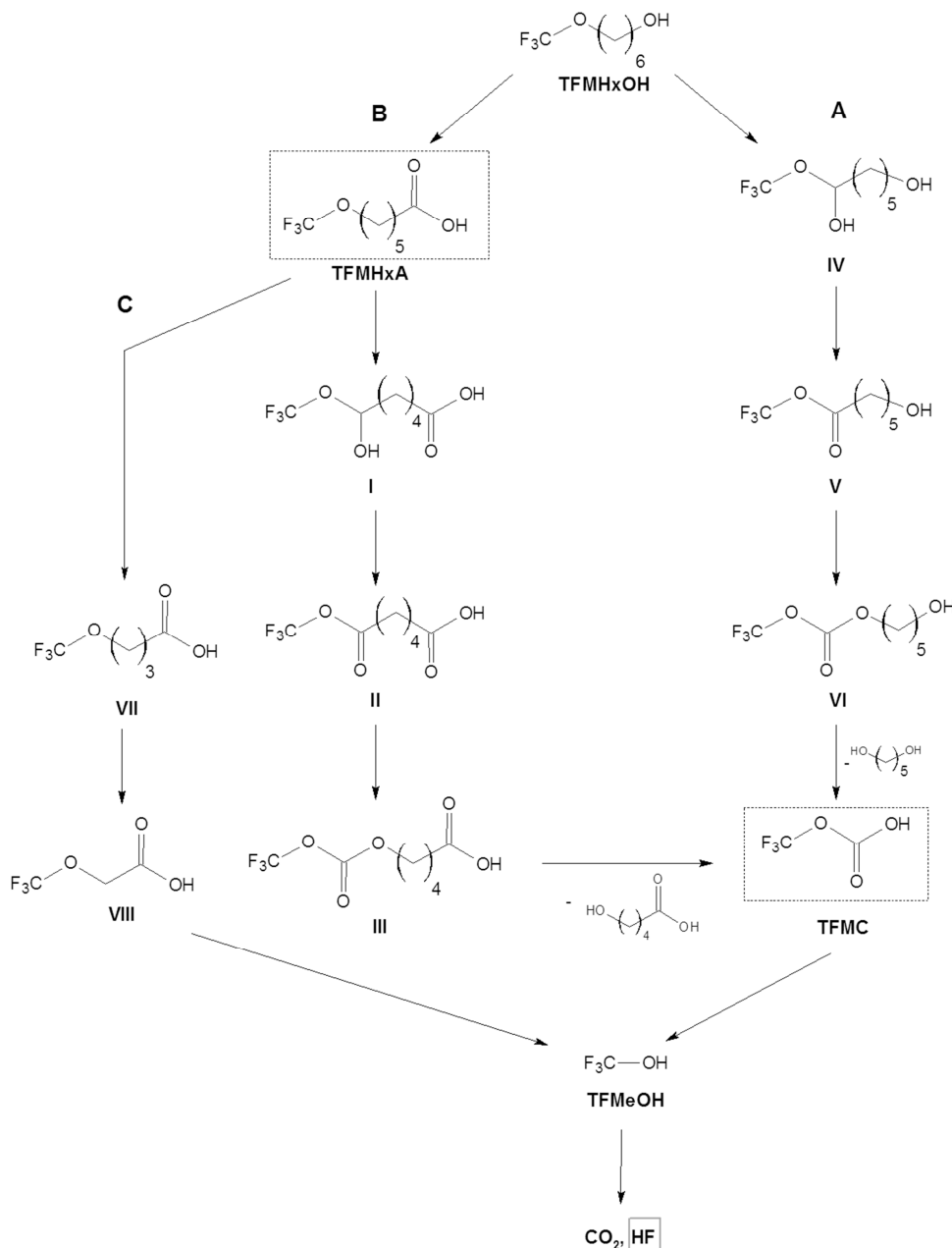


Figure 45: Proposed degradation pathways of TFMH_xOH; please note that possible transitions from the pathway A to pathway B are possible by oxidation, but not depicted here. For further information, see text. The dotted rectangles indicate the TPs identified by HPLC-ESI-MS/MS.

Since both TFMH_xA and TFMH_xO are degraded and no further organic TP was detected, it is hypothesized that both TPs – TFMH_xA and TFMH_xO – yield inorganic fluoride. Since the curves for TFMH_xA and TFMH_xO are not temporally shifted, no link between the two TPs can be made,

and yet, TFMHxA is assumed to be transformed to TFMC in a similar manner as TFMHxOH is metabolized itself. That is, TFMHxA is oxidized to an alcohol in proximity to the ether group yielding the hemiacetal **I**. In turn, this is oxidized to the ester **II**, which is oxidized to the Bayer-Villiger-like carbonate **III**. Ester hydrolysis yields TFMC, which is eventually mineralized, as explained in chapter 3.6.1. Simultaneously, oxidation of TFMHxOH analogous to TFMPrOH proceeds. Even more complex, TPs **IV** to **VI** might be oxidized to the respective molecule on the left side. For instance, **IV** might be oxidized to **I** by oxidation of the terminal hydroxyl group to the carboxylic acid. Which of these reactions take place, cannot be scrutinized here, because some of these reactions are supposed to proceed very rapidly.

Alternatively, TFMHxA might be shortened via β -oxidation, as was initially presumed during the investigation of 10-(trifluoromethoxy)decane-1-sulfonate by Peschka *et al.* [111] and also in other studies carried out with ω -substituted alkane-1-sulfonates, which were initially transformed to the respective carboxylates [112,113]. This would involve the two transient TPs **VII** and **VIII** (Figure 45) as shown in pathway C, whereas subsequent β -oxidation of **VIII** would contribute to the presence of TFMeOH. However, a β -oxidation pathway would not form TFMC, indicating that at least one other transformation pathway must be involved. Also, the TPs **VII** and **VIII** were not detected by MS, even though they are supposed to be analytes that can be detected in negative ESI mode in a straightforward way.

The complete defluorination renders the 6-(trifluoromethoxy)hex-1-oxo group a promising building block for environmentally friendly substitutes of PFASs, as explained in chapter 1.6. If implemented in larger organic molecules via an ester bridge, TFMHxOH is a likely TP, either by enzymatic or chemical ester hydrolysis. The transformation rate is probably highly depending on the structure of the whole molecule, especially when it comes to enzymatic cleavage, where steric aspects may predominate.

3.6.3 1-(2,2,3,3,4,4,4-Heptafluorobutoxy)-propan-2-ol

The C₃ perfluorinated building block 1-(2,2,3,3,4,4,4-heptafluorobutoxy)-propan-2-ol (HFBPrOH, see Figure 49) is a promising moiety for high-performance applications. The biodegradation potential of this moiety was assessed by assaying the actual alcohol, which may be formed by hydrolysis when connected to a larger molecule in form of a carboxylic acid ester.

The test compound itself was found to be measurable as the acetate adduct [M + acetate]⁻, similar to FTOHs. In order to increase reproducibility of the quantitative analysis, 6:2-FTOH was used as an internal standard. MS was operated in MRM mode by monitoring the transition [M + acetate]⁻ → acetate⁻.

As illustrated in Figure 46, the initially spiked concentration cannot be verified by HPLC-MS measurement, which is probably due to pronounced adsorption of the compound. In the

sterilized assay, concentration is stable around 20 μM for 45 days, whereas in the active assay, a drop in concentration can be observed after 8 days. Primary biodegradation then proceeds rapidly so that almost no HFBPrOH can be detected after 14 days.

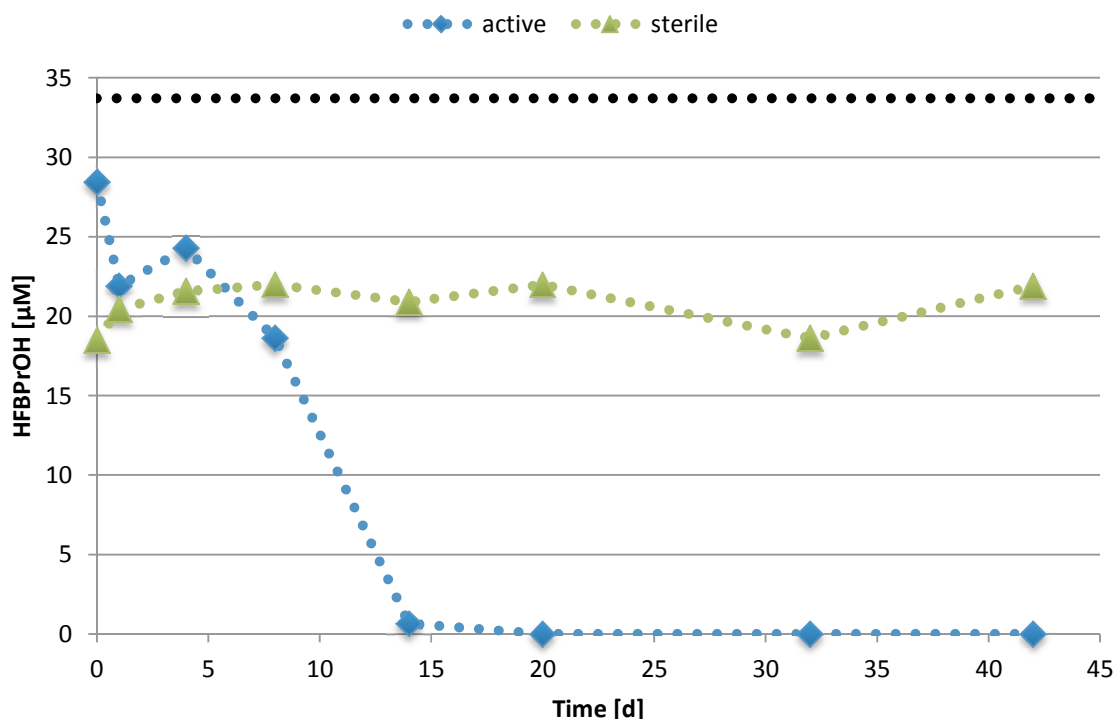


Figure 46: Temporal evolution of HFBPrOH in the active and sterilized biodegradation assay. The dotted line indicates the theoretical initial concentration

Different TPs were sought for by HPLC-MS/MS in MRM mode or SIM mode with subsequent verification by MS/MS measurements. Non-acidic potential TPs, i.e. those carrying only ether and hydroxyl groups, were monitored by $[\text{M} + \text{acetate}]^- \rightarrow \text{acetate}^-$. The structures of these TPs are summarized in Table 20 in the Annex.

Several TPs were observed, which were neither detected in the sterilized nor in the control assay. Unfortunately, for non-acidic compounds, no further verification of the structure could be made, since acetate adducts always fragment by decay to an acetate ion and the neutral molecule it was attached to, which disallows measurement by MS. For HFBAA however, verification by MS/MS experiments was carried out.

The product ion spectrum of HFBAA is presented in Figure 47. It is suggested that HFBAA initially fragments by loss of HF leading to the unsaturated molecule at m/z 237, which further decays to the alkenolate at m/z 179 and the well-known perfluoropropyl anion at m/z 169, which is known from PFCA fragmentation [154]. A different pathway leads to the aldehyde derivative at m/z 197.

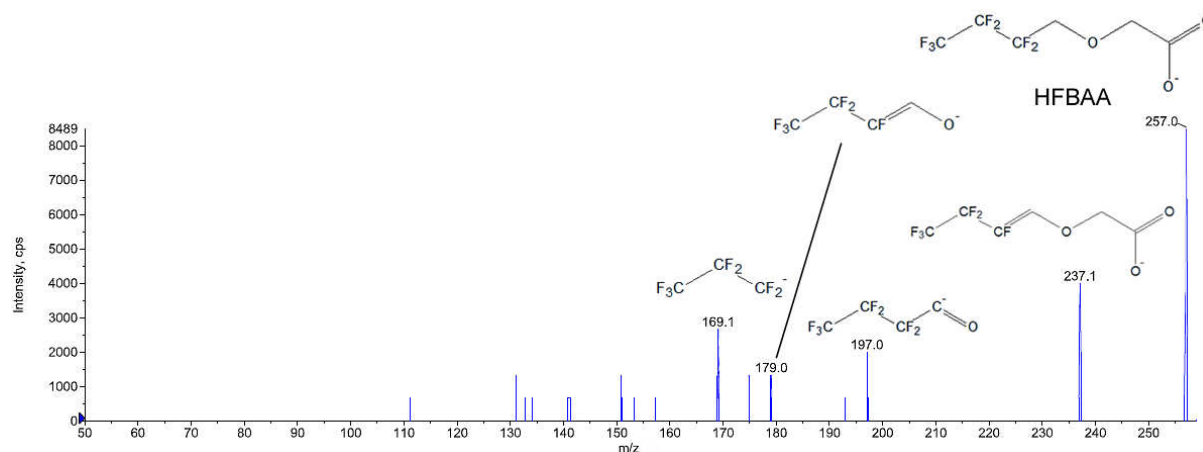


Figure 47: HPLC(-)ESI-MS/MS product ion spectrum of HFBA and proposed structures of product ions

HFBA fragmentation gives rise to several conclusions because of its structural similarity to FTEO₁Cs (see 3.2). Both are based on a perfluoroalkyl chain (although of different lengths), one or two methylene bridges, an ether function and an acetic acid moiety. In contrast to FTEO₁C, the perfluoroalkyl chain is separated from the ether bridge by only one methylene group, rather than two of them.

Despite the structural similarity, HFBA only loses one molecule of HF. This emphasizes the significance of the ethylene bridge for the manifold loss of HF, because in theory, four molecules of HF could be cleaved off from HFBA. Also similarities in the CID fragmentation pathway are obvious: Unlike many other aliphatic acids, HFBA as well as FTEOCs do not fragment by loss of carbon dioxide, which is probably related to the ether bridge located in β -position to the carboxylic acid moiety. It can be concluded that this ether bridge destabilizes a potentially generated carbanion by the positive mesomeric effect of the oxygen atom, and hence, its formation is suppressed.

The structure of HFBOHPa could not be verified. In SIM mode, a compound with an m/z of 287 was detected and its temporal evolution recorded as shown in Figure 48. However, no significant product ions were detected due to the rather low intensity. Thus, its structure was only postulated but not confirmed.

The temporal evolution of the TPs is illustrated in Figure 48. The first signals were obtained after four days, except for PFBA, which was only measured above the LOD after 14 days, which suggests that PFBA is generated via an indirect pathway, i.e. via other transient TPs.

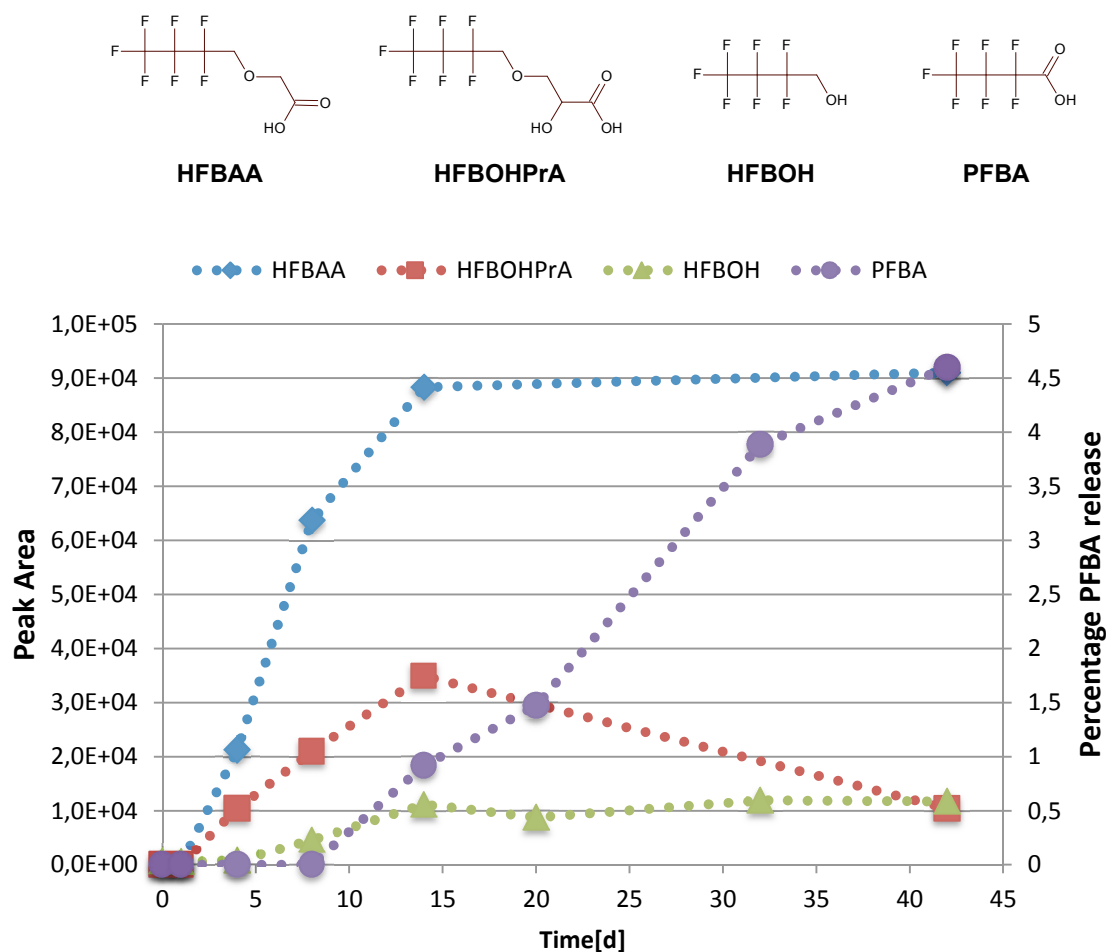


Figure 48: Temporal evolution of HFBPrOH TPs and their structural formulae

It is suggested that PFBA is generated by a complex pathway as shown in Figure 49. Beginning with a hydroxylation in α -position (Figure 49, I) and subsequent oxidation of this terminal hydroxyl group to the aldehyde (Figure 49, II) and the lactic acid derivative 3-(2,2,3,3,4,4,4-heptafluorobutoxy)-2-hydroxypropanoic acid (HFBOHPrA). This in turn is transformed to (2,2,3,3,4,4,4-heptafluorobutoxy)acetic acid (HFBA) by α -oxidation. β -oxidation then leads to 2,2,3,3,4,4,4-heptafluorobutan-1-ol (HFBOH), which is easily converted to PFBA, probably via an aldehyde. As expected, PFBA seems to be the dead-end TP of HFBPrOH, since no fluoride could be measured by IC.

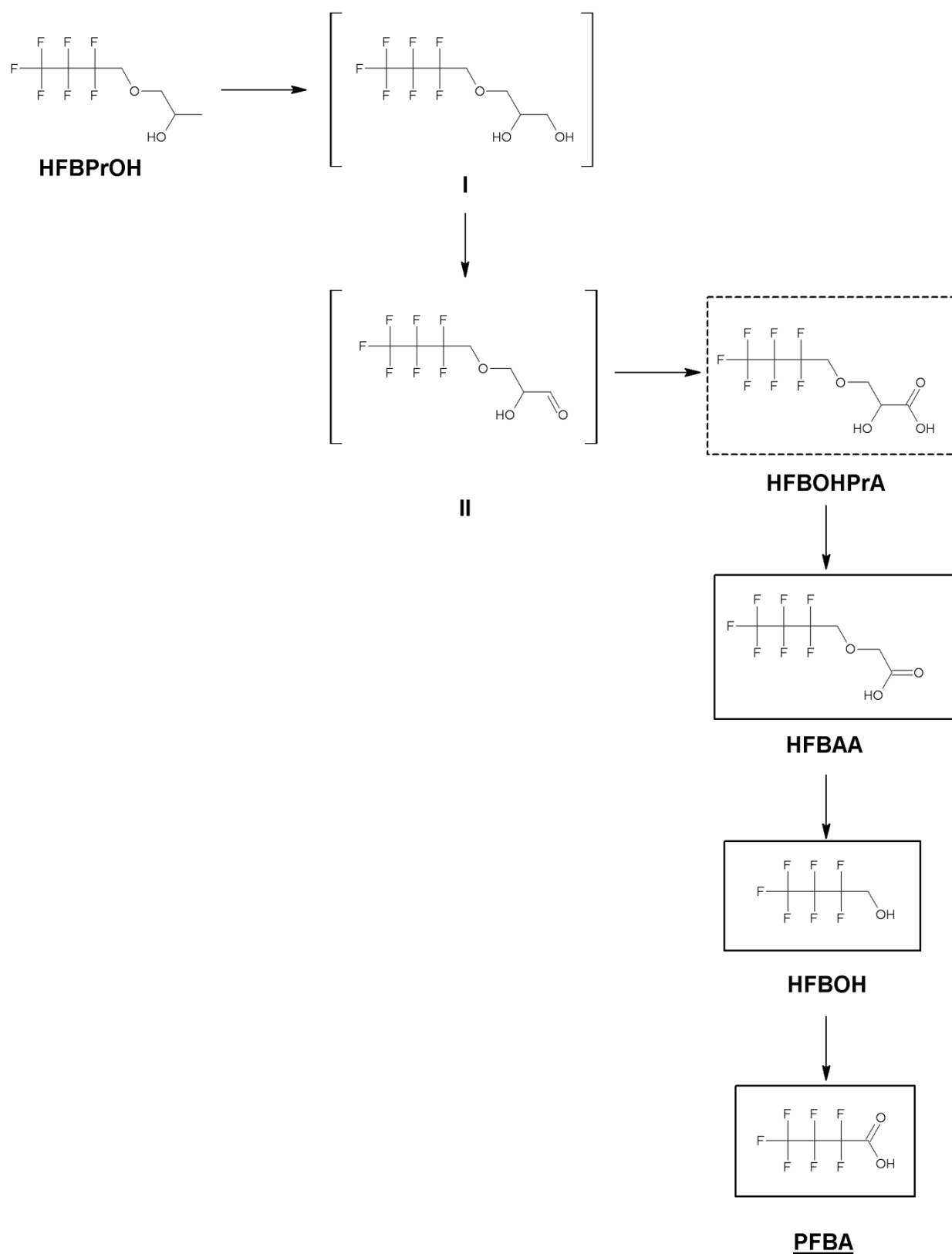


Figure 49: Proposed degradation scheme of HFBPrOH with PFBA being the dead-end transformation product. The dotted rectangle indicates detection of the TP without confirmation by MS/MS, the rectangle indicates detected and confirmed TPs. TPs I and II were not detected.

Unfortunately, the TPs I and II could not be detected, but such highly reductive and therefore transient TPs like aldehydes or vicinal diols are rarely detected in degradation studies, when no lysis of cell walls is carried out.

Under environmental aspects, HFBPrOH exhibits both advantageous and disadvantageous properties. Whereas it does not lead to precarious and hazardous TPs like PFOS or PFOA, it is also not mineralized, which would represent the ideal case.

Instead, the already known substance PFBA is generated via biotransformation. PFBA is not a novel PFAS and has been detected in environmental samples for several years [75,169-172]. PFBA has been proven to exhibit less environmentally adverse effects, such as less pronounced bioaccumulation and toxicity [173]. Ecotoxicity of PFBA has been restricted to one publication so far, but it also gives rise to dramatically reduced effects when compared with longer chained PFCAs [98]. Due to the scarcity of ecotoxicological data, PFBA was investigated in this respect, as presented in chapter 3.7.

Whereas most properties and environmental effects of short-chained PFASs seem to be more benign as compared with the long-chained counterparts, there is at least one drawback of the short perfluoroalkyl chain: their mobility. It was shown that PFBA is not retained during soil passage, which in turn indicates that it may easily reach groundwater and eventually drinking water [174], where it has already been detected [71,72,75], sometimes even up to the $\mu\text{g L}^{-1}$ range.

Thus, it can be stated that this C_3 perfluorinated building block represents a compromise between satisfactory performance and acceptable environmental and toxicological profile.

3.6.4 Conclusion

Three different candidates for building blocks in novel fluorinated surfactants were investigated with respect to their degradability.

The two structurally related TFMPPrOH and TFMHxOH showed analogous TPs, but a drastic difference in mineralization yield, expressed as the molar percentage release of fluoride. This is due to the stability of TFMPPrA, the carboxylic acid associated to TFMPPrOH, which is generated in the biotransformation assay, but not further degraded. In contrast to this, the carboxylic acid derivative of TFMHxOH, TFMHxA, is generated and completely transformed to other TPs. Thus, TFMHxOH biotransformation yielded nearly 100% of the theoretical fluoride, but TFMPPrOH was only defluorinated to an extent of 15%. It is assumed that the remaining 85% are accumulated in form of TFMPPrA.

The biotransformation pathways of TFMHxOH and TFMPPrOH were analyzed by combination of the observations for both compounds. Given the fact that TFMPPrA is not further degraded, but nonetheless, TFMC is formed during the biotransformation experiment of TFMPPrOH, an

insertion of oxygen into the alkyl chain must have occurred. Thus, it was hypothesized that TFMP_{OH} undergoes two different transformation pathways, one leading to non-degradable TFMP_A, and another one initiated by in-chain oxidation in proximity to the TFM group. The resulting hemiacetal is oxidized to the ester, which is then oxidized to a carbonic acid derivative by a Bayer-Villiger-like oxidation. This would be easily cleaved to form TFMC.

The transformation pathways are supposed to occur coherently for TFMH_xOH. However, the question remains, why TFMH_xA is further degraded and what the mechanism behind its degradation is. Several transformation pathways are to be considered: β -oxidation would lead to C₄ and C₂ acids. Another transformation pathway would include consecutive oxidation of the alkyl chain in proximity to the TFM group, just as proposed for TFMP_{OH} degradation. Unfortunately, none of the proposed theoretical intermediates was detected by HPLC-ESI/MS, although at least the acidic TPs are presumed to be measurable with good response.

The reason for the dissimilar stability of TFMH_xA and TFMP_A cannot be entirely explained with the knowledge obtained. One possible reason is a different accessibility of the methylene group in vicinity to the TFM group in the two compounds. In TFMP_A, the methylene group might be shielded by the polar carboxylic acid function, so that it cannot be hydroxylated enzymatically, which in turn could be possible in TFMH_xA, where the carboxylic acid group is separated by more methylene groups. However, these suggestions remain highly speculative unless one or several transient TPs are detected in other studies.

3.7 Ecotoxicological assessment of selected PFASs

3.7.1 Selection of compounds and background

The environmental effects of several PFASs were studied by two standardized ecotoxicity tests. The investigations were part of the two EU projects ECO-itn (see www.eco-itn.eu) and CADASTER (see www.cadaster.eu). These projects aim to develop more reliable computational models to calculate environmental properties of organic compounds, including environmentally important compounds, such as triazoles and benzotriazoles, polybrominated diphenylethers and also PFASs. In order to develop these models, several compounds were selected based on design of experiment and principle component analysis. One of the dead-end TPs of previous biodegradation measurements, namely PFBA, was included in the study.

Previous experiments with PFBA in the laboratory had resulted in EC₅₀ values much lower than expected from comparison with other PFCAs (data not shown). Thus, experiments were repeated to verify the validity of these results.

3.7.2 Acute toxicity on *Pseudokirchneriella subcapitata*

The acute effects on the green algae *Pseudokirchneriella subcapitata* were examined with the help of a standardized test, which measures the effects of chemicals on the photosynthetic system of the plant with the help of a pulsed-amperometric fluorometer.

It was discovered that problems associated with previous measurements were related to the acidity of the perfluorinated carboxylic acids. Even though problems in assessing the pKa values of perfluorinated acids exist [135], the pKa values are likely to be very low due to the electron-withdrawing effects of the perfluoroalkyl chain implying their occurrence in the environment mainly in the anionic form.

The ecotoxicity test to algae is carried out in so-called 'Dutch standard water' (DSW), which has a buffer capacity of approximately 1.4 mM. Therefore, concentrations of any perfluorinated acid above 1.4 mM will cause a major drop in pH, which in turn is likely to lead to a toxic effect on the algae. To circumvent this problem, the stock solutions used for the assay were adjusted to a pH above 8, just like the test medium, with hydrochloric acid and sodium hydroxide solution.

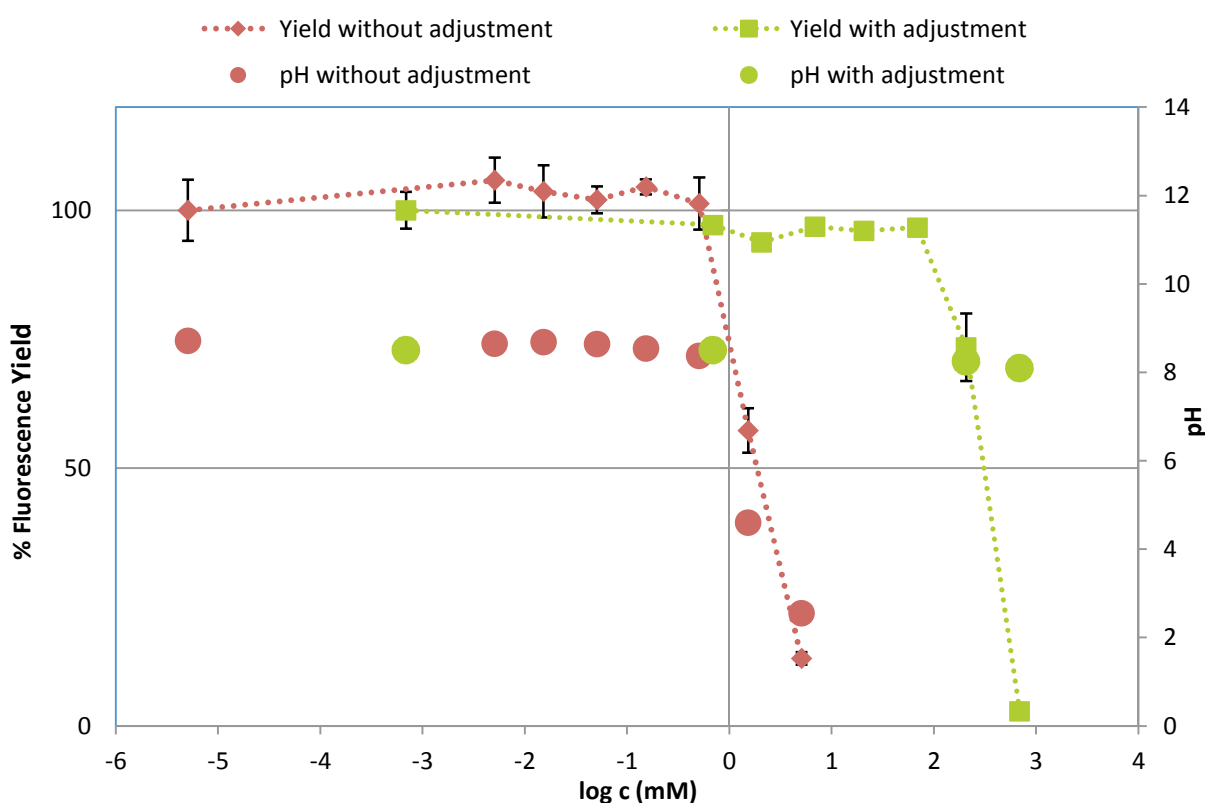


Figure 50: Logarithmic dose-effect curve for PFBA with and without pH adjustment. The dots represent the pH in the test vials at the respective PFBA concentrations. Red: without pH adjustment; green: with pH adjustment

Figure 50 shows the logarithmic dose-effect graph for PFBA and contrasts the curves with and without pH adjustment. It is obvious that the pH drop at $\log c = 0.2$ affects an increased toxicity,

which is not the case when pH is adjusted. Without pH adjustment, the toxicity is more than two orders of magnitude lower than with non-adjusted stock solution ($EC_{50} = 1.76 \text{ mM}$ vs. 279 mM). It could be shown that the previously measured values for other perfluorinated acids were equally biased by a pH effect. Figure 51 demonstrates that also for PFOA, pH adjustment is necessary. Here again, PFOA was measured with and without adjustment. A third assay was performed using the commercially available ammonium perfluorooctanoate (APFO). The dose-response curves for pH-adjusted PFOA and APFO were very similar, which is also expressed by very similar EC_{50} values.

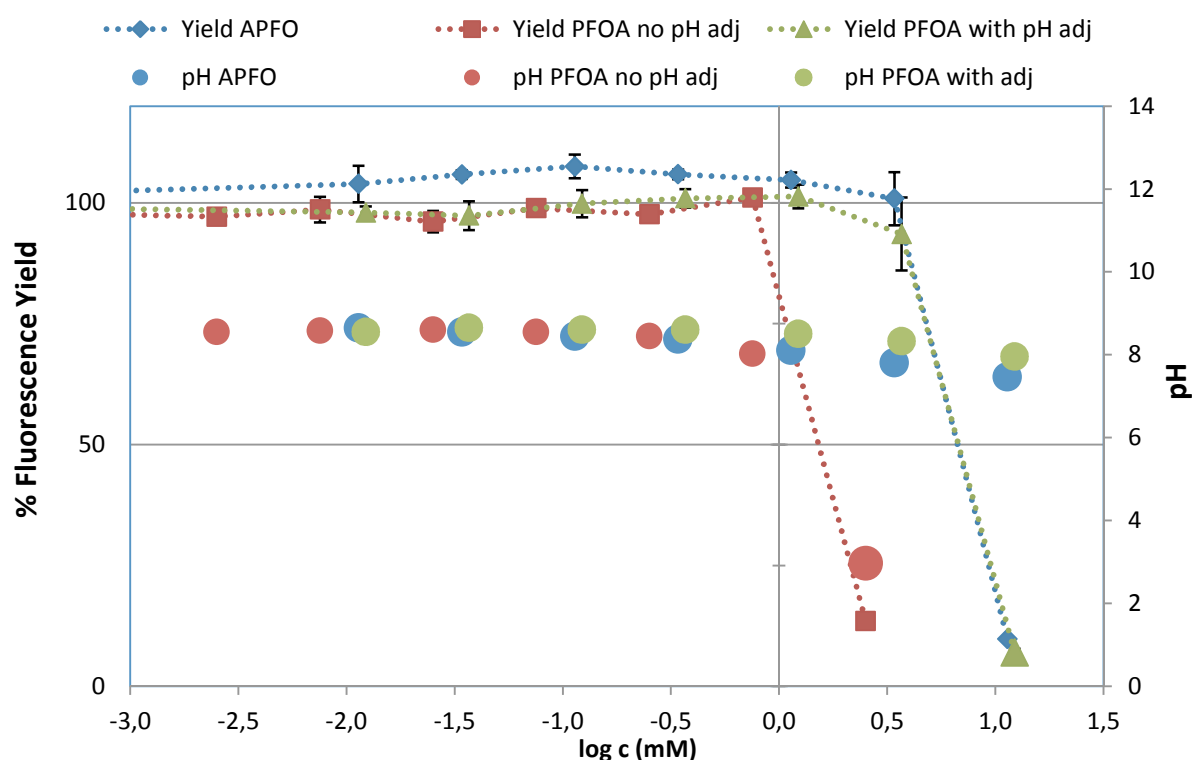


Figure 51: Dose-response curves for APFO, PFOA without pH adjustment and PFOA with pH adjustment. Dots indicate the pH measured in the vials after the test. Please note that nominal concentrations are given for better comparison of the data between PFOA without pH adjustment and APFO.

Various other perfluorinated compounds were tested in for acute toxicity on algae. The results are shown in Table 7. For a number of compounds, low water solubility prevented measurements of EC_{50} values, because even under saturated conditions, no effect was observed.

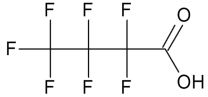
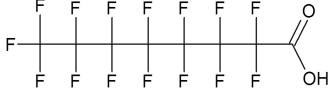
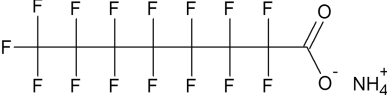
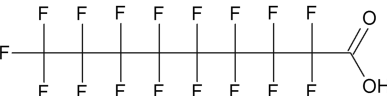
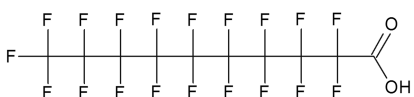
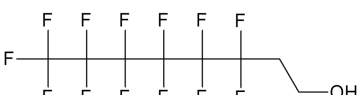
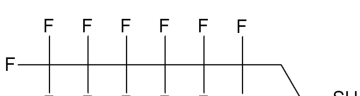
The comparison of THPFODiol and PFSubA clearly indicates that toxicity of a compound is not only related to the perfluoroalkyl chain length, but functional groups greatly affect the toxicity. In this case, the EC_{50} values will have a difference of at least two orders of magnitude, although both contain six difluoromethylene groups. The toxic effect of the two alcohol groups is much more pronounced than that of the two carboxylic acid functions. However, this may be different

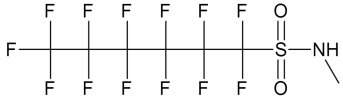
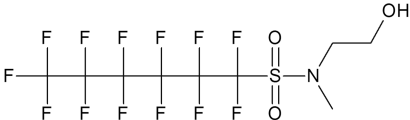
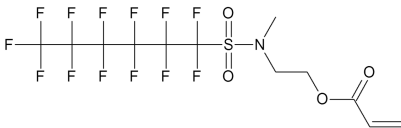
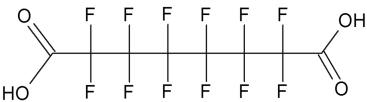
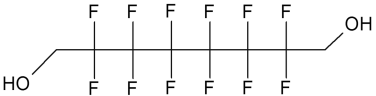
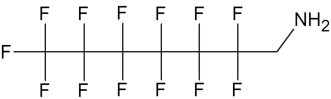
for other species, because the PAM test is very specific since an effect will only be observed if the photosynthetic system is affected.

The EC₅₀ values reported herein suggest that under environmental conditions, no acute toxicity will emanate from the compounds investigated.

PFOA, PFBA and the FTOH have been detected in numerous environmental samples, but have never been quantified in concentration levels close to the measured EC₅₀ values. In general, concentrations in environmental samples lie in the ng L⁻¹ range for samples with no direct sources such as PFAS manufacturing facilities or after application *in situ* (firefighting foams etc).

Table 7: Overview of results for acute toxicity of fluorinated compounds to *Pseudokirchneriella subcapitata*

Structure	Chemical name	Acronym	Concentrations verified	EC ₅₀ PAM test ^a [mM]	EC ₁₀ PAM test ^a [mM]
	Perfluorobutanoic acid ^b	PFBA	yes	257 (236 – 279)	156 (131 – 185)
	Perfluorooctanoic acid ^b	PFOA	yes	5.96 (5.43 – 6.53)	3.68 (3.27 – 4.15)
	Ammonium perfluorooctanoate	APFO	no	6.94 (6.07 – 7.94)	4.31 (3.60 – 5.16)
	Perfluorononanoic acid ^b	PFNA	yes	0.732 (0.599 – 0.894)	0.232 (0.169 – 0.519)
	Perfluorodecanoic acid ^b	PFDA	no	> S _w > 0.438 mM	
	1H,1H,2H,2H-Perfluorooctanol	6:2-FTOH	no	> S _w > 0.04	
	1H,1H,2H,2H-Perfluorooctanethiol	6:2-FTSH	no	> S _w > 0.038	

Structure	Chemical name	Acronym	Concentrations verified	EC ₅₀ PAM test ^a [mM]	EC ₁₀ PAM test ^a [mM]
	N-Methylperfluorohexanesulfonamide	N-MePFHxSA	no	> S _w > 0.02	
	N-Methyl,N-(2-hydroxyethyl)perfluorohexanesulfonamide	N-MeFHxSE	no	> S _w > 0.02	
	N-Methyl-perfluorohexane sulfonamidoethyl acrylate	N-MeFHxSEAc	no	> S _w > 0.02	
	Perfluorooctanedioic acid (Perfluorosuberic acid)	PFSubA	no	> 130	
	1H,1H,8H,8H-Perfluorooctane-1,8-diol	THPFOdiol	yes	0.659 (0.592 – 0.735)	0.182 (0.143 – 0.231)
	1H,1H-Perfluoroheptylamine	DHPFHpAm	no	> 0.151	

^a 95% confidence interval in brackets^b stock solutions neutralized with sodium hydroxide, therefore toxicity of the anion is assessed

3.7.3 Acute toxicity to *Chydorus sphaericus*

The acute toxicity of PFBA was also measured to the cladoceran *Chydorus sphaericus*, which is a common species in Central European waters. The endpoint of this assay is the immobility of the test species, which most often equals mortality. However, assessment of mortality is much too complicated for routine tests, thus immobility is chosen as the endpoint. Previous measurements yielded an EC₅₀ value of 2.51 mM.

However, also in this assay, a medium is used which contains low buffer concentration, in this case 0.77 mM sodium bicarbonate. Therefore, when the PFBA concentration exceeds the bicarbonate concentration, a major pH reduction will occur, although this could not be proven in the test because of the very small volume used.

Table 8: Results for acute toxicity of PFBA to *Chydorus sphaericus*

	24 h		48 h	
	[mM]	95% CI [mM]	[mM]	95% CI [mM]
EC ₅₀	30.6	25.4 - 35.2	22.3	16.8 - 26.6
EC ₁₀	16.6	11.0 - 20.9	13.1	7.5 - 17.2

95% CI: 95% confidence interval

The test was carried out with a stock solution with pH adjustment. The resulting values are much higher than previous ones with an EC₅₀ value of 22.3 mM after 48 h (see Table 8). This value is comparatively high and shows that toxic effects of PFBA are not likely to occur in the environment, where concentrations are usually in the pM to nM range, although its concentration might increase in the following years due to a shift towards rather short-chained PFASs. This increase is not suspected to be of several orders of magnitude, implying no acute toxicity of PFBA towards *Chydorus sphaericus*.

3.7.4 Conclusions

The ecotoxicological data collected on several PFASs illustrates several structure-activity relationships. The general correlation between the number of perfluorinated carbon atoms and toxicity was confirmed for the species tested. Short-chained compounds, such as PFBA, exhibit much higher EC₅₀ and EC₁₀ values as compared with their long-chained counterparts, like PFOA and PFNA. However, it must be pointed out that this relationship is only valid when comparing the same compound classes. This becomes particularly obvious when comparing the ecotoxicological characteristics of THPFODiol and its oxidized derivative PFSubA, whose EC₅₀ values are separated by at least a factor of 200, with the diol compound being more toxic. This highlights the influence of the functional group attached to the perfluoroalkyl chain, which

provides different modes of action by different physico-chemical interactions. For instance, PFSubA is capable of ionic interactions, whereas THPFODiol can merely interact with biomolecules via dipole-dipole interactions.

The algae toxicity test is very specific since effects can only be observed if the photosynthetic chain is hampered. This can be one explanation for the diverging ecotoxicological characteristics of PFASs with different functional groups. In contrast to this, toxicity assessment to *Chydorus sphaericus* is much less specific, since the immobility – which can be regarded as nearly equivalent to mortality – can be caused by numerous mechanisms.

The EC₅₀ and EC₁₀ values measured for PFASs are much higher than environmental concentrations without any point sources. This is true for all measurements of ecotoxicity on *Pseudokirchneriella subcapitata* and *Chydorus sphaericus*, although for the latter one, only toxicity of PFBA was assessed. If the rule of thumb regarding perfluoroalkyl chain length holds for *Chydorus sphaericus*, relatively low EC₁₀ and EC₅₀ values are to be expected for PFOA and PFNA, since the responsiveness of *Chydorus sphaericus* was approximately 10-fold higher than for *Pseudokirchneriella subcapitata*.

Toxicity measurements of PFBA and PFOA revealed that these tests should be carried out with care regarding the high acidity of PFCAs and PFSAs. Especially the pH value of the test media should be controlled in order to prevent false high toxicity assessments.

4 Perspectives

Evaluation of biodegradability of PFASs has been assessed for several compound classes in this thesis. Although general rules for degradability cannot be established, further biotransformation tests for structurally similar compounds may be carried out to gain more knowledge on the processes involved during transformation.

This is notably true for TFM-based alcohols, of which TFMP_{OH} and TFMH_xOH have been studied herein. The minimum chain length of TFM-based alcohols allowing for complete defluorination would be interesting to know. As has been explained above, complete defluorination can only occur if the respective TFM-alkanoic acid can be cleaved by subsequent multiple oxidation. Furthermore, verification of the biotransformation pathway by detection of at least one of the transient TPs would be desirable. The Bayer-Villiger-oxidation products are of particular importance to corroborate this degradation pathway. The detection of these compounds could be carried out with the help of interdisciplinary co-operation between analytical chemists and microbiologists, because the latter ones could bring in their knowledge on cell lysis and release of transient TPs into the biotransformation medium.

As for FTEOs, two different results concerning their degradability have been obtained herein. Whereas one experiment did not yield PFOA or PFH_xA as a stable TP, PFOA was released in the second experiment in considerable amounts. It is certain that FTEOs are transformed to PFCAs by biodegradation, but the reasons for the different observations are not yet clear. Thus, different parameters, such as the inoculum, the concentration of the test compound and the oxygen supply, could be varied and their effects on the formation of PFCAs could be assessed. Also the biotransformation pathway of long-chained FTEOCs to PFCAs is not yet entirely evident, although the presence of 1*H*-PFOA suggests a transformation pathway via FTOH. The latter one could be captured and detected if higher concentrations of fractionated FTEO were applied in the assay. Finally, shorter-chained fractionated FTEOs could be examined, since it would be interesting to see similarities or differences in formation of FTEOCs and PFCAs.

It is recommended that the characteristic product ions obtained during CID of fluorotelomer-based compounds be used in precursor ion scans of environmental or consumer product samples. This allows for the detection of novel fluorinated contaminants whose structure can be elucidated via different MS techniques, especially high-resolution MS. The exact structures of these product ions could be found out by sophisticated mass spectrometric investigations, e.g. by isotopic labeling, and computational methods like density functional theory methods.

5 Summary

The present thesis aimed at investigating different aspects regarding environmental occurrence, fate and effects of perfluorinated and polyfluorinated alkyl substances (PFASs).

In two different studies, the aerobic biotransformation of the commercially available fluorotelomer ethoxylates (FTEOs) was studied. The first biodegradation study was carried out with a commercial FTEO mixture, which was found to be a vast mixture of compounds with different perfluoroalkyl chain lengths as well as a strongly varying degree of ethoxylation. With the help of HPLC-ESI-MS/MS methods, it was possible to show that the FTEOs were transformed to the respective ω -oxidized carboxylic acids (FTEOCs) by biotransformation. Long FTEOCs acids were degraded to shorter FTEOCs, which showed recalcitrance in this experiment. Perfluorocarboxylic acids (PFCAs) formation, more precisely perfluorooctanoic acid (PFOA) and perfluorohexanoic acid (PFHxA), was reasoned by biotransformation of residual unreacted fluorotelomer alcohols (FTOHs), which had been known to degrade to PFCAs before.

In order to verify if the PFCAs generated in the previous experiment were effectively only due to FTOH degradation, the commercial mixture was fractionated two-dimensionally by perfluoroalkyl chain length as well as ethoxylate chain length with the help of column chromatography. One of the fractions containing mostly 8:2-FTEO₁₅ and 8:2-FTEO₁₆, were subjected to an individual biotransformation study. Surprisingly, formation of PFOA could be identified to approximately 7%, which is coherent to PFOA formation from 8:2-FTOH as shown before by other research groups. Thus, FTEOs are another source of PFOA in the environment.

In a monitoring campaign of 17 Hessian WWTP effluents and four Hessian surface waters, the widespread PFCAs and perfluorosulfonic acids (PFSAs) could be detected alongside one quantitative detection of 8:2-FTEO₁C and 6:2-FTEO₁C, the short-chained TPs of FTEO. PFAS concentrations in WWTP effluents showed an average of approximately 40 ng L⁻¹, which is considered comparable with previous results. The surface waters showed relatively high PFAS burdens of up to 760 ng L⁻¹, which can be attributed to sources of industrial wastewaters.

Three building blocks for potential PFAS substitutes were investigated in view of their potential to form inorganic fluoride or other environmentally benign dead-end TPs. Two of these compounds were structurally very similar, namely 6-(trifluoromethoxy)-hexan-1-ol (TFMHxOH) and 3-(trifluoromethoxy)-propan-1-ol (TFMPrOH). Whereas TFMPrOH yielded only 15 mol% of inorganic fluoride, TFMHxOH yielded stoichiometric amount of fluoride after 35 days. Both TFMHxOH and TFMPrOH were found to be metabolized to their ω -oxidized carboxylic acid as well as to trifluoromethoxy carbonate (TFMC), which was further degraded in both experiments. However, the acid derived from TFMHxOH could be degraded after its formation, whereas the TFMPrOH derivative was recalcitrant. It is assumed that at least two biotransformation pathways occur for both alcohols. The first one includes initial oxidation of the alcohol to the

respective carboxylic acid, probably via the aldehyde intermediate. The second one is suggested to include oxidation of the methylene group adjacent to the trifluoromethoxy group to a hemiacetal and subsequently to an ester. This ester is oxidized in terms of a Bayer-Villiger-like oxidation leading to a carbonic acid diester which is hydrolyzed under release of TFMC. However, the intermediates could not be detected with the analytical methods used.

A third fluorosurfactant building block candidate investigated for biodegradation potential was 1-(2,2,3,3,4,4,4-heptafluorobutoxy)-propan-2-ol (HFBPrOH). It could be shown that it is transformed consecutively via oxidation, α -oxidation and β -oxidation with perfluorobutanoic acid (PFBA) being the dead-end TP accounting for 4.5 mol%. PFBA is not further degradable, but its toxic potential is much lower than long-chained PFCAs, which was studied in what follows.

The acute environmental effects of a set of PFASs were determined by comparative measurements of toxicity on the green algae *Pseudokirchneriella subcapitata* in the context of a molecular modeling study. It could be shown that short-chained compounds such as PFBA show much lower effective concentrations (EC_{50}) than those with longer chains, e.g. PFOA. It was discovered as well that not only the perfluoroalkyl chain length is of importance, but also the functional groups were of high importance. Perfluorosuberic acid toxicity was lower by nearly a factor of 200 than that of the equally long-chained 1*H*,1*H*,2*H*,2*H*-perfluorooctane-1,8-diol (THPFODiol). EC_{50} values of all compounds were higher by several orders of magnitude than the concentration levels detected in the environment on a regular basis.

The acute toxicity of PFBA, the dead-end TP of HFBPrOH, on the central European cladoceran *Chydorus sphaericus*, was assessed. The EC_{50} value of 22.6 mM after 48 h of exposure suggest no acute environmental effects of PFBA to the species examined.

Since all measurements carried out in this thesis were performed with electrospray ionization-mass spectrometry (ESI-MS) using collision-induced dissociation (CID), fragmentation pathways of a large set of compounds could be directly compared with each other allowing for enlightenment of characteristic fragmentation patterns. In this context, the characteristic fragmentation pathway of fluorotelomer-based compounds, i.e. such compounds that bear a $F-(CF_2-CF_2)_n-CH_2-CH_2-O-$ function), in negative polarity could be unveiled. All compounds of that kind that were measured in this thesis, namely FTOHs, FTEOs and FTEOCs lead to the same characteristic pattern of product ions at m/z 403, 383, 355 and 317 (for 8:2-fluorotelomer based compounds). With the help of MS^3 scans as well as high-resolution orbitrap MS, the fragmentation pathway as well as the chemical formulae of the product ions were determined unequivocally.

6 Annex

6.1 Materials and methods

6.1.1 Solvents, reagents, reference materials and instrumentation

All solvents and mobile phase modifiers used for HPLC, MS and biodegradation study applications were at least of HPLC grade and are summarized in Table 9.

Table 9: List of solvents and reagents and their purities

Solvent	Manufacturer	Purity
MeOH	Merck, Darmstadt, Germany	SupraSolv®
Acetic acid	Merck, Darmstadt, Germany	100%
Acetone	Merck, Darmstadt, Germany	SupraSolv®
Acetone (cleaning)	Roth, Karlsruhe, Germany	>99.5%
ACN	Merck, Darmstadt, Germany	LiChrosolv®
NH ₄ OAc	Fluka, Seelze, Germany	>99%
Ethyl acetate	Merck, Darmstadt, Germany	SupraSolv®
i-Propanol	Merck, Darmstadt, Germany	p.a.

Milli-Q water was prepared using a Millipore Simplicity 185 with a Slimpak 2 Cartridge (Millipore, Milford, USA). If not stated differently, this Milli-Q water was used for preparation of solutions and dilution, when 'water' is mentioned.

A commercial mixture of FTEO was from DuPont (Neu-Isenburg, Germany), named 'Zonyl FSH'. Its active content is 50%, the remainder being dipropyleneglycol methyl ether and H₂O at equal shares [159].

TFMP₂OH (98% purity), TFMH₂OH (unknown purity) and HFBP₂OH (87% purity, 5% methyl isomer impurity, HFBOH present in unknown fraction) were synthesized and supplied by Merck (Darmstadt, Germany).

Fluorosurfactant reference materials were purchased from Wellington Laboratories (Guelph, Ontario, Canada) or from Neochema (Mainz, Germany). 6:2-FTOH, 8:2-FTOH and bromoacetic acid for synthesis were purchased from Sigma (Seelze, Germany).

SPE was carried out on a Baker-10 SPE System (Baker, Phillipsburg, USA) coupled to a MPC 101Z, 0.06 kW vacuum pump (Ilmvac, Ilmenau, Germany).

Ion exchange chromatography was carried out on a Metrohm modular system consisting of a 709 IC Pump, a 752 Pump Unit, a 733 Separation Center, a 732 IC Detector and a 762 IC Interface (all from Metrohm, Herisau, Switzerland). Ion chromatographic separations were carried out on a Metrosep A Supp 5 100 x 4.0 mm (Metrohm, Herisau, Switzerland) and a

Varian C₁₈ 3 µm precolumn (Varian, Frankfurt, Germany). The eluent was aqueous Na₂CO₃ (1.6 mM) and NaHCO₃ (0.5 mM) at a flow rate of 0.8 mL/min.

A fluoride stock solution was prepared from analytical grade sodium fluoride (Sigma, Seelze, Germany) at a concentration of approximately 1 mg mL⁻¹. Standards were prepared at fluoride concentrations of 0.1 mg mL⁻¹, 0.25 mg mL⁻¹, 0.5 mg mL⁻¹, 0.75 mg mL⁻¹, 1 mg mL⁻¹ and 2.5 mg mL⁻¹.

6.1.2 HPLC-ESI/MS analysis

6.1.2.1 General setup and methods

The chromatographic setup consisted of two Series 200 Micro Pumps, a Series 200 vacuum degasser, and a Series 200 autosampler (Perkin Elmer, Norwalk, CT, USA).

The chromatograph was coupled to a hybrid triple quadrupole linear ion trap tandem mass spectrometer 3200 Q Trap (Applied Biosystems, Foster City, CA, USA) using a Turbo Ionspray interface in ESI ("Turbo Spray"). Nitrogen used for MS was generated by a Membrane nitrogen generator NGM-22-LC/MS (CMC, Eschborn, Germany) coupled to a SF 4 FF oil-free orbiting scroll compressor (Atlas Corpo, Stockholm, Sweden). Operation and data acquisition of the HPLC-MS system was carried out via Analyst Software, versions 1.4 and 1.5, respectively. Important parameters, which were used for all measurements on the 3200 Q Trap are summarized in Table 10.

Table 10: MS parameters which were used throughout the whole thesis

Setting	Value
IonSpray Voltage (IS)	+5500 V / -4500 V
Curtain Gas (CUR)	25 psi
Nebulizer Gas (GS1)	55 psi
Turbo Gas (Desolvation) (GS2)	65 psi
CAD Gas (CAD)	Medium (equals 5 on an arbitrary scale from 1 to 12)
Interface heater (ihe)	On

For target compound analysis, optimization of the MS parameters was performed via syringe pump injection of a solution of the analyte at an approximate concentration of 0.1-20 µg mL⁻¹ depending on response factors. Optimization was either carried out automatically by the Analyst

software or manually by variation of the parameters DP, EP, CE and CXP. For FTOH analysis, optimization was carried out via syringe pump injection of the compounds into a stream of the eluent via a T-piece. Besides the abovementioned parameters, temperature of the desolvation gas ('Turbo Gas') was optimized.

When CID spectra were recorded under constant infusion via a syringe pump, the settings governing the degree of fragmentation (CE or excitation energy) were always ramped through the whole range. Spectra shown in this thesis are averaged spectra of the most indicative settings. When such spectra were recorded by using preceding HPLC separation, the same gradient was used as for MRM or SIM measurement and CE or excitation energy were estimated by comparison with previous measurements.

For biodegradation experiments, standards of the parent compounds were always prepared from 10% (or lower) of the theoretical concentration up to approximately 125-150% of the initial concentration. At least five calibration points were used.

6.1.2.2 PFCA, PFSA and FTEO₁C analysis

Instrumental analysis of PFCAs, PFSA and FTEO₁Cs was optimized throughout the whole study. Only the final methodology is presented here.

Besides the analytical column, which is a MZ Aqua C18 50 x 2.1 mm, 5 µm particle size, equipped with a guard column with dimensions of 10 x 2.1 mm of the same material, a further column (Phenomenex Aqua C18, 50 x 2.0 mm, 5 µm particle size from Phenomenex, Aschaffenburg, Germany) was placed between the mixing chamber of the eluent pumps and the sample loop in order to achieve separation of PFASs injected from those which were present as instrumental contaminations by tubings or PTFE parts in the degasser. Contaminant PFASs are trapped on this column and are eluted slightly later than PFASs injected.

Injection volume was 50 µL, HPLC flow rate was set to 300 µL min⁻¹ and the eluents were A: H₂O/MeOH 95/5 (V/V) and B: H₂O/MeOH (5/95) (V/V) both containing 5 mM NH₄OAc. The chromatographic gradient is shown in Table 11.

Table 11: Chromatographic gradient for HPLC-MS analysis of PFCAs, PFSA's and FTEO₁Cs

Time [min]	Conditions
0 – 2	100% A
2 - 15	→ 0% A
15 – 20	0% A
20 – 25	→ 100% A
25 – 35	100% A

The MS was run in MRM mode under negative ESI polarity. The compound-dependent parameters for all compounds are listed in Table 12 and ESI temperature was set to 600°C.

Table 12: MS settings used for analysis of PFCAs, PFSA's and FTEO₁Cs. Please note that only one of the mass-labeled internal standards of PFOA was used at any time.

Compound	Q1 mass (m/z)	Q3 mass (m/z)	DP [V]	EP [V]	CE [V]	CXP [V]
6:2-FTEO ₁ C	421	75/255	-25	-9	-30/-44	0/-4
8:2-FTEO ₂ C	521	75/355	-25	-9	-40/-44	0/-4
¹³ C ₂ -PFHxA	315	270/120	-10	-5	-10/-26	-4/0
¹³ C ₂ -PFOA	415	370/170	-15	-4.5	-14/-24	-4/-2
¹³ C ₄ -PFOA	417	372/169	-15	-6	-12/-26	-4/0
PFBA	213	169	-13	-5	-16	-4
PFPeA	263	219	-10	-8	-10	-6
PFHxA	313	269/169	-15	-5	-10/-28	-4/0
PFHeA	363	319/169	-15	-4	-12/-22	-4/-4
PFOA	413	369/169	-15	-5.5	-12/-24	-4/-2
PFNA	463	419/169	-15	-7.5	-14/-26	-14/-2
PFDA	513	469/269	-10	-5	-14/-24	-16/-4
PFBS	299	80/99	-55	-5	-48/-38	-2/0
PFHxS	399	80/99	-45	-8.5	-70/-60	-2
PFOS	499	80/99	-50	-10	-72/-70	-2
PFDS	599	80/99	-75	-7	-98/-82	0

6.1.2.3 FTOH analysis

HPLC was carried out on an MZ Aqua C18 50 x 2.1 mm, 5 µm particle size, equipped with a guard column with dimensions of 10 x 2.1 mm of the same material. Injection volume was 50 µL, HPLC flow rate was set to 200 µL min⁻¹ and the eluents were A: H₂O/MeOH (95/5; V/V) + and B: H₂O/MeOH (5/95; V/V) both containing 5 mM NH₄OAc. The chromatographic gradient is displayed in Table 13.

Table 13: Chromatographic gradient for HPLC-MS analysis of FTOHs

Time [min]	Conditions
0 – 2	50% A
2 – 8	→ 0% A
8 – 10	0% A
10 – 12	→ 50% A
12 - 25	50% A

The MS was operated in MRM mode under negative ESI conditions. Compound-dependent parameters are shown in Table 14. ESI temperature was set at 150°C, which is an important parameter. The response factor will decrease drastically if much higher temperatures are used.

Table 14: Compound-dependent MS parameters for FTOH analysis

Compound	Q1 mass (m/z)	Q3 mass (m/z)	DP [V]	EP [V]	CE [V]	CXP [V]
6:2-FTOH	421	59	-2	-10	-29	-1
8:2-FTOH	521	59	-2	-10	-33	-1
² H ₂ , ¹³ C ₂ -8:2-FTOH	315	59	-2	-10	-50	-1

6.1.2.4 FTEO and FTEOC analysis

Biotransformation of whole Zonyl FSH:

Chromatography was carried out on a HALO C₁₈ column (Advanced Materials Technology, Wilmington, DE, USA), 50 × 2.1 mm, 2.7 µm particle size (2.2 µm solid core), 90 Å pore size. Mobile phases were A: H₂O/ACN (95/5; V/V) and B: H₂O/ACN (20/80; V/V) both containing 5 mM NH₄OAc.

A binary gradient, starting with 60 % A, held for 0.5 min, followed by a linear decrease to 0 % A within 5.5 min was used. The column was then rinsed at 0 % A for 3 min, brought back to

60 % A within 4 min and reequilibrated for 5 min. The flow rate was 300 $\mu\text{L min}^{-1}$ and the injection volume was 50 μL .

The MS was operated in multiple-reaction monitoring (MRM) mode. FTEO were measured as their ammonium adducts in positive ESI mode. The MRM transitions and the compound-dependent parameters are given in Table 15. EP was set to 10 V and the CXP was 3 V for all transitions.

Table 15: Compound-dependent MS parameters of 6:2-FTEO and 8:2-FTEO congeners used during biotransformation study of a technical FTEO mixture. The dotted line indicates a change in the MRM detection window

Compound	Q1 mass <i>m/z</i>	Q3 mass <i>m/z</i>	DP [V]	CE [V]	Dwell Time [ms]
6:2-FTEO ₃	514	89	40	55	25
6:2-FTEO ₄	558	89			
6:2-FTEO ₅	602	89			
6:2-FTEO ₆	646	89			
6:2-FTEO ₇	690	89			
6:2-FTEO ₈	734	89			
6:2-FTEO ₉	778	89			
6:2-FTEO ₁₀	822	89			
6:2-FTEO ₁₁	866	89			
6:2-FTEO ₁₂	910	89			
6:2-FTEO ₁₃	954	89			
8:2-FTEO ₃	614	89			
8:2-FTEO ₄	658	89			
8:2-FTEO ₅	702	89			
8:2-FTEO ₆	746	89			
8:2-FTEO ₇	790	89			
8:2-FTEO ₈	834	89			
8:2-FTEO ₉	878	89			
8:2-FTEO ₁₀	922	89			
8:2-FTEO ₁₁	966	89			
8:2-FTEO ₁₂	1010	89			
8:2-FTEO ₁₃	1054	89			
NPEO ₂	326	183.3	25	10	50
NPEO ₂	326	309.5			30

FTEO TP, namely FTEOCs, were analyzed with the same HPLC-MS setup as for FTEOs. Data was gathered both in positive and negative ESI in 'Q1 Multiple Ions' mode (similar to SIM in single quadrupole instruments). In positive mode, the acids were measured as their $[\text{M} + \text{NH}_4]^+$ adduct, whereas in negative mode, deprotonated molecules were measured and peak area ratios were calculated by dividing the peak areas of the FTEOC by that for the internal standard

($^{13}\text{C}_2$ -PFHxA for 6:2-FTEOCs and $^{13}\text{C}_2$ -PFOA for 8:2-FTEOCs). No internal standard was used for positive ionization measurements.

Biotransformation study of fractionated FTEO:

The MS was operated in Q1 SIM mode under positive ESI conditions. Ions with m/z 524 -1360 at 44 Da difference (for 8:2-FTEO ammonium adducts) and m/z 540 – 1376 at a difference of 44 Da were monitored. Internal standard was NPEO₂ at m/z 326 ($[\text{M}+\text{NH}_4]^+$). Temperature was set at 600°C and DP = 40 V and EP = 10 V were set for all compounds.

HPLC was carried out on a MZ Aqua C18 column with precolumn. Injection volume was 25 μL , HPLC flow rate was set to 300 $\mu\text{L min}^{-1}$ and the eluents were A: H₂O/MeOH (95/5; V/V) + and B: H₂O/MeOH (5/95; V/V) both containing 5 mM NH₄OAc. The chromatographic gradient is presented in Table 16.

Table 16: Chromatographic gradient for HPLC-MS analysis of 8:2-FTEO and 8:2-FTEOC during biotransformation study of purified 8:2-FTEO₁₄₋₁₆

Time [min]	Conditions
0 – 0.5	60% A
0.5 – 6	→ 0% A
6 – 9	0% A
9 – 13	→ 60% A
13 – 18	60% A

Determination of relative intensities

Relative intensities of FTEO congeners were determined at different DP values (see 3.1) with a solution containing 10 $\mu\text{g mL}^{-1}$ of whole Zonyl FSH, implying an FTEO concentration of 5 $\mu\text{g mL}^{-1}$, which was dissolved in the mobile phase of whole Zonyl FSH biodegradation study (eluent A/B 10/90; V/V). Chromatography was carried out as described for investigation of whole Zonyl FSH degradation, but isocratic elution at 10% A was performed. The injection volume was 50 μL .

The MS was operated in positive ESI polarity and in SIM mode monitoring the masses of FTEO ammonium adduct from $x = 2-14$ (even numbers only) and $y = 0-20$. Three different DP settings were used, namely 10 V, 25 V and 40 V. Gas temperature was maintained at 500°C and EP was set to 10 V.

6.1.2.5 TFMP_{OH} TPs

Chromatography was carried out on a HALO C₁₈ column (Advanced Materials Technology, Wilmington, DE, USA), 50 × 2.1 mm, 2.7 µm particle size (2.2 µm solid core), 90 Å pore size. Mobile phases were A: water/ACN (95/5; V/V) and B: water/ACN (20/80; V/V) both containing 5 mM NH₄OAc. HPLC flow rate was 300 µL min⁻¹ and injection volume was set to 5 µL. The chromatographic gradient is presented in Table 17.

Table 17: Chromatographic gradient for HPLC-MS analysis of TFMP_{OH} TPs

Time [min]	Conditions
0 – 0.5	80% A
0.5 – 6	→ 5% A
6 – 9	5% A
9 – 13	→ 80% A
13 – 19	80% A

The MS was operated in negative ESI polarity and MRM mode monitoring the transitions m/z 157 → 85 (CE = -30 V), 141 → 85 (CE = -30 V), 127 → 85 (CE = -30 V) / 83 (CE = -12 V) / 63 (CE = -12 V) representing the TFM-alkanoic acids. Temperature was set to 550°C and DP, EP and CXP were maintained at -20 V, -10 V and -2 V, respectively.

6.1.2.6 TFMH_xOH and its TPs

TFMH_xOH

Chromatographic conditions were the same as those for analysis of TFMP_{OH} TPs (see chapter 6.1.2.5) except for the injection volume, which was set to 50 µL. Details about the chromatographic gradient are given in Table 18.

Table 18: Chromatographic gradient for HPLC-MS analysis of TFMH_xOH

Time [min]	Conditions
0 – 0.5	90% A
0.5 – 8	→ 5% A
5 – 8	5% A
8 – 12	→ 90% A
12 – 21	90% A

The MS was operated in positive ESI polarity and in MRM mode. Transitions monitored were m/z 187 \rightarrow 83 (CE = 11 V) and m/z 187 \rightarrow 55 (CE = 23 V). Temperature was set to 400°C, DP, EP and CXP were held constant at 16 V, 9 V and 4 V, respectively.

TPs

Chromatographic conditions were the same as for the parent compound, except for the injection volume, which was changed to 5 μ L.

The MS was operated in negative ESI polarity and in SIM mode monitoring m/z 199, 185, 171, 157, 143, and 129 representing the deprotonated TFM-alkanoic acids C₁-C₆. Temperature was set to 400°C, DP was -20 V and EP was -5 V.

6.1.2.7 HFBPrOH and its TPs

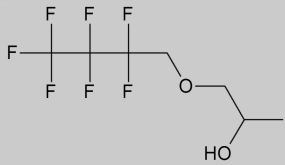
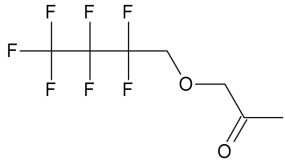
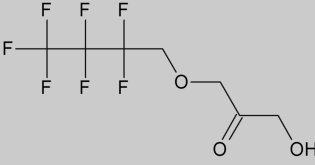
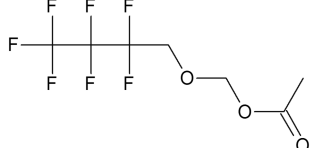
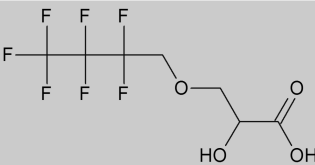
HFBPrOH and its TPs were chromatographed with a MZ Aqua C18 50 x 2.1 mm, 5 μ m particle size, equipped with a guard column with dimensions of 10 x 2.1 mm of the same material. Eluents were A: H₂O/ACN (90/10; V/V) and B: H₂O/ACN (10/90; V/V) both containing 5 mM triethylamine and 5 mM acetic acid. Two different HPLC-MS methods were used, one for non-acidic compounds (alcohols and potential ketone and aldehyde TPs) and one for acidic TPs. The different gradients are presented in Table 19. Flow rate was set to 300 μ L min⁻¹ and injection volume for non-acidic compounds was 5 μ L and for acids 10 μ L.

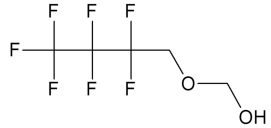
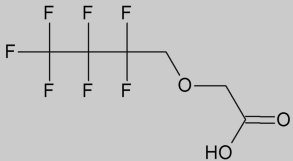
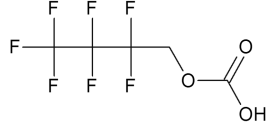
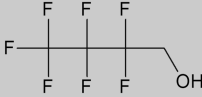
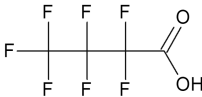
Table 19: Chromatographic gradient used for analysis of HFBPrOH and its potential non-acidic (left) and acidic (right) TPs

<i>Non-acidic</i>		<i>Acidic</i>	
Time [min]	Conditions	Time [min]	Conditions
0 – 2	40% A	0 – 1	95% A
2 – 4	\rightarrow 0% A	1 – 7	\rightarrow 0% A
4 – 7	0% A	7 – 10	0% A
7 – 8	\rightarrow 40% A	10 – 12	\rightarrow 95% A
8 – 15	40% A	12 – 20	95% A

MS analysis was carried out under negative ESI in MRM mode. For non-acidic compounds the transition $[M + \text{acetate}]^- \rightarrow m/z$ 59 (acetate) was monitored. Temperature was set to 300°C for non-acidic compounds and to 550°C for acids. An overview of the compounds analyzed and the respective parameters are summarized in Table 20.

Table 20: Overview of HFBPrOH and its TP's analyzed

Structure	Name	Acronym	Molecular Weight [Da]	MRM transition	MS Parameters [V]	Detected
	1-(2,2,3,3,4,4,4-heptafluorobutoxy)propan-2-ol	HFBPrOH	258.1	317 → 59 [M + acetate] ⁻ → acetate	DP: -1 EP: -2 CE: -25 CXP: -1	yes
	1-(2,2,3,3,4,4,4-heptafluorobutoxy)propan-2-one	HFBPon	256.1	315 → 59 [M + acetate] ⁻ → acetate	DP: -1 EP: -2 CE: -25 CXP: -1	no
	1-(2,2,3,3,4,4,4-heptafluorobutoxy)-3-hydroxypropan-2-one	OH-HFBPon	272.1	331 → 59 [M + acetate] ⁻ → acetate	DP: -5 EP: -2 CE: -25 CXP: -3	no
	(2,2,3,3,4,4,4-heptafluorobutoxy)methyl acetate	HFBMAc	272.1	331 → 59 [M + acetate] ⁻ → acetate	DP: -5 EP: -2 CE: -25 CXP: -3	no
	3-(2,2,3,3,4,4,4-heptafluorobutoxy)-2-hydroxypropanoic acid	HFBPrOHPrA	288.19	287 (SIM)		yes

	(2,2,3,3,4,4,4-heptafluorobutoxy)methanol	HFBM	230.1	289 → 59 [M + acetate] ⁻ → acetate	DP: -5 EP: -2 CE: -25 CXP: -3	no
	(2,2,3,3,4,4,4-heptafluorobutoxy)acetic acid	HFBA	258.1	257 (SIM)		yes
	2,2,3,3,4,4,4-heptafluorobutyl hydrogen carbonate	HFBC	244.1	243 → 199 [M-H] ⁻ → [M-H-CO ₂] ⁻	DP: -30 EP: -10 CE: -25 CXP: -3	no
	2,2,3,3,4,4,4-heptafluorobutan-1-ol	HFBOH	200.1	259 → 59 [M + acetate] ⁻ → acetate	DP: -1 EP: -10 CE: -25 CXP: -3	yes (also impurity of FS-alcohol!)
	heptafluorobutanoic acid	PFBA	214.0	213 → 169 [M-H] ⁻ → [M-H-CO ₂] ⁻	DP: -25 EP: -10 CE: -30 CXP: -3	yes

6.1.3 Biotransformation setup and sample preparation

6.1.3.1 Biotransformation of a technical FTEO mixture

Biodegradation experiments were carried out at approximately 25 °C in amber 1 L glass bottles filled with 1 L of unfiltered effluent water of the municipal waste water treatment plant Beuerbach (Hesse, Germany). Aerobic conditions were maintained by aerating the bottles regularly (1-2 h per day) with an aquarium pump. Permanent aeration was not chosen in order to reduce potential volatilization of TPs. In order to distinguish microbial degradation from adsorption to particles or the glass surface, additional experiments were carried out in waste water spiked with 10 g L⁻¹ sodium azide, analogous to OECD guideline 309 [175]. The bottles were spiked with 9.5 mL of a solution containing 1.2 mg mL⁻¹ Zonyl FSH in MilliQ water, resulting in an effective FTEO concentration of 5.7 mg L⁻¹. Blank bottles containing WWTP effluent only were also prepared. Sample intervals decreased from daily in the beginning of the experiment to weekly after several weeks had passed.

For FTEO analysis, 100 µL of the fresh samples were mixed with 500 µL of a 10 mM aqueous NH₄OAc solution, 380 µL ACN and 20 µL of internal standard solution (10 ng NPEO₂ µL⁻¹ in ACN). The samples were vortex-shaken and filtered through a 0.2 µm nylon membrane filter (Carl Roth, Karlsruhe, Germany). For TP analysis, 500 µL of the samples were mixed with 300 µL 10 mM aqueous NH₄OAc solution, 180 µL ACN and 20 µL of internal standard solution (¹³C₂-PFHxA and ¹³C₂-PFOA, 100 pg µL⁻¹ in MeOH).

6.1.3.2 Biotransformation of purified FTEO

The experiment was carried out with the fractionated FTEO congeners, which contain 8:2-FTEO₁₄ (33.1 %) and 8:2-FTEO₁₅ (60.6 %) as well as traces of 8:2-FTEO₁₆ (ca. 2.7%) and 8:2-FTEO₆₋₁₃ (< 1%). This fraction is called 'F001'. The total mass concentration in the stock solution is 0.7 mg mL⁻¹ MeOH as determined by weighing. It is free of FTOH (< 0.01 mass%), PFOA (< 1 ppm), PFHxA and 6:2-FTEO congeners.

Six 50 mL PP centrifuge tubes were filled with 20 mL WWTP effluent (WWTP Beuerbach, Germany, 16.08.2011), which was previously aerated.

The active bottles contained 20 mL WWTP effluent, 14.3 µL 'F001' stock solution ('F001', 0.7 mg mL⁻¹ MeOH). Sterilized controls were prepared analogously to active experiments, but 200 mg NaN₃ were added, dissolved in effluent prior to addition of FTEOs. Blank controls were prepared as described for active experiments, but 14.3 µL MeOH instead of FTEO solution was added to the effluent.

After 15 minutes of shaking, t₀ samples were drawn and prepared according to dilution procedure. The tubes were opened and aerated for 30 s daily.

Furthermore, 25 mL glass bottles with screw-cap and septum were filled with 15 mL of WWTP effluent and 10.72 μL 'F001' stock solution (active and sterilized test) or MeOH (blank test) and 150 mg NaN_3 (sterilized test only). After 30 min of automatic shaking, t_0 samples were drawn.

300 μL of the freshly drawn samples were transferred into 1.5 mL Eppendorf caps previously filled with 228 μL MeOH, 12 μL NPEO₂ solution (10 ng μL^{-1} MeOH) and 60 μL PFAS-IS solution (100 pg μL^{-1} MeOH). The solution was vortexed for 5 s and centrifuged for 5 min at XXX g. Samples of the polypropylene (PP) centrifuge tube experiment were drawn just before aerating them (in order to sample potential volatile TPs).

Sampling of the glass bottles was carried out in multiple steps:

Firstly, an 8 x 40 mm Sterican needle (Braun, Melsungen, Germany) connected to an SPE cartridge (Varian Nexus ABS Elut, 60 mg, 3 mL) was pierced through the septum. The bottle was aerated for 30 s with compressed air by introducing a 120 mm Sterican needle into the solution, which was connected to an emptied SPE cartridge and a plastic nozzle. Thus, potential volatile TPs were captured on the SPE cartridges, which were then stored in a refrigerator at 4°C. The SPE cartridges were used several times.

After aeration, the emptied SPE cartridge was disconnected from the needle and replaced with a plastic syringe. Ca. 0.3-0.35 mL of the test solution was withdrawn and temporarily filled into a 0.65 mL PP Eppendorf cap. After that, the SPE cartridge was also removed from the bottle. 0.3 mL of the sample were then prepared as explained above.

Elution of the SPE cartridges was performed with 2 x 1.5 mL MeOH. After elution, the remaining liquid was squeezed out of the cartridge with the help of an air stream. 60 μL of $^{13}\text{C}_2, ^2\text{H}_2$ -8:2-FTOH (1 ng μL^{-1} MeOH) was added to the eluate, which was vortexed for 5 s and partially transferred into a 500 μL PP vial.

The sample from 'PP2' after 105 d was enriched by SPE to confirm the presence of 2H-PFOA. 10 mL samples were drawn through a WAX SPE cartridge (30 mg sorbent, 60 μm , 3 cm^3) (Waters, Eschborn, Germany) previously conditioned with 3 mL MeOH + 0.1% NH_3 and 3 mL of water. The cartridges were dried under nitrogen for 5 min and the compounds were eluted with 2 x 1.5 mL MeOH + 0.1% NH_3 . After evaporation to dryness under a gentle stream of nitrogen at 50°C \pm 1°C, the residue was reconstituted in 0.5 mL $\text{H}_2\text{O}/\text{MeOH}$ (1/1; V/V).

6.1.3.3 Biodegradation of TFMPPrOH

Three 1 L amber glass bottles were filled with 0.5 L effluent waste water from waste water treatment plant Beuerbach, Germany, taken at 18 February 2009. The inoculum was aerated for 0.5 h with an aquarium pump.

A stock solution was prepared by dissolving 12.6 mg TFMPPrOH in 2 mL MeOH. The active biodegradation sample contained 794 μL of the stock solution. The sterilized assay was

prepared in the same way, but 5 g NaN_3 were added prior to adding TFMPrOH. A control assay was prepared by mixing 500 mL WWTP effluent and 794 μL MeOH.

The bottles were stirred for 30 min and a sample of 10 mL was taken into a 22 mL glass vial. Initial TFMPrOH concentration in the active and sterilized sample was 9.8 mg L^{-1} ($68.1 \mu\text{M}$).

The bottles were closed with a glass plug and parafilm for four days and continuously shaken at 100 rpm on an automatic shaker. After four days, the glass plug and parafilm were removed and from then on, the bottles were aerated daily for half an hour with an aquarium pump.

For IC analysis, the frozen samples were put in an ultrasonic bath for 5 min and 3.5 mL of the sample were mixed with 3.5 mL mQ- H_2O . The samples were vortexed and filtered through a $0.2 \mu\text{m}$ membrane filter.

6.1.3.4 Biodegradation of TFMHxOH

The biodegradation assay for TFMHxOH was essentially carried out in the same way as for TFMPrOH (see 6.1.3.3). The following changes were made:

The stock solution was prepared by mixing 13.0 mg TFMHxOH and 2 mL MeOH. The active and sterilized assays contained 769 μL of the stock solution. Initial TFMHxOH concentration was 10 mg L^{-1} ($53.7 \mu\text{M}$).

6.1.3.5 Biodegradation of HFBPrOH

A stock solution of HFBPrOH was prepared by weighing 33.0 mg into a 25 mL volumetric flask and filling up with water. The biodegradation assay was carried out in amber 1 L glass bottles. The bottles were filled with 500 g WWTP effluent (December 2 2010). After aerating the bottles for 1 min, 5 g of sodium azide were added to the sterilized bottle and shaken for several minutes. To the active assay and the sterilized assay, 3.79 mL of the stock solution were added and stirred with a magnetic stirrer for 45 minutes. Then, approximately 10 mL of a sample was transferred into a 22 mL glass vial and frozen.

The bottles were aerated regularly (see table) and samples of 1 mL (in 1.5 mL Eppendorf PP caps) or 10 mL (in 22 mL glass vials) were taken approximately once a week.

Sample preparation was carried out by transferring 300 μL of the sample into a 1.5 mL Eppendorf cap and mixing with 60 μL 6:2-FTOH solution ($10 \text{ ng } \mu\text{L}^{-1}$ ACN) and 240 μL ACN. The samples were vortexed and centrifuged for 5 min. The supernatant was transferred into 500 μL PP vials with a glass pipette.

6.1.4 Trace analysis of PFASs in wastewater treatment plant effluents

WWTP effluents were filtered through a Whatman GF6 glass fiber filter (Whatman, Dassen, Germany) with the help of a water-jet vacuum pump and spiked with 50 μL of internal standard ($^{13}\text{C}_2$ -PFHxA and $^{13}\text{C}_2$ -PFOA, 100 $\text{pg } \mu\text{L}^{-1}$ MeOH each). pH was adjusted to 6 ± 0.1 with 10% aqueous acetic acid.

Enrichment of PFASs was achieved on Oasis[®] WAX cartridges (30 mg sorbent, 60 μm , 3 cm^3) (Waters, Eschborn, Germany) previously conditioned with 2 mL n-hexane, 2 mL MeOH + 0.1% NH_3 , 2 x 2 mL MeOH and 5 x 2 mL H_2O mQ. The sample was drawn through the cartridge under vacuum at a flow rate of approximately 15 mL min^{-1} .

The cartridges were under a stream of nitrogen for 10 min and subsequently eluted with 2 x 2 mL MeOH/acetone (1/1) and 3 x 2 mL MeOH containing 0.1% NH_3 . The latter eluate was evaporated at $T \leq 40^\circ\text{C}$ under a gentle stream of nitrogen.

The residue was reconstituted in 500 μL H_2O /MeOH (1/1; V/V), vortexed for 15 s and filtered into a 500 μL PP vial through a 0.45 μm membrane filter made of regenerated cellulose.

Calibration was done by extraction of spiked PFASs from ground water (Niedernhausen, Germany) in the same manner as explained above. The PFAS concentrations were 0, 0.5, 1, 2.5, 5 and 10 $\text{ng } 200 \text{ mL}^{-1}$ for PFCA and PFSA and 0, 1, 2.5, 5, 10 and 25 $\text{ng } 200 \text{ mL}^{-1}$ for FTEO₁Cs. To all calibration points, 50 μL of the internal standard solution (see above) were added. Validation parameters are summarized in Table 21. If concentrations exceeded the calibration range, samples were diluted accordingly.

Table 21: Validation parameters for trace analysis of PFASs. Recovery is expressed as method recovery of spiked WWTP samples (n=3), relative standard deviation in brackets. Repeatability is expressed as instrumental repeatability (n=4)

Compound	LOD [ng L^{-1}]	LOQ [ng L^{-1}]	Recovery [%]	Repeatability [%]
6:2-FTEO ₁ C	1.0	1.8	98.8 (2.7)	9.4
8:2-FTEO ₁ C	14.6	25.3	79.1 (5.9)	7.5
PFHxA	0.6	0.9	95.7 (15.2)	3.6
PFHeA	0.3	0.5	120.5 (6)	7.6
PFOA	0.7	1.2	79.5 (10.5)	7.6
PFNA	0.2	0.5	63.1 (6.6)	7.7
PFDA	0.7	1.2	86.7 (3.7)	8.1
PFBS	0.3	0.5	150.8 (22.1)	4.3
PFHxS	0.2	0.5	195.2 (48.2)	6.2
PFOS	0.5	0.9	83.3 (9.3)	7.7
PFDS	0.2	0.5	76.5 (10)	14.7

6.1.5 Two-dimensional fractionation of FTEO

6.1.5.1 Reversed-phase column chromatography

The crude FTEO mixture was chromatographed two-dimensionally in order to allow a comprehensive biodegradation test of only longer chained FTEOs with respect to the ethoxylate chain length. Therefore, the mixture was initially separated under reversed-phase conditions leading to separation mainly according to the perfluorocarbon chain length. Afterwards, NP chromatography was used to separate the compounds according to their ethoxylate chain length.

500 mg Zonyl FSH (= 250 mg FTEO) were weighed and dissolved in H₂O. A glass column was packed with 20 g C₁₈ material (Bakerbond Octadecyl (C₁₈), 40 µm particle size, J.T. Baker, Phillipsburg, NJ, USA) and the compounds were eluted with mixtures of H₂O and MeOH. Initial conditions were H₂O/MeOH (50/50; V/V) and the MeOH fraction were increased stepwise towards 90%. Fractions of approximately 4 mL (in the beginning 10 mL) were collected in 12 mL centrifuge tubes previously rinsed with acetone.

The fractions were diluted 1:200 with H₂O/MeOH + 5 mM NH₄OAc and measured by flow-injection analysis on the 3200 Q Trap. Basic parameters were: 'Enhanced MS' mode (*m/z* 300-1700), 5 µL injected, eluent: H₂O/ACN (20/80; V/V) + 5 mM NH₄OAc

The fractions containing compounds with one perfluorocarbon chain length only were pooled and evaporated on a rotary evaporator. If foaming occurred, the remainder was evaporated at 70°C under a stream of nitrogen.

The residue was dissolved in 2 mL of the eluting solvent for normal-phase chromatography.

6.1.5.2 Normal-phase column chromatography

The 8:2-FTEO fraction was chromatographed under NP conditions on 30 g flash silica gel (Silica Gel 60, 40-63 µm particle size, Carl Roth, Karlsruhe, Germany) with an eluent consisting of ethyl acetate/acetone/water (55/35/10; V/V/V) (based on Ref. [176]). Fractions of 2 to 15 mL were collected in 12 mL centrifuge tubes.

Fractions were dissolved 1:100 with H₂O/MeOH (1/1; V/V) + 5 mM NH₄OAc and measured under the same conditions as described above (except: injection volume 100 µL).

Fractions were pooled in a 22 mL glass vial according to the degree of ethoxylation (two to five ethoxymers each) and evaporated at 50°C ± 1°C under nitrogen.

In order to determine the mass, the residues were reconstituted in 1 mL acetone, vortexed for 15 s and transferred into a 2 mL glass vial previously washed with acetone and weighed. After evaporation to dryness, the vials were weighed again. A blank was prepared by transferring 1 mL into such a vial in order to check for potential problems in the weighing procedure.

6.1.6 Synthesis of TPs

6.1.6.1 8:2-FTEO₁C

Synthesis of crude FTEO₁Cs was adopted from the work of Abello et al. [177]. 172.5 mg sodium hydride (NaH, suspension in mineral oil, 4 eq.) were weighed into a round-bottom flask under nitrogen and washed twice with 10 mL n-pentane. After suspending in 3 mL dry THF, 500 mg 8:2-FTOH (1 eq.) dissolved in 10 mL dry tetrahydrofuran (THF) were slowly added to the suspension. After stirring for 0.5 h, 180 mg bromoacetic acid (1.2 eq.) dissolved in 5 mL dry THF were added dropwise to the stirring solution. The reaction progress was monitored by means of thin layer chromatography on silica gel (Polygram[®] SIL G/UV₂₅₄ with fluorescent indicator, Macherey Nagel, Düren, Germany) using ethyl acetate as the eluent (R_f (8:2-FTOH) = 0.59).

The mixture was stirred overnight, filtered, washed with 2 x 10 mL 1 M HCl and dried in a vacuum desiccator over silica gel for one week.

6.1.6.2 6:2-FTEO₁C

438 mg sodium hydride (NaH, suspension in mineral oil, 4 eq.) were weighed into a round-bottom flask under nitrogen and washed twice with 10 mL n-pentane. After suspending in 5 mL dry THF, 1 g 6:2-FTOH (1 eq.) dissolved in 5 mL dry THF were slowly added to the suspension. After stirring for 0.5 h, 457 mg bromoacetic acid (1.2 eq.) dissolved in 5 mL dry THF were added in little portions to the stirred solution. The reaction progress was monitored by means of thin layer chromatography on silica gel (Polygram[®] SIL G/UV₂₅₄ with fluorescent indicator, Macherey Nagel, Düren, Germany) using ethyl acetate as the eluent (R_f (8:2-FTOH) = 0.59).

The mixture was stirred overnight and filtered. The residue was suspended in 50 mL 1 M HCl and extracted with 2 x 20 mL dichloromethane. The organic phase was evaporated with a rotary evaporator.

6.1.6.3 Clean-up

The crude products were dissolved in acetone, diluted 1:100 with water and purified in small portions on Oasis[®] MAX cartridges (6 cm³, 150 mg sorbent) (Waters, Eschborn, Germany) previously conditioned with 5 mL n-hexane, 5 mL MeOH and 2 x 5 mL 7.5 % aq. NH₃. The FTEO₁C solution was passed through the cartridge and the filtrate recovered in a centrifuge tube. The cartridge was washed with 5 mL 7.5 % aq. NH₃, 5 mL MeOH/7.5 % aq. NH₃ (1/1; V/V), 5 mL MeOH and 5 mL acetone/ethyl acetate (1/1; V/V) prior to elution with 10 mL MeOH/formic acid (100/5; V/V).

5 μL of all solutions were transferred into a HPLC Vial and 995 μL H_2O were added. These samples were measured on the by HPLC-ESIMS/MS in MRM mode for 8:2-FTEO₂C and 6:2-FTEO₁C. Only the eluate contained significant amounts of FTEO₁C

The eluate was transferred into a 22 mL vial, which had been previously weighed, and evaporated under a nitrogen stream at $T \leq 50^\circ\text{C}$.

Due to the laborious clean-up procedure, the crude products were not entirely processed. Therefore, a determination of the overall yield of the synthesis is not possible. Clean-up of the crude products was ceased when approximately 5 mg of the final product was present.

6.1.6.4 Analysis

The final products were analyzed by (HPLC-)ESI-MS, (HPLC-)ESI-MS/MS, (HPLC-)ESI-orbitrap-MS and NMR. ESI-MS, ESI-MS/MS and ESI-orbitrap-MS data are presented in the results and discussion section.

The LC-ESI-MS measurements showed approximately 1% of cross-contamination of the FTEO₁C products, which is due to non-pure educts (FTOH). No other contaminations were detected with any of the abovementioned methods, thus, the purity was determined to be 100%.

NMR data

6:2-FTEO₁C:

¹H NMR (400 MHz, MeOD) δ 3.99 (s, 2H), 3.75 (t, $^3J_{HH} = 5.3$ Hz, 2H), 2.44 (t, $J = 19.0$ Hz, 2H).

¹³C NMR (101 MHz, MeOD) δ 175.62 (s), 115.47 (m), 70.27 (s), 65.09 (s), 33.14 (t, $J = 21.4$ Hz).

¹⁹F NMR (188 MHz, MeOD) δ -82.96 (tt, $J = 9.9, 2.2$ Hz, 3F, CF₃-CF₂-), -114.92 (m, 2F, -CF₂-CF₂-CH₂-), -123.40 (m, 2F, -CF₂-CF₂-CF₂-CH₂-), -124.42 (m, 2F, CF₃-CF₂-CF₂-CF₂-), -125.15 (m, 2F, -CF₂-CF₂-CF₂-CF₂-CH₂-), -127.84 (m, 1F, CF₃-CF₂-CF₂-).

¹⁹F NMR (1H decoupled) (188 MHz, MeOD) δ -82.96 (tt, $J = 10.1, 2.2$ Hz, 3F), -114.91 (m, 2F), -123.38 (m, 2F), -124.39 (m, 2F), -125.18 (m, 2F), -127.83 (m, 2F).

8:2-FTEO₁C:

¹H NMR (400 MHz, MeOD) δ 4.02 (s, 2H, -O-CH₂-COOH), 3.79 (t, $^3J_{HH} = 6.1$ Hz, -CH₂-CH₂-O-2H), 2.49 (t, $J = 19.2$ Hz, 2H, -CF₂-CH₂-CH₂-).

¹³C NMR (101 MHz, MeOD) δ 174.88 (s, -CH₂-COOH), 117.50 (m, perfluoroalkyl carbon atoms), 69.64 (s, -O-CH₂-COOH), 64.34 (s, -CH₂-CH₂-O-), 32.44 (t, $^2J_{CF} = 21.4$ Hz, -CF₂-CH₂-CH₂-).

^{19}F NMR (188 MHz, MeOD) δ -82.90 (t, J = 10.1 Hz, 3 F, $\text{CF}_3\text{-CF}_2\text{-}$), -114.88 (m, 2F, $\text{-CF}_2\text{-CF}_2\text{-CH}_2\text{-}$), -123.35 (m, 6F, $\text{CF}_2\text{-CF}_2\text{-CF}_2\text{-CF}_2\text{-CF}_2\text{-CH}_2\text{-}$), -124.22 (s, 2F, $\text{CF}_3\text{-CF}_2\text{-CF}_2\text{-CF}_2\text{-}$), -125.14 (m, 2F, $\text{-CF}_2\text{-CF}_2\text{-CF}_2\text{-CH}_2\text{-}$), -127.77 (m, 2F, $\text{CF}_3\text{-CF}_2\text{-CF}_2\text{-}$).

^{19}F NMR (1H decoupled) (188 MHz, MeOD) δ -82.90 (t, J = 10.0 Hz, 3F), -114.90 (m, 2F), -123.36 (m, 6F), -124.22 (s, 2F), -125.14 (m, 2F), -127.77 (m, 2F).

6.1.7 Ecotoxicological experiments

6.1.7.1 Acute toxicity on *Pseudokirchneriella subcapitata*

Acute toxicity to algae was carried out with the "PAM test" (pulsed amplitude modulation) developed by the Rijksinstituut voor Volksgezondheid en Milieu (RIVM, National institute for Public Health and the Environment) and the University of Amsterdam [178]. Briefly, photosynthetic activity of the green algae *Pseudokirchneriella subcapitata* is measured by a pulsed-amperometric fluorometer under the influence of the selected chemical at different concentrations. Seven geometrically distributed concentrations and one blank are prepared and measured in duplicate. The end-point of the test is fluorescence yield compared with a blank after 4.5 h.

The test is carried out in so-called 'Dutch Standard Water', which consists of 100 mg L⁻¹ NaHCO₃, 20 mg L⁻¹ KHCO₃ and 180 mg L⁻¹ MgSO₄·7H₂O dissolved in milli-Q water.

6.1.7.2 Acute toxicity on *Chydorus sphaericus*

Acute toxicity to *Chydorus sphaericus* was assessed by the help of a test developed at RIVM [178]. Briefly, a minimum number of 20 juvenile (age < 24 h) animals were exposed to a series of at least six concentrations of the test chemical and a blank. The animals were divided into at least four groups and the test was carried out in 2 mL HPLC vials with a test volume of 250 μL . Immobilization was assessed after 24 h and 48 h under a microscope after gently shaking the HPLC vial. EC₅₀ and EC₁₀ values were calculated with the Probit software provided by the US Environmental Protection Agency.

6.1.7.3 Verification of concentrations

Concentrations of the compounds in assays with PFBA (with pH adjustment), PFOA (with pH adjustment), perfluorononanoic acid (PFNA) and 1*H*,1*H*,8*H*,8*H*-perfluorooctane-1,8-diol (THPFODiol) were confirmed by means of HPLC-ESI-MS/MS. Samples were drawn right after the test and immediately diluted 1:10 (V:V) with MeOH to prevent adsorption. For further measurement, these samples were subsequently diluted with water/MeOH (1:1; V:V) to fit into the calibration curve. For measurement of PFOA, PFNA and THPFODiol, internal standard $^{13}\text{C}_2\text{-PFOA}$ was added to the samples and used for quantification.

6.2 List of abbreviations

ACN	Acetonitrile
AFFF	Aqueous firefighting foam
APFO	Ammonium perfluorooctanoate
API	Atmospheric pressure ionization
CAD	Collisionally-activated dissociation
CE	Collision energy
CID	Collision-induced dissociation
CRM	Charge residue model
cps	Counts per second
CXP	Collision-cell exit potential
DOC	Dissolved organic carbon
DP	Declustering potential
EC ₅₀	Half maximal effective concentration
EP	Entrance potential
ESI	Electrospray ionization
FTEO	Fluorotelomer ethoxylate
FTEOC	Fluorotelomer ethoxycarboxylic acid
FTO	Fluorotelomer olefin
FTOH	Fluorotelomer alcohol
FTS	Fluorotelomer sulfonate
FWHH	Full width at half height
HFB	2,2,3,3,4,4,4-Heptafluorobutoxy-
HPLC	High-performance liquid chromatography
IEM	Ion evaporation model
LIT	Linear ion trap
LOD	Limit of detection
LOQ	Limit of quantification
<i>m/z</i>	Mass-to-charge ratio
MeOH	Methanol
MS	Mass spectrometry
MS/MS	Tandem mass spectrometry
N-EtFOSE	N-Ethyl-perfluorooctane sulfonamidoethanol
N-MeFOSE	N-Methyl-perfluorooctane sulfonamidoethanol
NH ₄ OAc	Ammonium acetate
NMR	Nuclear magnetic resonance
NOEC	No observed effect concentration
NP	Normal phase
NPEO ₂	Nonylphenol diethoxylate
OECD	Organisation for Economic Co-Operation and Development

PBT	Persistent, bioaccumulative, toxic
PFAS	Perfluoroalkyl and polyfluoroalkyl substance
PFBA	Perfluorobutanoic acid
PFBS	Perfluorobutane sulfonate
PFCA	Perfluorinated carboxylic acid
PFDA	Perfluorodecanoic acid
PFDS	Perfluorodecane sulfonate
PFHeA	Perfluoroheptanoic acid
PFHxA	Perfluorohexanoic acid
PFHxS	Perfluorohexane sulfonate
PFNA	Perfluorononanoic acid
PFOA	Perfluorooctanoic acid
PFOS	Perfluorooctane sulfonate
PFPeA	Perfluoropentanoic acid
PFSA	Perfluorinated sulfonic acid
PFSuA	Perfluorosuberic acid
POP	Persistent organic pollutant
PP	Polypropylene
ppm	Parts per million
PTFE	Polytetrafluoroethylene
PVDF	Polyvinylidene difluoride
Q (q)	Quadrupole
QqQ	Triple quadrupole
QqQ _{LIT}	Hybrid triple quadrupole / linear ion trap
RDBE	Ring and double bond equivalents
RF	Radio frequency
RP	Reversed phase
RSD	Relative standard deviation
SIM	Single ion monitoring
SPE	Solid-phase extraction
TFES	2,2,2-Trifluoroethane sulfonate
TFM	Trifluoromethoxy
TFMC	Trifluoromethyl carbonate
TFMeOH	Trifluoromethanol
TFMHxA	6-Trifluoromethoxyhexanoic acid
TFMHxOH	6-Trifluoromethoxyhexan-1-ol
TFMPrA	3-Trifluoromethoxypropanoic acid
TFMPrOH	3-Trifluoromethoxypropan-1-ol
TFMS	Trifluoromethane sulfonate
THF	Tetrahydrofuran

THPFOdiol	<i>1H, 1H, 8H, 8H</i> -Tetrahydroperfluorooctanediol
TP	Transformation product
WWTP	Wastewater treatment plant

6.3 List of figures

Figure 1: Overview of biotic and abiotic processes involved in the formation of transformation products ..	9
Figure 2: Toxicity of a set of pesticides versus the toxicity of its TP..	12
Figure 3: Biotransformation pathways of 8:2-FTOH.....	19
Figure 4: Schematic illustration of a novel PFASs and its transformation pathway.....	21
Figure 5: Biotransformation routes of the surfactant candidate 10-(trifluoromethoxy)decane-1-sulfonate.	22
Figure 6: Definition of mass resolving power by the FWHM method.....	26
Figure 7: Basic setup and functionality of an ESI ion source and the ESI process	28
Figure 8: Simplified scheme of a quadrupole mass analyzer.....	29
Figure 9 Setup of the Applied Biosystems 3200 Q Trap [®]	31
Figure 10: Schematic illustration of one linear ion trap scan cycle.	31
Figure 11: Schematic illustration of an orbitrap mass analyzer.....	34
Figure 12: Structure and acronymization of fluorotelomer ethoxylates	37
Figure 13: (+)ESI-MS Q1MS spectrum of 15 $\mu\text{g mL}^{-1}$ Zonyl FSH.....	38
Figure 14: (+)ESI-MS Q1MS spectrum of 15 $\mu\text{g mL}^{-1}$ Zonyl FSH with 5 mM ammonium acetate.....	39
Figure 15: Percentage gain in relative and absolute intensity of FTEO ammonium adducts	41
Figure 16: Relative molar intensities of FTEOs in technical mixture Zonyl FSH.....	42
Figure 17: HPLC-(+)-ESI-MS/MS chromatogram of 750 ng Zonyl FSH mL^{-1}	44
Figure 18: (+)ESI-MS/MS product ion spectrum of 6:2-FTEO ₇	46
Figure 19: (+)ESI-MS/MS product ion spectrum of the ammonium adduct of 6:2-FTEO ₅ C	46
Figure 20: (-)ESI-MS/MS enhanced product ion spectra of 8:2-FTEO ₇ and 8:2-FTOH.....	47
Figure 21: Proposed fragmentation pathway of 8:2-FTEO ₇ after negative ESI.	48
Figure 22: (-)ESI-MS/MS spectra of 8:2-FTEO ₁ C measured on orbitrap and QqLIT.....	49
Figure 23: CID Fragmentation scheme of 8:2-FTEO ₁ C.	52
Figure 24: Tentative fragmentation pathway of FTOH-related product ions of 8:2-FTEO ₁ C..	54
Figure 25: HPLC-(-)ESI-MS/MS XICs for FTOHs in Zonyl FSH	56
Figure 26: Structural formula and acronyms of FTEO in sterilized controls.....	57
Figure 27: Biodegradation of FTEO expressed as concentration divided by initial concentration.....	58
Figure 28: Temporal evolution of FTEOCs.....	59
Figure 29: Course of FTEO in experiment 'PP1' and 'G'	62
Figure 30: PFOA formation in three different FTEO biotransformation.experiments.....	64
Figure 31: HPLC-(-)ESI-MS/MS enhanced product ion spectrum of 2H-PFOA (m/z 395)	65
Figure 32: Temporal course of 8:2-FTEO ₁₃₋₁₅ C in experiment 'PP1' and 'G'	66
Figure 33: Synthetic route to FTEO ₁ C.....	68
Figure 34: LC-(+)ESI-MS/MS XICs for 8:2-FTEO ₄₋₇ C in sample from WWTP-14.....	71
Figure 35: (+)ESI-MS/MS product ion spectrum of TFMPPrOH.....	73
Figure 36: HPLC-(-)ESI-MS/MS precursor ion scan of a TFMPPrOH biodegradation sample	74
Figure 37: HPLC-(-)ESI-MS/MS enhanced product ion spectrum of TFMC and TFMPPrA.....	75
Figure 38: Temporal evolution of TFMPPrOH TPs TFMPPrA and TFMC	76
Figure 39: Proposed biotransformation pathways of TFMPPrOH	78

Figure 40: (+)-ESI-MS/MS CID enhanced product ion spectrum of TFMHxOH	79
Figure 41: Proposed fragmentation mechanism of the carbenium ion at m/z 169.....	80
Figure 42: Temporal evolution of TFMHxOH in active and sterile biodegradation assays.	80
Figure 43: (-)ESI-MS/MS product ion scan of TFMHxA and proposed structures of the product ions.	81
Figure 44: Temporal evolution of TFMHxOH TPs TFMC and TFMHxA and fluoride release.....	81
Figure 45: Proposed degradation pathways of TFMHxOH;	82
Figure 46: Temporal evolution of HFBPrOH in the active and sterilized biodegradation assay.	84
Figure 47: HPLC-(-)ESI-MS/MS product ion spectrum of HFBAA	85
Figure 48: Temporal evolution of HFBPrOH TPs and their structural formulae.....	86
Figure 49: Proposed degradation scheme of HFBPrOH.....	87
Figure 50: Logarithmic dose-effect curve for PFBA with and without pH adjustment.	90
Figure 51: Dose-response curves for APFO as well as PFOA with and without pH adjustment.	91

6.4 List of tables

Table 1: Selected modes, which the Applied Biosystems 3200 Q Trap can be operated with.....	33
Table 2: Measured versus theoretical m/z of orbitrap MS measurement of FTEO ₁ Cs.....	50
Table 3: Summarized parameters for biotransformation experiments of fractionated FTEO	61
Table 4: PFAS concentration measured in selected WWTP effluents and surface waters	70
Table 5: Linear coefficient of determination (R^2) between concentrations of PFCAs	72
Table 6: Fluoride determination in TFMP ₁ OH biodegradation samples after 77 days.....	77
Table 7: Overview of results for acute toxicity of fluorinated compounds to <i>Pseudokirchneriella subcapitata</i>	93
Table 8: Results for acute toxicity of PFBA to <i>Chydorus sphaericus</i>	95
Table 9: List of solvents and reagents and their purities.....	100
Table 10: MS parameters which were used throughout the whole thesis.....	101
Table 11: Chromatographic gradient for HPLC-MS analysis of PFCAs, PFSA and FTEO ₁ Cs.....	103
Table 12: MS settings used for analysis of PFCAs, PFSA and FTEO ₁ Cs.	103
Table 13: Chromatographic gradient for HPLC-MS analysis of FTOHs	104
Table 14: Compound-dependent MS parameters for FTOH analysis.....	104
Table 15: Compound-dependent MS parameters of 6:2-FTEO and 8:2-FTEO congeners	105
Table 16: Chromatographic gradient for HPLC-MS analysis of 8:2-FTEO and 8:2-FTEOC during biotransformation study of purified 8:2-FTEO ₁₄₋₁₆	106
Table 17: Chromatographic gradient for HPLC-MS analysis of TFMP ₁ OH TPs	107
Table 18: Chromatographic gradient for HPLC-MS analysis of TFMHxOH.....	107
Table 19: Chromatographic gradient used for analysis of HFBP ₁ OH and its potentia TPs	108
Table 20: Overview of HFBP ₁ OH and its TPs analyzed.....	109
Table 21: Validation parameters for trace analysis of PFASs.....	114
Table 22: Acronyms of perfluorocarbon chains.....	125
Table 23: General structures and acronyms of classic PFASs.....	126
Table 24: Structures and acronyms of fluorotelomer-based compounds	126
Table 25: Structures and acronyms of compounds related to biotransformation of TFMHxOH, TFMP ₁ OH and HFBP ₁ OH	128
Table 26: Structures and acronyms of miscellaneous fluorinated compounds.....	129

6.5 List of compounds and their acronyms

Acronymization of classic PFASs, such as PFCAs, is based on a common acronym for the compound class and inserting an acronym for the respective perfluorocarbon chain length.

The acronyms for perfluoroalkyl chain lengths are depicted in Table 22.

Table 22: Acronyms of perfluorocarbon chains. Please notice that in PFCAs the number of carbon atoms includes the carboxylic acid carbon.

Number of carbon atoms	Acronym
3	Pr
4	B
5	Pe
6	Hx
7	Hp
8	O
9	N
10	D
11	Un
12	Do
13	Tr
14	Te

Table 23 summarizes the acronymization for PFCAs, PFSA and their sulfonamide derivatives.

The X must be substituted with the correct acronym for the chain length as shown in Table 22.

Table 23: General structures and acronyms of classic PFASs. The 'X' must be replaced with the acronym referring to the perfluoroalkyl chain length as presented in Table 22.

Structure	Acronym substance class	Acronym single compounds
$\text{F}-(\text{CF}_2)_n-\text{C} \begin{array}{l} \text{O} \\ \parallel \\ \text{OH} \end{array}$	PFCA	PFXA
$\text{F}-(\text{CF}_2)_n-\text{S} \begin{array}{l} \text{O} \\ \parallel \\ \text{OH} \\ \parallel \\ \text{O} \end{array}$	PFSA	PFXS
$\text{F}-(\text{CF}_2)_n-\text{S} \begin{array}{l} \text{O} \\ \parallel \\ \text{NH}_2 \\ \parallel \\ \text{O} \end{array}$		FXSA
$\text{F}-(\text{CF}_2)_n-\text{S} \begin{array}{l} \text{O} \\ \parallel \\ \text{NH} \\ \parallel \\ \text{O} \end{array} \text{R}$ <p>R = Me, Et</p>		N-Me/N-EtFXSA
$\text{F}-(\text{CF}_2)_n-\text{S} \begin{array}{l} \text{O} \\ \parallel \\ \text{N} \begin{array}{l} \text{CH}_2-\text{CH}_2 \\ \parallel \\ \text{OH} \end{array} \\ \parallel \\ \text{O} \end{array} \text{R}$ <p>R = Me, Et</p>		N-Me/N-EtFXSE

Fluorotelomer compounds are a group of chemicals with both perfluorinated carbon chains and one or several methylene groups as well as their derivatives. These compounds are named by special nomenclature, which is presented in Table 24.

Table 24: Structures and acronyms of fluorotelomer-based compounds

Structure	Acronym substance class	Acronym single compounds
$\text{F}-(\text{CF}_2)_x-\text{CH}_2-\text{CH}_2-\text{OH}$	FTOH	x:2-FTOH
$\text{F}-(\text{CF}_2)_x-\text{CH}_2-\text{C} \begin{array}{l} \text{O} \\ \parallel \\ \text{H} \end{array}$	FTAI	x:2-FTAI
$\text{F}-(\text{CF}_2)_x-(\text{CH}_2)_y-\text{C} \begin{array}{l} \text{O} \\ \parallel \\ \text{OH} \end{array}$	FTA	x:y-FTA
$\text{F}-(\text{CF}_2)_x-\text{CF}=\text{CH}-\text{C} \begin{array}{l} \text{O} \\ \parallel \\ \text{OH} \end{array}$	FTUA	x:2-FTUA
$\text{F}-(\text{CF}_2)_x-\text{CH}=\text{CH}-\text{C} \begin{array}{l} \text{O} \\ \parallel \\ \text{OH} \end{array}$	FTUA	x:3-FTUA
$\text{F}-(\text{CF}_2)_x-\text{CH}(\text{OH})-\text{CH}_3$	sFTOH	x:2-sFTOH
$\text{F}-(\text{CF}_2)_x-\text{C} \begin{array}{l} \text{O} \\ \parallel \\ \text{CH}_3 \end{array}$	FT ketone	x:2-FT ketone
$\text{F}-(\text{CF}_2)_x-\text{CH}_2-\text{CH}_2-\text{S} \begin{array}{l} \text{O} \\ \parallel \\ \text{OH} \end{array}$	FTS	x:2-FTS altern.: 1H,1H,2H,2H-PFXS
$\text{F}-(\text{CF}_2)_x-\text{CH}_2-\text{CH}_2-\text{O}-(\text{CH}_2-\text{CH}_2-\text{O})_y\text{H}$	FTEO	x:2-FTEO _y
$\text{F}-(\text{CF}_2)_x-(\text{CH}_2-\text{CH}_2-\text{O})_y-\text{CH}_2-\text{C} \begin{array}{l} \text{O} \\ \parallel \\ \text{OH} \end{array}$	FTEOC	x:2-FTEO _y C
$\text{F}-(\text{CF}_2)_x-(\text{CH}_2-\text{CH}_2-\text{O})_y-\text{CH}_2-\text{C} \begin{array}{l} \text{O} \\ \parallel \\ \text{H} \end{array}$	FTEOAI	x:2-FTEO _y AI
$\text{F}-(\text{CF}_2)_x-\text{CH}=\text{CH}_2$	FTO	x:2-FTO

Substances containing the TFM group or the HFB group are summarized in Table 25.

Table 25: Structures and acronyms of compounds related to biotransformation of TFMHxOH, TFMPrOH and HFBPrOH

Structure	Acronym
$\text{F}_3\text{C}-\text{O}-(\text{CH}_2)_3-\text{OH}$	TFMPrOH
$\text{F}_3\text{C}-\text{O}-(\text{CH}_2)_6-\text{OH}$	TFMHxOH
$\text{F}_3\text{C}-\text{O}-(\text{CH}_2)_2-\text{C}(=\text{O})\text{OH}$	TFMPrA
$\text{F}_3\text{C}-\text{O}-(\text{CH}_2)_5-\text{C}(=\text{O})\text{OH}$	TFMHxOH
$\text{F}_3\text{C}-\text{O}-\text{C}(=\text{O})\text{OH}$	TFMC
$\text{F}-(\text{CF}_2)_3-\text{CH}_2-\text{O}-\text{CH}_2-\text{CH}(\text{OH})\text{CH}_3$	HFBPrOH
$\text{F}-(\text{CF}_2)_3-\text{CH}_2-\text{O}-\text{CH}_2-\text{CH}(\text{OH})\text{C}(=\text{O})\text{OH}$	HFBOHPrA
$\text{F}-(\text{CF}_2)_3-\text{CH}_2-\text{O}-\text{CH}_2-\text{C}(=\text{O})\text{OH}$	HFBA
$\text{F}-(\text{CF}_2)_3-\text{CH}_2-\text{OH}$	HFBOH

Compounds, which do not belong to substance classes presented above, are summarized in Table 26.

Table 26: Structures and acronyms of miscellaneous fluorinated compounds

Structure	Acronym
$\text{F}-(\text{CF}_2)_6-\text{CH}_2-\text{CH}_2-\text{SH}$	6:2-FTSH
$\text{HO}-\text{C}(=\text{O})-(\text{CF}_2)_6-\text{C}(=\text{O})-\text{OH}$	PFSubA
$\text{F}-(\text{CF}_2)_6-\text{S}(=\text{O})_2-\text{N}(\text{CH}_3)-\text{CH}_2-\text{CH}_2-\text{O}-\text{C}(=\text{O})-\text{CH}=\text{CH}_2$	N-MeFHxSEAc
$\text{F}-(\text{CF}_2)_6-\text{CH}_2-\text{NH}_2$	DHPFHpAm
$\text{HO}-\text{CH}_2-(\text{CF}_2)_6-\text{CH}_2-\text{OH}$	THPFOdiol

6.6 List of references

1. Hirsch, R., Ternes, T., Haberer, K., Kratz, K. L. Occurrence of antibiotics in the aquatic environment, *Science of The Total Environment* (1999) 225: 109-118.
2. Richardson, S. D. Environmental Mass Spectrometry, *Analytical Chemistry* (2000) 72: 4477-4496.
3. Wania, F., MacKay, D. Peer Reviewed: Tracking the Distribution of Persistent Organic Pollutants, *Environmental Science & Technology* (1996) 30: 390A-396A.
4. Reemtsma, T., Jekel, M. Organic Pollutants in the Water Cycle. Wiley VCH, Weinheim (2006).
5. Anonymous. Persistent pesticides and PCBs in the environment, *Nature* (1972) 240.
6. Jones, K. C., de Voogt, P. Persistent organic pollutants (POPs): state of the science, *Environmental Pollution* (1999) 100: 209-221.
7. Daughton, C. G., Ternes, T. A. Pharmaceuticals and personal care products in the environment: Agents of subtle change?, *Environmental Health Perspectives* (1999) 107: 907-938.
8. Reemtsma, T., Weiss, S., Mueller, J., Petrovic, M., Gonzalez, S., Barcelo, D., Ventura, F., Knepper, T. P. Polar pollutants entry into the water cycle by municipal wastewater: a European perspective, *Environmental Science & Technology* (2006) 40: 5451-5458.
9. Eichhorn, P., Knepper, T. P., Ventura, F., Diaz, A. The behavior of polar aromatic sulfonates during drinking water production: a case study on sulfophenyl carboxylates in two European waterworks, *Water Research* (2002) 36: 2179-2186.
10. Bernhard, M., Eubeler, J. P., Zok, S., Knepper, T. P. Aerobic biodegradation of polyethylene glycols of different molecular weights in wastewater and seawater, *Water Research* (2008).
11. Bernhard, M., Muller, J., Knepper, T. P. Biodegradation of persistent polar pollutants in wastewater: comparison of an optimised lab-scale membrane bioreactor and activated sludge treatment, *Water Research* (2006) 40: 3419-3428.
12. Wick, A., Wagner, M., Ternes, T. A. Elucidation of the Transformation Pathway of the Opium Alkaloid Codeine in Biological Wastewater Treatment, *Environmental Science & Technology* (2011) 45: 3374-3385.
13. Boreen, A. L., Arnold, W. A., McNeill, K. Photodegradation of pharmaceuticals in the aquatic environment: A review, *Aquatic Sciences - Research Across Boundaries* (2003) 65: 320-341.
14. Atkinson, R., Arey, J. Atmospheric Degradation of Volatile Organic Compounds, *Chemical Reviews* (2003) 103: 4605-4638.
15. Bond, T., Huang, J., Templeton, M. R., Graham, N. Occurrence and control of nitrogenous disinfection by-products in drinking water - A review, *Water Research* (2011) 45: 4341-4354.
16. Mitch, W. A., Sedlak, D. L. Formation of N-Nitrosodimethylamine (NDMA) from Dimethylamine during Chlorination, *Environmental Science & Technology* (2001) 36: 588-595.
17. Schmidt, C. K., Brauch, H. J. N,N-dimethylsulfamide as precursor for N-nitrosodimethylamine (NDMA) formation upon ozonation and its fate during drinking water treatment, *Environmental Science & Technology* (2008) 42: 6340-6346.
18. Stehl, R. H., Lamparski, L. L. Combustion of Several 2,4,5-Trichlorophenoxy Compounds: Formation of 2,3,7,8-Tetrachlorodibenzo-p-dioxin, *Science* (1977) 197: 1008-1009.

-
19. Giger, W., Brunner, P. H., Schaffner, C. 4-Nonylphenol in sewage sludge: accumulation of toxic metabolites from nonionic surfactants, *Science* (1984) 225: 623-625.
 20. The European Parliament and The Council of the European Union, Directive 2003/53/EC of the European Parliament and of The Council (2003), <http://eur-lex.europa.eu/LexUriServ/LexUriServ.do?uri=OJ:L:2003:178:0024:0027:en:PDF>, last access: 2-2-2012.
 21. Boxall, A. B. A., Sinclair, C. J., Fenner, K., Kolpin, D., Maund, S. J. Peer Reviewed: When Synthetic Chemicals Degrade in the Environment, *Environmental Science & Technology* (2004) 38: 368A-375A.
 22. Glaze, W. H. Sustainability engineering and green chemistry, *Environmental Science & Technology* (2000) 34: 449A.
 23. The European Parliament and The Council of the European Union, Regulation (EC) No 1907/2006 of The European Parliament and of The Council (2006), http://eur-lex.europa.eu/LexUriServ/site/en/oj/2006/l_396/l_39620061230en00010849.pdf, last access: 2-2-2012.
 24. European Chemicals Agency, Guidance on information requirements and chemical safety assessment, Chapter R.7b: Endpoint specific guidance (2008), http://echa.europa.eu/documents/10162/17224/information_requirements_r7b_en.pdf, last access: 13-2-2012.
 25. Organisation for Economic Co-Operation and Development, OECD Guidelines for the Testing of Chemicals, Section 3 (2011), OECD, last access: 27-12-2011.
 26. Sinclair, C. J., Boxall, A. B. A. Assessing the Ecotoxicity of Pesticide Transformation Products, *Environmental Science & Technology* (2003) 37: 4617-4625.
 27. Organisation for Economic Co-Operation and Development, Lists of PFOS, PFAS, PFOA, PFCA, related compounds and chemicals that may degrade to PFCA (2007), [http://www.ois.oecd.org/olis/2006doc.nsf/LinkTo/NT00000F9A/\\$FILE/JT03231059.PDF](http://www.ois.oecd.org/olis/2006doc.nsf/LinkTo/NT00000F9A/$FILE/JT03231059.PDF), last access: 23-9-2009.
 28. Lindstrom, A. B., Strynar, M. J., Libelo, E. L. Polyfluorinated Compounds: Past, Present, and Future, *Environmental Science & Technology* (2011) 45: 7954-7961.
 29. Murphy, C. D., Schaffrath, C., O'Hagan, D. Fluorinated natural products: the biosynthesis of fluoroacetate and 4-fluorothreonine in *Streptomyces cattleya*, *Chemosphere* (2003) 52: 455-461.
 30. O'Hagan, D., Harper, B. Fluorine-containing natural products, *Journal of Fluorine Chemistry* (1999) 100: 127-133.
 31. Bondi, A. Van der Waals Volumes and Radii, *The Journal of Physical Chemistry* (1964) 68: 441-451.
 32. Robinson, E. A., Johnson, S. A., Tang, T. H., Gillespie, R. J. Reinterpretation of the Lengths of Bonds to Fluorine in Terms of an Almost Ionic Model, *Inorganic Chemistry* (1997) 36: 3022-3030.
 33. Gillespie, R. J., Robinson, E. A. Bond lengths in covalent fluorides. A new value for the covalent radius of fluorine, *Inorganic Chemistry* (1992) 31: 1960-1963.
 34. Brockway, L. O. The Internuclear Distance in the Fluorine Molecule, *Journal of the American Chemical Society* (1938) 60: 1348-1349.
 35. Pauling, L. The Nature of the Chemical Bond and the Structure of Molecules and Crystals; An Introduction to Modern Structural Chemistry. Cornell University Press, Ithaca (1960).
-

-
36. Blanksby, S. J., Ellison, G. B. Bond Dissociation Energies of Organic Molecules, *Accounts of Chemical Research* (2003) 36: 255-263.
 37. Natarajan, R., Azerad, R., Badet, B., Copin, E. Microbial cleavage of CF bond, *Journal of Fluorine Chemistry* (2005) 126: 424-435.
 38. Lemal, D. M. Perspective on Fluorocarbon Chemistry, *The Journal of Organic Chemistry* (2004) 69: 1-11.
 39. Key, B. D., Howell, R. D., Criddle, C. S. Fluorinated Organics in the Biosphere, *Environmental Science & Technology* (1997) 31: 2445-2454.
 40. Kissa, E. Fluorinated Surfactants and Repellents. Marcel Dekker, New York (2001).
 41. Liu, J., Lee, L. S. Effect of fluorotelomer alcohol chain length on aqueous solubility and sorption by soils, *Environmental Science & Technology* (2007) 41: 5357-5362.
 42. Wang, N., Szostek, B., Buck, R. C., Folsom, P. W., Sulecki, L. M., Gannon, J. T. 8-2 Fluorotelomer alcohol aerobic soil biodegradation: Pathways, metabolites, and metabolite yields, *Chemosphere* (2009) 75: 1089-1096.
 43. Wang, N., Szostek, B., Buck, R. C., Folsom, P. W., Sulecki, L. M., Capka, V., Berti, W. R., Gannon, J. T. Fluorotelomer alcohol biodegradation - Direct evidence that perfluorinated carbon chains breakdown, *Environmental Science & Technology* (2005) 39: 7516-7528.
 44. Arp, H. P. H., Niederer, C., Goss, K. U. Predicting the partitioning behavior of various highly fluorinated compounds, *Environmental Science & Technology* (2006) 40: 7298-7304.
 45. Liu, J., Lee, L. S. Solubility and sorption by soils of 8:2 fluorotelomer alcohol in water and cosolvent systems, *Environmental Science & Technology* (2005) 39: 7535-7540.
 46. Lei, Y. D., Wania, F., Mathers, D., Mabury, S. A. Determination of vapor pressures, octanol-air, and water-air partition coefficients for polyfluorinated sulfonamide, sulfonamidoethanols, and telomer alcohols, *Journal of Physical Chemistry A* (2004) 49: 1013-1022.
 47. Goss, K. U., Bronner, G., Harner, T., Hertel, M., Schmidt, T. C. The partition behavior of fluorotelomer alcohols and olefins, *Environmental Science & Technology* (2006) 40: 3572-3577.
 48. 3M, Fluorochemical Use, Distribution and Release Overview; U.S. Public Docket AR-226-0550 (1999), <http://www.chemicalindustryarchives.org/dirtysecrets/scotchgard/pdfs/226-0550.pdf>, last access: 1-12-2011.
 49. Prevedouros, K., Cousins, I. T., Buck, R. C., Korzeniowski, S. H. Sources, fate and transport of perfluorocarboxylates, *Environmental Science & Technology* (2006) 40: 32-44.
 50. Rhoads, K. R., Janssen, E. M. L., Luthy, R. G., Criddle, C. S. Aerobic biotransformation and fate of N-ethyl perfluorooctane sulfonamidoethanol (N-EtFOSE) in activated sludge, *Environmental Science & Technology* (2008) 42: 2873-2878.
 51. Ellis, D. A., Martin, J. W., Mabury, S. A., Hurley, M. D., Andersen, M. P. S., Wallington, T. J. Atmospheric lifetime of fluorotelomer alcohols, *Environmental Science & Technology* (2003) 37: 3816-3820.
 52. Ellis, D. A., Martin, J. W., De Silva, A. O., Mabury, S. A., Hurley, M. D., Andersen, M. P. S., Wallington, T. J. Degradation of fluorotelomer alcohols: A likely atmospheric source of perfluorinated carboxylic acids, *Environmental Science & Technology* (2004) 38: 3316-3321.
 53. Wallington, T. J., Hurley, M. D., Xia, J., Wuebbles, D. J., Sillman, S., Ito, A., Penner, J. E., Ellis, D. A., Martin, J., Mabury, S. A., Nielsen, O. J., Andersen, M. P. S. Formation of C₇F₁₅COOH
-

- (PFOA) and other perfluorocarboxylic acids during the atmospheric oxidation of 8:2 fluorotelomer alcohol, *Environmental Science & Technology* (2006) 40: 924-930.
54. D'Eon, J. C., Hurley, M. D., Wallington, T. J., Mabury, S. A. Atmospheric chemistry of N-methyl perfluorobutane sulfonamidoethanol, $C_4F_9SO_2N(CH_3)CH_2CH_2OH$: kinetics and mechanism of reaction with OH, *Environmental Science & Technology* (2006) 40: 1862-1868.
 55. Taves, D. R. Evidence that there are Two Forms of Fluoride in Human Serum, *Nature* (1968) 217: 1050-1051.
 56. Taves, D. R., Grey, W. S., Brey, W. S. J. Abstracts of papers for the Fifteenth Annual Meeting of the Society of Toxicology, Atlanta, Georgia March 14, 1976 No. 69: Organic Fluoride in Human Plasma: Its Distribution and Partial Identification, *Toxicology and Applied Pharmacology* (1976) 37: 93-192.
 57. Fenn, J. B., Mann, M., Meng, C. K., Wong, S. F., Whitehouse, C. M. Electrospray ionization for mass spectrometry of large biomolecules, *Science* (1989) 246: 64-71.
 58. Whitehouse, C. M., Dreyer, R. N., Yamashita, M., Fenn, J. B. Electrospray interface for liquid chromatographs and mass spectrometers, *Analytical Chemistry* (1985) 57: 675-679.
 59. Dole, M., Mack, L. L., Hines, R. L., Mobley, R. C., Ferguson, L. D., Alice, M. B. Molecular Beams of Macroions, *The Journal of Chemical Physics* (1968) 49: 2240-2249.
 60. Olsen, G. W., Burris, J. M., Mandel, J. H., Zobel, L. R. Serum perfluorooctane sulfonate and hepatic and lipid clinical chemistry tests in fluorochemical production employees, *Journal of Occupational and Environmental Medicine* (1999) 41: 799-806.
 61. Olsen, G. W., Church, T. R., Larson, E. B., van, B. G., Lundberg, J. K., Hansen, K. J., Burris, J. M., Mandel, J. H., Zobel, L. R. Serum concentrations of perfluorooctanesulfonate and other fluorochemicals in an elderly population from Seattle, Washington, *Chemosphere* (2004) 54: 1599-1611.
 62. Olsen, G. W., Huang, H. Y., Helzlsouer, K. J., Hansen, K. J., Butenhoff, J. L., Mandel, J. H. Historical comparison of perfluorooctanesulfonate, perfluorooctanoate, and other fluorochemicals in human blood, *Environmental Health Perspectives* (2005) 113: 539-545.
 63. Kannan, K., Corsolini, S., Falandysz, J., Fillmann, G., Kumar, K. S., Loganathan, B. G., Mohd, M. A., Olivero, J., Van, W. N., Yang, J. H., Aldoust, K. M. Perfluorooctanesulfonate and related fluorochemicals in human blood from several countries, *Environmental Science & Technology* (2004) 38: 4489-4495.
 64. Olsen, G. W., Mair, D. C., Church, T. R., Ellefson, M. E., Reagen, W. K., Boyd, T. M., Herron, R. M., Medhdizadehkashi, Z., Nobiletti, J. B., Rios, J. A., Butenhoff, J. L., Zobel, L. R. Decline in perfluorooctanesulfonate and other polyfluoroalkyl chemicals in American Red Cross adult blood donors, 2000-2006, *Environmental Science & Technology* (2008) 42: 4989-4995.
 65. Olsen, G. W., Mair, D. C., Reagen, W. K., Ellefson, M. E., Ehresman, D. J., Butenhoff, J. L., Zobel, L. R. Preliminary evidence of a decline in perfluorooctanesulfonate (PFOS) and perfluorooctanoate (PFOA) concentrations in American Red Cross blood donors, *Chemosphere* (2007) 68: 105-111.
 66. Giesy, J. P., Kannan, K. Global distribution of perfluorooctane sulfonate in wildlife, *Environmental Science & Technology* (2001) 35: 1339-1342.
 67. Butt, C. M., Berger, U., Bossi, R., Tomy, G. T. Levels and trends of poly- and perfluorinated compounds in the arctic environment, *Science of The Total Environment* (2010) 408: 2936-2965.

-
68. Houde, M., Martin, J. W., Letcher, R. J., Solomon, K. R., Muir, D. C. Biological monitoring of polyfluoroalkyl substances: A review, *Environmental Science & Technology* (2006) 40: 3463-3473.
 69. Houde, M., De Silva, A. O., Muir, D. C., Letcher, R. J. Monitoring of perfluorinated compounds in aquatic biota: an updated review, *Environmental Science & Technology* (2011) 45: 7962-7973.
 70. 3M, Environmental Monitoring - Multi-City Study (2001), http://www.ewg.org/files/multicity_full.pdf, last access: 28-12-2011.
 71. Mak, Y. L., Taniyasu, S., Yeung, L. W., Lu, G., Jin, L., Yang, Y., Lam, P. K., Kannan, K., Yamashita, N. Perfluorinated compounds in tap water from China and several other countries, *Environmental Science & Technology* (2009) 43: 4824-4829.
 72. Wilhelm, M., Bergmann, S., Dieter, H. H. Occurrence of perfluorinated compounds (PFCs) in drinking water of North Rhine-Westphalia, Germany and new approach to assess drinking water contamination by shorter-chained C4-C7 PFCs, *International Journal of Hygiene and Environmental Health* (2010).
 73. Rumsby, P. C., McLaughlin, C. L., Hall, T. Perfluorooctane sulphonate and perfluorooctanoic acid in drinking and environmental waters, *Philosophical Transactions of The Royal Society A - Mathematical, Physical & Engineering Sciences* (2009) 367: 4119-4136.
 74. Skutlarek, D., Exner, M., Färber, H. Perfluorierte Tenside (PFT) in der aquatischen Umwelt und im Trinkwasser, *Umweltwissenschaften und Schadstoff-Forschung* (2006) 18: 151-154.
 75. Knepper, T. P., Lange, F. T. Polyfluorinated Chemicals and Transformation Products. Springer Verlag, Heidelberg (2011).
 76. Zhang, X., Chen, L., Fei, X. C., Ma, Y. S., Gao, H. W. Binding of PFOS to serum albumin and DNA: insight into the molecular toxicity of perfluorochemicals, *BMC Molecular Biology* (2009) 10: 16.
 77. Organisation for Economic Co-Operation and Development, Hazard Assessment of Perfluorooctane Sulfonate (PFOS) and its Salts (2002), <http://www.oecd.org/dataoecd/23/18/2382880.pdf>, last access: 13-2-2012.
 78. Intrasukri, U., Rangwala, S. M., O'Brien, M., Noonan, D. J., Feller, D. R. Mechanisms of peroxisome proliferation by perfluorooctanoic acid and endogenous fatty acids, *General Pharmacology: The Vascular System* (1998) 31: 187-197.
 79. Intrasukri, U., Feller, D. R. Comparison of the effects of selected monocarboxylic, dicarboxylic and perfluorinated fatty acids on peroxisome proliferation in primary cultured rat hepatocytes, *Biochemical Pharmacology* (1991) 42: 184-188.
 80. Berthiaume, J., Wallace, K. B. Perfluorooctanoate, perfluorooctanesulfonate, and N-ethyl perfluorooctanesulfonamido ethanol; peroxisome proliferation and mitochondrial biogenesis, *Toxicological Letters*. (2002) 129: 23-32.
 81. Haugthom, B., Spydevold, O. The mechanism underlying the hypolipemic effect of perfluorooctanoic acid (PFOA), perfluorooctane sulphonic acid (PFOSA) and clofibrilic acid, *Biochimica et Biophysica Acta* (1992) 1128: 65-72.
 82. Ikeda, T., Aiba, K., Fukuda, K., Tanaka, M. The induction of peroxisome proliferation in rat liver by perfluorinated fatty acids, metabolically inert derivatives of fatty acids, *The Journal of Biochemistry* (1985) 98: 475-482.
 83. Seacat, A. M., Thomford, P. J., Hansen, K. J., Clemen, L. A., Eldridge, S. R., Elcombe, C. R., Butenhoff, J. L. Sub-chronic dietary toxicity of potassium perfluorooctanesulfonate in rats, *Toxicology* (2003) 183: 117-131.
-

-
84. Seacat, A. M., Thomford, P. J., Hansen, K. J., Olsen, G. W., Case, M. T., Butenhoff, J. L. Subchronic toxicity studies on perfluorooctanesulfonate potassium salt in cynomolgus monkeys, *Toxicological Sciences* (2002) 68: 249-264.
 85. Peden-Adams, M. M., Stuckey, J. E., Gaworecki, K. M., Berger-Ritchie, J., Bryant, K., Jodice, P. G., Scott, T. R., Ferrario, J. B., Guan, B., Vigo, C., Boone, J. S., McGuinn, W. D., Dewitt, J. C., Keil, D. E. Developmental toxicity in white leghorn chickens following in ovo exposure to perfluorooctane sulfonate (PFOS), *Reproductive Toxicology* (2009) 27: 307-318.
 86. Lau, C., Butenhoff, J. L., Rogers, J. M. The developmental toxicity of perfluoroalkyl acids and their derivatives, *Toxicology and Applied Pharmacology* (2004) 198: 231-241.
 87. Butenhoff, J. L., Gaylor, D. W., Moore, J. A., Olsen, G. W., Rodricks, J., Mandel, J. H., Zobel, L. R. Characterization of risk for general population exposure to perfluorooctanoate, *Regulatory Toxicology and Pharmacology* (2004) 39: 363-380.
 88. Bonefeld-Jorgensen, E. C., Long, M., Bossi, R., Ayotte, P., Asmund, G., Kruger, T., Ghisari, M., Mulvad, G., Kern, P., Nzulumiki, P., Dewailly, E. Perfluorinated compounds are related to breast cancer risk in Greenlandic Inuit: a case control study, *Environmental Health* (2011) 10: 88.
 89. Peden-Adams, M. M., Keller, J. M., Eudaly, J. G., Berger, J., Gilkeson, G. S., Keil, D. E. Suppression of humoral immunity in mice following exposure to perfluorooctane sulfonate, *Toxicological Sciences* (2008) 104: 144-154.
 90. Corsini, E., Sangiovanni, E., Avogadro, A., Galbiati, V., Viviani, B., Marinovich, M., Galli, C. L., Dell'agli, M., Germolec, D. R. In vitro characterization of the immunotoxic potential of several perfluorinated compounds (PFCs), *Toxicology and Applied Pharmacology* (2011).
 91. Fair, P. A., Driscoll, E., Mollenhauer, M. A., Bradshaw, S. G., Yun, S. H., Kannan, K., Bossart, G. D., Keil, D. E., Peden-Adams, M. M. Effects of environmentally-relevant levels of perfluorooctane sulfonate on clinical parameters and immunological functions in B6C3F1 mice, *Journal of Immunotoxicology* (2011) 8: 17-29.
 92. Stockholm Convention Secretariat, Governments unite to step-up reduction on global DDT reliance and add nine new chemicals under international treaty (2009), <http://chm.pops.int/Convention/Pressrelease/COP4Geneva8May2009/tabid/542/language/en-US/Default.aspx>, last access: 28-12-2011.
 93. European Commission, Environment and Water: proposal to reduce water pollution risks (2012), <http://europa.eu/rapid/pressReleasesAction.do?reference=IP/12/88&format=HTML&aged=0&language=EN&guiLanguage=en>, last access: 25-1-2012.
 94. The European Parliament and The Council of the European Union, Directive 2008/105/EC of The European Parliament and of The Council (2008), <http://eur-lex.europa.eu/LexUriServ/LexUriServ.do?uri=OJ:L:2008:348:0084:0097:EN:PDF>, last access: 2-2-2012.
 95. Mulkiewicz, E., Jastorff, B., Skladanowski, A. C., Kleszczynski, K., Stepnowski, P. Evaluation of the acute toxicity of perfluorinated carboxylic acids using eukaryotic cell lines, bacteria and enzymatic assays, *Environmental Toxicology and Pharmacology* (2007) 23: 279-285.
 96. Latala, A., Nedzi, M., Stepnowski, P. Acute toxicity assessment of perfluorinated carboxylic acids towards the Baltic microalgae, *Environmental Toxicology and Pharmacology* (2009) 28: 167-171.
 97. Mitchell, R. J., Myers, A. L., Mabury, S. A., Solomon, K. R., Sibley, P. K. Toxicity of fluorotelomer carboxylic acids to the algae *Pseudokirchneriella subcapitata* and *Chlorella vulgaris*, and the amphipod *Hyaella azteca*, *Ecotoxicology and Environmental Safety* (2011) 74: 2260-2267.
-

-
98. Hagenaaers, A., Vergauwen, L., De, C. W., Knapen, D. Structure-activity relationship assessment of four perfluorinated chemicals using a prolonged zebrafish early life stage test, *Chemosphere* (2011) 82: 764-772.
 99. Key, B. D., Howell, R. D., Criddle, C. S. Defluorination of Organofluorine Sulfur Compounds by *Pseudomonas* Sp. Strain D2, *Environmental Science & Technology* (1998) 32: 2283-2287.
 100. Schultz, M. M., Barofsky, D. F., Field, J. A. Quantitative determination of fluorotelomer sulfonates in groundwater by LC MS/MS, *Environmental Science & Technology* (2004) 38: 1828-1835.
 101. Wang, N., Liu, J., Buck, R. C., Korzeniowski, S. H., Wolstenholme, B. W., Folsom, P. W., Sulecki, L. M. 6:2 fluorotelomer sulfonate aerobic biotransformation in activated sludge of waste water treatment plants, *Chemosphere* (2011) 82: 853-858.
 102. Parsons, J. R., Saez, M., Dolfig, J., de Voogt, P. Biodegradation of Perfluorinated Compounds, *Reviews of Environmental Contamination and Toxicology* (2008) 53-71.
 103. Butt, C. M., Mabury, S. A., Muir, D. C. G., Braune, B. M. Prevalence of long-chained perfluorinated carboxylates in seabirds from the Canadian arctic between 1975 and 2004, *Environmental Science & Technology* (2007) 41: 3521-3528.
 104. Furdui, V. I., Stock, N. L., Ellis, D. A., Butt, C. M., Whittle, D. M., Crozier, P. W., Reiner, E. J., Muir, D. C. G., Mabury, S. A. Spatial distribution of perfluoroalkyl contaminants in lake trout from the Great Lakes, *Environmental Science & Technology* (2007) 41: 1554-1559.
 105. Wang, N., Szostek, B., Folsom, P. W., Sulecki, L. M., Capka, V., Buck, R. C., Berti, W. R., Gannon, J. T. Aerobic biotransformation of ¹⁴C-labeled 8-2 telomer B alcohol by activated sludge from a domestic sewage treatment plant, *Environmental Science & Technology* (2005) 39: 531-538.
 106. Dinglasan, M. J. A., Ye, Y., Edwards, E. A., Mabury, S. A. Fluorotelomer alcohol biodegradation yields poly- and perfluorinated acids, *Environmental Science & Technology* (2004) 38: 2857-2864.
 107. Liu, J., Lee, L. S., Nies, L. F., Nakatsu, C. H., Turcot, R. F. Biotransformation of 8:2 fluorotelomer alcohol in soil and by soil bacteria isolates, *Environ. Sci. Technol.* (2007) 41: 8024-8030.
 108. Liu, J., Wang, N., Buck, R. C., Wolstenholme, B. W., Folsom, P. W., Sulecki, L. M., Bellin, C. A. Aerobic biodegradation of [¹⁴C] 6:2 fluorotelomer alcohol in a flow-through soil incubation system, *Chemosphere* (2010) 80: 716-723.
 109. Liu, J., Wang, N., Szostek, B., Buck, R. C., Panciroli, P. K., Folsom, P. W., Sulecki, L. M., Bellin, C. A. 6-2 Fluorotelomer alcohol aerobic biodegradation in soil and mixed bacterial culture, *Chemosphere* (2010) 78: 437-444.
 110. Schröder, H. F. Determination of fluorinated surfactants and their metabolites in sewage sludge samples by liquid chromatography with mass spectrometry and tandem mass spectrometry after pressurised liquid extraction and separation on fluorine-modified reversed-phase sorbents, *Journal of Chromatography A* (2003) 1020: 131-151.
 111. Peschka, M., Fichtner, N., Hierse, W., Kirsch, P., Montenegro, E., Seidel, M., Wilken, R. D., Knepper, T. P. Synthesis and analytical follow-up of the mineralization of a new fluorosurfactant prototype, *Chemosphere* (2008) 72: 1534-1540.
 112. Peschka, M., Frömel, T., Fichtner, N., Hierse, W., Kleinedam, M., Montenegro, E., Knepper, T. P. Mechanistic studies in biodegradation of the new synthesized fluorosurfactant 9-[4-(trifluoromethyl)phenoxy]nonane-1-sulfonate, *Journal of Chromatography A* (2008) 1187: 79-86.
-

-
113. Frömel, T., Peschka, M., Fichtner, N., Hierse, W., Ignatiev, N. V., Bauer, K. H., Knepper, T. P. ω-(Bis(trifluoromethyl)amino)alkane-1-sulfonates: synthesis and mass spectrometric study of the biotransformation products, *Rapid Communications in Mass Spectrometry* (2008) 22: 3957-3967.
 114. Schneider, W. F., Wallington, T. J., Huie, R. E. Energetics and Mechanism of Decomposition of CF₃OH, *The Journal of Physical Chemistry* (1996) 100: 6097-6103.
 115. Zachariah, M. R., Tsang, W., Westmoreland, P. R., Burgess, D. R. F. Theoretical Prediction of the Thermochemistry and Kinetics of Reactions of CF₂O with Hydrogen Atom and Water, *The Journal of Physical Chemistry* (1995) 99: 12512-12519.
 116. Russell, M. H., Berti, W. R., Szostek, B., Buck, R. C. Investigation of the biodegradation potential of a fluoroacrylate polymer product in aerobic soils, *Environmental Science & Technology* (2008) 42: 800-807.
 117. Washington, J. W., Ellington, J. J., Jenkins, T. M., Evans, J. J., Yoo, H., Hafner, S. C. Degradability of an Acrylate-Linked, Fluorotelomer Polymer in Soil, *Environmental Science & Technology* (2009) 43: 6617-6623.
 118. Eubeler, J. P., Zok, S., Bernhard, M., Knepper, T. P. Environmental biodegradation of synthetic polymers I. Test methodologies and procedures, *TrAC Trends in Analytical Chemistry* (2009) 28: 1057-1072.
 119. Renner, R. Do perfluoropolymers biodegrade into PFOA?, *Environmental Science & Technology* (2008) 42: 648-650.
 120. DuPont Company, Hydrolytic Stability Study Report. U.S. EPA Administrative Record OPPT2003-0012-2607 (2004), www.regulations.gov, last access: 23-9-2009.
 121. Kromidas, S. HPLC Made to Measure: A Practical Handbook for Optimization. John Wiley & Sons, (2008).
 122. Mallet, C. R., Lu, Z. L., Mazzeo, J. R. A study of ion suppression effects in electrospray ionization from mobile phase additives and solid-phase extracts, *Rapid Communications in Mass Spectrometry* (2004) 18: 49-58.
 123. Clifford, M. N., Lopez, V., Poquet, L., Williamson, G., Kuhnert, N. A systematic study of carboxylic acids in negative ion mode electrospray ionisation mass spectrometry providing a structural model for ion suppression, *Rapid Communications in Mass Spectrometry* (2007) 21: 2014-2018.
 124. Remane, D., Meyer, M. R., Wissenbach, D. K., Maurer, H. H. Ion suppression and enhancement effects of co-eluting analytes in multi-analyte approaches: systematic investigation using ultra-high-performance liquid chromatography/mass spectrometry with atmospheric pressure chemical ionization or electrospray ionization, *Rapid Communications in Mass Spectrometry* (2010) 24: 3103-3108.
 125. van Leeuwen, S. P. J., de Boer, J. Extraction and clean-up strategies for the analysis of poly- and perfluoroalkyl substances in environmental and human matrices, *Journal of Chromatography A* (2007) 1153: 172-185.
 126. Langlois, I., Oehme, M. Structural identification of isomers present in technical perfluorooctane sulfonate by tandem mass spectrometry, *Rapid Communications in Mass Spectrometry* (2006) 20: 844-850.
 127. McLafferty, F. W. A Century of Progress in Molecular Mass Spectrometry, *Annual Review of Analytical Chemistry* (2011) 4: 1-22.
 128. Hansen, K. J., Clemen, L. A., Ellefson, M. E., Johnson, H. O. Compound-Specific, Quantitative Characterization of Organic Fluorochemicals in Biological Matrices, *Environmental Science & Technology* (2001) 35: 766-770.
-

-
129. Iribarne, J. V., Thomson, B. A. On the evaporation of small ions from charged droplets, *Journal of Chemical Physics* (1976) 64: 2287-2294.
 130. Thomson, B. A., Iribarne, J. V. Field induced ion evaporation from liquid surfaces at atmospheric pressure, *Journal of Chemical Physics* (1979) 71: 4451-4463.
 131. Cech, N. B., Enke, C. G. Practical implications of some recent studies in electrospray ionization fundamentals, *Mass Spectrometry Reviews* (2001) 20: 362-387.
 132. Kebarle, P., Peschke, M. On the mechanisms by which the charged droplets produced by electrospray lead to gas phase ions, *Analytica Chimica Acta* (2000) 406: 11-35.
 133. Brace, N. O. Long Chain Alkanoic and Alkenoic Acids with Perfluoroalkyl Terminal Segments¹, *The Journal of Organic Chemistry* (1962) 27: 4491-4498.
 134. Burns, D. C., Ellis, D. A., Li, H., McMurdo, C. J., Webster, E. Experimental pKa Determination for Perfluorooctanoic Acid (PFOA) and the Potential Impact of pKa Concentration Dependence on Laboratory-Measured Partitioning Phenomena and Environmental Modeling, *Environmental Science & Technology* (2008) 42: 9283-9288.
 135. Goss, K. U. The pKa values of PFOA and other highly fluorinated carboxylic acids, *Environmental Science & Technology* (2008) 42: 456-458.
 136. Blades, A. T., Ikononou, M. G., Kebarle, P. Mechanism of electrospray mass spectrometry. Electrospray as an electrolysis cell, *Analytical Chemistry* (1991) 63: 2109-2114.
 137. Kebarle, P., Tang, L. From ions in solution to ions in the gas phase - the mechanism of electrospray mass spectrometry, *Analytical Chemistry* (1993) 65: 972A-986A.
 138. Kebarle, P., Verkerk, U. H. Electrospray: From ions in solution to ions in the gas phase, what we know now, *Mass Spectrometry Reviews* (2009) 28: 898-917.
 139. Schröder, H. F., Meesters, R. J. Stability of fluorinated surfactants in advanced oxidation processes--A follow up of degradation products using flow injection-mass spectrometry, liquid chromatography-mass spectrometry and liquid chromatography-multiple stage mass spectrometry, *Journal of Chromatography A* (2005) 1082: 110-119.
 140. Sottani, C., Minoia, C. Quantitative determination of perfluorooctanoic acid ammonium salt in human serum by high-performance liquid chromatography with atmospheric pressure chemical ionization tandem mass spectrometry, *Rapid Communications in Mass Spectrometry* (2002) 16: 650-654.
 141. Linge, K. L., Jarvis, K. E. Quadrupole ICP-MS: Introduction to Instrumentation, Measurement Techniques and Analytical Capabilities, *Geostandards and Geoanalytical Research* (2009) 33: 445-467.
 142. Miller, P. E., Denton, M. B. The quadrupole mass filter: Basic operating concepts, *Journal of Chemical Education* (1986) 63: 617.
 143. Willoughby, R., Sheehan, E. W., Mitrovich, S. A global view of LC/MS: how to solve your most challenging analytical problems. Global View Publ., Pittsburgh (2002).
 144. Applied Biosystems. Applied Biosystems 3200 Q Trap operator manual (2012)
 145. Hager, J. W. A new linear ion trap mass spectrometer, *Rapid Communications in Mass Spectrometry* (2010) 16: 512-526.
 146. Hu, Q., Noll, R. J., Li, H., Makarov, A., Hardman, M., Graham Cooks, R. The Orbitrap: a new mass spectrometer, *Journal of Mass Spectrometry* (2005) 40: 430-443.
-

-
147. Kingdon, K. H. A Method for the Neutralization of Electron Space Charge by Positive Ionization at Very Low Gas Pressures, *Physical Review* (1923) 21: 408-418.
 148. Knight, R. D. Storage of ions from laser-produced plasmas, *Applied Physics Letters* (1981) 38: 221-223.
 149. Makarov, A., Denisov, E., Kholomeev, A., Balschun, W., Lange, O., Strupat, K., Horning, S. Performance Evaluation of a Hybrid Linear Ion Trap/Orbitrap Mass Spectrometer, *Analytical Chemistry* (2006) 78: 2113-2120.
 150. Marshall, A. G., Hendrickson, C. L. High-Resolution Mass Spectrometers, *Annual Review of Analytical Chemistry* (2008) 1: 579-599.
 151. Levsen, K., Schwarz, H. Gas-phase chemistry of collisionally activated ions, *Mass Spectrometry Reviews* (1983) 2: 77-148.
 152. McLafferty, F. W. Mass Spectrometric Analysis. Molecular Rearrangements, *Analytical Chemistry* (1959) 31: 82-87.
 153. Levsen, K., Schiebel, H.-M., Terlouw, J. K., Jobst, K. J., Elend, M., Preiß, A., Thiele, H., Ingendoh, A. Even-electron ions: a systematic study of the neutral species lost in the dissociation of quasi-molecular ions, *Journal of Mass Spectrometry* (2007) 42: 1024-1044.
 154. Arsenault, G., McAlees, A., McCrindle, R., Riddell, N. Analysis of perfluoroalkyl anion fragmentation pathways for perfluoroalkyl carboxylates and sulfonates during liquid chromatography/tandem mass spectrometry: evidence for fluorine migration prior to secondary and tertiary fragmentation, *Rapid Communications in Mass Spectrometry* (2007) 21: 3803-3814.
 155. Lyon, P. A., Tomer, K. B., Gross, M. L. Fast atom bombardment and tandem mass spectrometry for characterizing fluoroalkanesulfonates, *Analytical Chemistry* (1985) 57: 2984-2989.
 156. Berger, U., Langlois, I., Oehme, M., Kallenborn, R. Comparison of three types of mass spectrometer for high-performance liquid chromatography/mass spectrometry analysis of perfluoroalkylated substances and fluorotelomer alcohols, *European Journal of Mass Spectrometry* (2004) 10: 579-588.
 157. Szostek, B., Prickett, K. B., Buck, R. C. Determination of fluorotelomer alcohols by liquid chromatography/tandem mass spectrometry in water, *Rapid Communications in Mass Spectrometry* (2006) 20: 2837-2844.
 158. Liu, J. X., Lee, L. S. Effect of fluorotelomer alcohol chain length on aqueous solubility and sorption by soils, *Environmental Science & Technology* (2007) 41: 5357-5362.
 159. DuPont Company, Zonyl FSH Data Sheet (2001), http://www2.dupont.com/Zonyl_Foraperle/en_US/assets/downloads/Zonyl_FSH.pdf, last access: 13-2-2011.
 160. Frömel, T., Knepper, T. P. Mass spectrometry as an indispensable tool for studies of biodegradation of surfactants, *TrAC Trends in Analytical Chemistry* (2008) 27: 1091-1106.
 161. Knepper, T. P., Barcelo, D., de Voogt, P. Analysis and fate of surfactants in the aquatic environment. Elsevier, Amsterdam (2003).
 162. Dinglasan, M. J. A., Mabury, S. A. Significant residual fluorinated alcohols present in various fluorinated materials, *Environmental Science & Technology* (2006) 40: 1447-1453.
 163. Liu, J., Lee, L. S., Nies, L. F., Nakatsu, C. H., Turco, R. F. Biotransformation of 8 : 2 fluorotelomer alcohol in soil and by soil bacteria isolates, *Environmental Science & Technology* (2007) 41: 8024-8030.
-

-
164. Di Corcia, A., Crescenzi, C., Marcomini, A., Samperi, R. Liquid Chromatography- Electrospray- Mass Spectrometry as a Valuable Tool for Characterizing Biodegradation Intermediates of Branched Alcohol Ethoxylate Surfactants, *Environmental Science & Technology* (1998) 32: 711-718.
 165. Jonkers, N., Knepper, T. P., deVoogt, P. Aerobic biodegradation studies of nonylphenol ethoxylates in river water using liquid chromatography-electrospray tandem mass spectrometry, *Environmental Science & Technology* (2001) 35: 335-340.
 166. Bernhard, M., Eubeler, J. P., Zok, S., Knepper, T. P. Aerobic biodegradation of polyethylene glycols of different molecular weights in wastewater and seawater, *Water Research* (2008) 42: 4791-4801.
 167. Eubeler, J. P., Bernhard, M., Knepper, T. P. Environmental biodegradation of synthetic polymers II. Biodegradation of different polymer groups, *TrAC Trends in Analytical Chemistry* (2010) 29: 84-100.
 168. Kawai, F. Microbial degradation of polyethers, *Applied Microbiology and Biotechnology* (2002) 58: 30-38.
 169. Busch, J., Ahrens, L., Sturm, R., Ebinghaus, R. Polyfluoroalkyl compounds in landfill leachates, *Environmental Pollution* (2010) 158: 1467-1471.
 170. Möller, A., Ahrens, L., Sturm, R., Westerveld, J., van der Wielen, F., Ebinghaus, R., de Voogt, P. Distribution and sources of polyfluoroalkyl substances (PFAS) in the River Rhine watershed, *Environmental Pollution* (2010) 158: 3243-3250.
 171. Ahrens, L., Gerwinski, W., Theobald, N., Ebinghaus, R. Sources of polyfluoroalkyl compounds in the North Sea, Baltic Sea and Norwegian Sea: Evidence from their spatial distribution in surface water, *Marine Pollution Bulletin* (2010) 60: 255-260.
 172. Scott, B. F., Moody, C. A., Spencer, C., Small, J. M., Muir, D. C., Mabury, S. A. Analysis for perfluorocarboxylic acids/anions in surface waters and precipitation using GC-MS and analysis of PFOA from large-volume samples, *Environmental Science & Technology* (2006) 40: 6405-6410.
 173. Das, K. P., Grey, B. E., Zehr, R. D., Wood, C. R., Butenhoff, J. L., Chang, S. C., Ehresman, D. J., Tan, Y. M., Lau, C. Effects of perfluorobutyrate exposure during pregnancy in the mouse, *Toxicological Sciences* (2008) 105: 173-181.
 174. Gellrich, V., Stahl, T., Knepper, T. P. Behavior of perfluorinated compounds in soils during leaching experiments, *Chemosphere* (2012) 87: 1052-1056.
 175. Organisation for Economic Co-Operation and Development. OECD Guideline for the Testing of Chemicals - Aerobic Mineralisation in Surface Water - Simulation Biodegradation Test (2004)
 176. Sato, H., Shibata, A., Wang, Y., Yoshikawa, H., Tamura, H. Characterization of biodegradation intermediates of nonionic surfactants by MALDI-MS. 2. Oxidative biodegradation profiles of uniform octylphenol polyethoxylate in O-18-labeled water, *Biomacromolecules* (2003) 4: 46-51.
 177. Abello, N., Geurink, P. P., Toorn, M. v. d., Oosterhout, A. J. M., Lugtenburg, J., Marel, G. A., Kerstjens, H. A. M., Postma, D. S., Overkleeft, H. S., Bischoff, R. Poly(ethylene glycol)-Based Stable Isotope Labeling Reagents for the Quantitative Analysis of Low Molecular Weight Metabolites by LC-MS, *Analytical Chemistry* (2008) 80: 9171-9180.
 178. Verweij, W., Durand, A. M., Maas, J. L., and van der Grinten, E. Protocols belonging to the report 'Toxicity measurements in concentrated water samples' - RIVM Report 607013010/2010 (2010)
-